Title
Ligand-induced upregulation of TGF-beta type I and type II receptors at the cell surface amplifies the TGF-beta response

Author
Duan, Dana

Publication Date
2017

Peer reviewed|Thesis/dissertation

Ligand-induced upregulation of TGF-β type I and type II receptors at the cell surface amplifies the TGF-β response

by

Dana Duan

DISSERTATION

Submitted in partial satisfaction of the requirements for the degree of

DOCTOR OF PHILOSOPHY

in

Biochemistry and Molecular Biology

in the

GRADUATE DIVISION

of the

UNIVERSITY OF CALIFORNIA, SAN FRANCISCO

I dedicate this dissertation to my parents—my father who inspired my pursuit of scientific research, and my mother who supported those efforts.

ACKNOWLEDGEMENTS

To my research advisor Dr. Rik Derynck—Thank you for your patience and vast knowledge in mentoring me through the process of completing this research, for inspiring me to approach my work with an innovative mind, and for being a calming presence during inevitable times of stress. (Also, thank you for taking time to educate your mentees about fine art, fine wine, and aspiring for finer things in general.)

I would like to express my sincere gratitude to the other two members of my committee, Dr. Brian Black and Dr. Geeta Narlikar. You took the time to guide my research from a handful of nascent observations to the complete project presented in this manuscript, offering insights that shaped this work and counsel that got me through this degree.

I thank the other members of the Derynck lab for providing discussion and unique perspectives on my research, for occasionally lending your hands and reagents when my experiments were short on both, and for making the lab a second home to me.

Special thanks to my lab mate Dr. Erine Budi, without whose initial observations this project would not exist. You took the time to help me troubleshoot finicky experiments and interpret confusing results, and I am ever appreciative of your support.

Lastly, I am grateful my friends and family for believing in me when I was unsure of myself, for keeping me grounded in the face of the uncertainty inherent to scientific research, and without whom I could not have completed this endeavor.

PREVIOUSLY PUBLISHED MATERIALS

The text of Section III of this dissertation is a reprint of the material as it appears in The Journal of Clinical Investigation. The co-author listed in this publication (Dr. Hal Chapman) directed and supervised the research that forms the basis for this section of the dissertation.

> Wei, Y. et al. Fibroblast-specific inhibition of TGF-beta1 signaling attenuates lung and tumor fibrosis. *J Clin Invest* **127**, 3675-3688 (2017).

The text of Section IV of this dissertation is a reprint of the material as it appears in Trends in Cell Biology. This review was co-authored by Dr. Erine Budi and directed and supervised by my research advisor Dr. Rik Derynck.

> Budi, E.H., Duan, D. & Derynck, R. Transforming Growth Factor-beta Receptors and Smads: Regulatory Complexity and Functional Versatility. *Trends Cell Biol* **27**, 658-672 (2017).

The following is a statement from Dr. Derynck, regarding co-authorship of published materials:

> The major focus of Dana's research was on the control of TGF-β presentation at the cell surface, elucidating a novel mechanism of Akt-mediated enhancement of the cell surface levels of the TGF-β receptors in response to TGF-β, resulting in signal auto-amplification. This is outlined in the first section of her dissertation and essentially corresponds to a manuscript to be submitted.
>
> The work in collaboration with the lab of Hal Chapman was aimed at defining the effect of treatment of the cells with ellagic acid, and later with the related corilagin, on TGF-β-induced Smad activation. In this context, Dana found that pre-treatment, but not simultaneous treatment, of the cells inhibited TGF-β-induced Smad activation, in a time-dependent manner, thus suggesting that a metabolite of ellagic acid or corilagin might inhibit the TGF-β response. She subsequently found that this inhibitory effect resulted from a direct inhibition by corilagin-like derivatives on the kinase activity of the type I TGF-β receptor. These key observations were incorporated in a very large and substantial paper that largely focused on the antitumoral and antifibrotic effects of corilagin and involved

several research groups. One could argue that being a co-author on such extensive paper does not give sufficient visibility to Dana's work, but this is probably also the case for the contributing research by the other collaborating labs. However, the nature of this paper, going from organic chemistry and biochemistry to cell-based research and in vivo models, dictates required contributions by different labs. Data that were not incorporated in the paper, yet are important observations, are shown in section II.

Section IV represents a review on new insights into mechanisms of TGF-β signaling that was published in Trends in Cell Biology. Dana reviewed some important aspects of the mechanisms of Smad-mediated differentiation decisions in cells, including cell death, and wrote the corresponding sections, while also contributing to the overall manuscript. As Erine Budi had more extensive contributions to this review than Dana, Erine became first author, and Dana became second author.

ABSTRACT

Ligand-induced upregulation of TGF-β type I and type II receptors at the cell surface amplifies the TGF-β response

Dana Duan

The transforming growth factor (TGF)-β family of proteins drive normal embryonic development, while dysregulation of TGF-β signaling contributes to developmental disorders, and plays major roles in cancer progression and dissemination, and fibrosis. Signaling by TGF-β initiates upon ligand binding to transmembrane receptor proteins, which then promote gene expression changes through phosphorylation and activation of intracellular Smad proteins. Functional activation of the TGF-β receptors is carefully regulated through integration of post-translational modifications, spatial regulation at the cellular level, and receptor availability at the cell surface.

While the majority of TGF-β receptors reside intracellularly, they can be rapidly mobilized to the cell surface in response to Akt activation and signaling, thereby increasing the cell's responsiveness to TGF-β. Because TGF-β is known to induce phosphorylation of Akt, I investigated whether TGF-β regulates translocation of its own receptors to the cell surface and thus amplifies its own response. Through selective biotinylation of cell surface proteins, I found that TGF-β induced a rapid increase of type I and type II TGF-β receptors at the plasma membrane. This receptor upregulation was inhibited by blocking Akt phosphorylation, or in the presence of TGF-β type I receptor kinase inhibitors. Furthermore, attenuation of the Akt-mediated increase in cell surface receptor presentation decreased Smad activation and TGF-β-

induced gene expression responses. I also observed that while TGF-β treatment caused an overall increase in cell surface TGF-β receptors, it also induced an increased rate of receptor endocytosis, suggesting an overall amplification of TGF-β receptor cycling. Together, these data outline a novel response amplification mechanism, through a ligand-induced, rapid mobilization of cell surface receptors from intracellular stores.

Furthermore, BMP-4 caused cells to upregulate TGF-β receptors, leading to subsequent autocrine activation of TGF-β-responsive Smads and gene expression. Inhibition of Akt phosphorylation or inhibition of TGF-β type I receptor kinase attenuated the autocrine TGF-β signaling activation in response to BMP. The balance between BMP and TGF-β signaling pathways is essential for proper spatial and temporal regulation of tissue specification during development, and has been observed biochemically, although the underlying mechanisms are not clear. This work provides context for activation of TGF-β signaling by BMP, presenting a means by which cells could gain sensitivity to TGF-β in the presence of BMP.

TABLE OF CONTENTS

SECTION III

Attenuation of lung and tumor fibrosis by fibroblast-specific inhibition of TGFβ1 signaling

SECTION IV

TGF-β Receptors and Smads: Regulatory Complexity and Functional Versatility

LIST OF FIGURES

SECTION I.

Ligand-induced upregulation of TGF-β type I and type II receptor increases responsiveness to TGF-β

Chapter 1. Introduction

Embryonic development is characterized by precise regulation of cellular processes. The integration of multiple signaling pathways is necessary for cells to undergo differentiation, proliferation, migration, and cell death. Delicate coordination and control of signal transduction inform correct tissue formation and patterning in both the developing embryo and in tissue homeostasis, while dysregulation of signaling pathways underlies developmental disorders and cancers.

1.1 Spatial regulation of transmembrane receptor proteins

Transmembrane receptor serine/threonine and tyrosine kinases are critical to transduction of extracellular signals, and regulation of receptors is important to developmental and disease processes. Aberrant receptor function has been implicated in multiple disease processes, with mutation or dysregulation of receptor kinases often leading to ligand-independent signaling.[1,2]

Altered receptor expression and activation are the best characterized modes of receptor dysfunction.[1] However, modulation of ligand responsiveness through spatial regulation has been observed in receptor tyrosine kinases (RTKs). In general, the abundance of RTKs at the cell surface is determined not only the expression levels of the receptors, but also by receptor cycling between the plasma membrane and endocytic vesicles.[1-3] In many cases, ligand binding induces receptor endocytosis and, depending on context, receptor recycling or degradation.[3] While historically ligand-induced receptor internalization was viewed as a negative feedback mechanism, our current understanding is that endocytic transport is often required for signaling, and that both endocytosis and recycling of receptors function in complex spatial regulation of signaling.[1,2]

Among the RTKs, trafficking and endosomal signaling of the epidermal growth factor receptor (EGFR) has been well studied. Endocytic EGFR, which is capable of authophosphorylation, remains associated with co-internalized signaling molecules and is catalytically active.[4-8] Likewise, inhibition of EGFR internalization has been shown to alter cell response.[9,10] Receptor internalization after ligand binding has also been reported for other RTKs, including the insulin, vascular endothelial growth factor (VEGF), and platelet-derived growth factor (PDGF) receptors.[3] Radiolabeling assays suggest that the endocytic population of insulin receptors is highly activated in response to insulin, while disruption of dynamin-mediated inhibition of insulin receptor internalization was shown to impair downstream signaling.[11,12] Ligand-induced clathrin-mediated internalization of VEGF receptor type 2 (VEGFR2) regulates contact-dependent inhibition of cell growth, while ephrin B2 was found to control internalization and subsequent endosomal signaling of both VEGFR2 and VEGFR3.[13-15] A system to selectively activate endosome-associated PDGF receptor (PDGFR), without stimulating plasma membrane PDGFR, was used to demonstrate recruitment and subsequent activation of multiple PDGFR-interacting signaling proteins.[16]

Much less is known about the internalization, routing and transport of the TGF-β receptors.[17] In response to TGF-β, the distribution of TGF-β receptors between clathrin-mediated and caveolar endocytic compartments is likely an important determinant of the outcome of signal activation, with Smad signaling occurring primarily in clathrin-associated endosomes while activation of PI3K-Akt and Erk-MAP kinase pathways occurs in caveolar vesicles.[17-21] Additionally, proteasomal degradation of TGF-β receptors as a result of ubiquitylation has been associated with the caveolae.[22,23] Similarly, sorting of EGFR between clathrin- vs caveolin-

containing compartments determines whether the receptor undergoes degradation or recycling, respectively.[2,24,25]

These studies highlight the importance of cell surface distribution of transmembrane receptor kinases in determining the outcome and responsiveness to extracellular ligand. This is further emphasized by the prevalence of aberrant regulation of cell surface RTK levels in disease.[2] For example, overexpression of ErbB2 in cancer leads to increased cell surface levels which results in ligand-independent signaling, likely as a result of receptor autophosphorylation.[26-28] Correspondingly, overexpression of ErbB2 animal models amplifies tumorigenic potential.[29,30] Mutation of caveolin-1, a mediator of endocytic transport of RTKs including EGFR and ErbB2, which can function to sequester RTKs in membrane associated lipid rafts, has also been implicated in several types of cancer.[3,31,32] Interestingly, overexpression of caveolin-1 was shown to promote ligand-independent EGF receptor activation as a result of increased localized EGFR density in caveolae.[33]

Here, I describe research delineating a novel mechanism in which ligand binding induces receptor presentation at cell surface, thus amplifying signal response. While the regulation of the distribution of tyrosine kinases has been shown to modulate cellular response, this is the first report to my knowledge of a signaling molecule causing rapid post-translational upregulation of its own receptor at the cell surface, resulting in amplified cell responsiveness.

1.2 TGF-β signaling context and mechanism

Transforming growth factor (TGF)-β family proteins, and the closely related activins and bone morphogenic protein (BMPs), are involved in regulation of cell morphology, proliferation, and differentiation in both normal developmental and disease contexts[34-36] TGF-β receptors direct

cell differentiation and control cell physiology, proliferation, and growth, thus playing key roles in normal development.[17,37-39] In mice, inactivation of TGF-β receptor expression was found to cause impaired vasculogenesis characterized by defects in capillary tube formation.[40,41] Genetic aberrations in TGF-β receptors signaling components have been linked to developmental deficiencies and disorders including Marfan syndrome, Loeys-Dietz syndrome, multiple sclerosis, autism, and various cardiovascular defects.[42] Dysfunction in receptor expression, activation, and localization is implicated in development and progression of disease as well, including the initiation and progression of fibrosis and cancer.[35,36] Somatic mutations of TGF-β type I receptors (TβRI) have been identified in 16% of breast cancer patients, while TβRII mutations occur in colorectal and gastric cancers at a rate of 30% and 15%, respectively.[43] In biochemical studies, inactivation of (TβRII) illustrates the requirement of TGF-β signaling in invasion and metastasis of both skin and mammary epithelial cancers.[44,45] Treatment of nude mice with TβRII-loaded adenovirus has been shown to cause breast tumor regression, and pretreatment of mammary adenocarcinoma cells with TGF-β enhances invasion potential and metastasis in a xenograft model.[46,47]

The mechanisms of how TGF-β family ligands direct changes in gene expression through Smad activation are often seen as established. In brief, BMPs, activins, and TGF-β proteins are secreted as latent propeptides. Upon cleavage of latency-associated peptides, ligand dimers are able to signal through transmembrane receptors.[34,48] Ligand binding brings homodimers of type I and type II receptors in proximity, allowing receptor transphosphorylation and activation of receptor kinase.[49] Activated type I receptor in turn associates with and phosphorylates intracellular receptor-activated Smads (R-Smads) on two C-terminal serine residues, with Smad1, Smad5, and Smad8 as the effectors of BMP signaling, while Smad2 and Smad3 are

responsive to TGF-β.[38,50] The receptor-activated Smads dissociate from the receptors, bind with the co-Smad (Smad4), and translocate to the nucleus where the trimeric Smad complexes interact with DNA-binding transcription factors and cofactors to directly modulate gene expression.[51,52] Although Smads directly interact with Smad-binding elements (SBEs), the interaction is weak and requires stabilization by Smad-interacting transcription factors that bind DNA with greater affinity.[38,51-53]

Although the broad picture of Smad activation in response to TGF-β is well studied, TGF-β receptors activate several non-Smad signaling pathways, including ERK-MAP kinase, p38 MAP kinase, JNK, Rho-like GTPase, and PI3K-Akt.[54,55] Of particular relevance to my research is activation of PI3K-Akt signaling. In this vein, Akt phosphorylation in response to TGF-β was observed in epithelial cells in a manner requiring active TβRI kinase.[56,57] Furthermore, interaction of Akt with Smad3 was demonstrated to inhibit TGF-β signaling through sequestration of Smad3 in the cytosol.[58]

1.3 Regulation of TGF-β receptors

In signaling by TGF-β family of proteins, the cellular response has been shown to be dictated by the abundance and responsiveness of receptors at the cell surface. Regulation of cell sensitivity to TGF-β occurs through a variety of mechanisms, including post-translational modifications as well as regulation of receptor levels and compartmentalization at the cell surface.[17]

Phosphorylation activates TGF-β receptor kinases

The activity of TGF-β receptor kinases is regulated by both transphosphorylation between Type I and Type II receptors, and autophosphorylation.[59] The TGF-β type II receptor (TβRII) occurs as

a dimer and undergoes auto-/transphosphorylation on Serine 213 and Serine 409, which is likely required for activity.[60] The type I TGF-β receptor (TβRI), which also occurs as a dimer, is a direct substrate of the TβRII kinase. The TβRI receptor requires TβRII-mediated phosphorylation of its juxtamembrane GS domain (TTSGSGSG) in order to activate Smads, and mutation of two or more residues in this GS motif prevents full activation of the TβRI kinase.[61] While initially characterized as serine/threonine kinases, the TGF-β receptors are able to phosphorylate tyrosine residues, thus establishing them as dual-specificity kinases.[59] In a homology modeling study, both TβRI and TβRII were identified as having sequence similarity to tyrosine kinases.[62] Indeed, autophosphorylation of TβRII on tyrosine 259, tyrosine 336 and tyrosine 424 contributes to its kinase activity.[63] TβRI was also shown to phosphorylate the adapter protein ShcA on both tyrosine and serine residues, effecting TGF-β-mediated Erk-MAP kinase signaling activation and contributing to TGF-β-induced epithelial-mesenchymal transition.[64-66]

Post-translational modifications of TGF-β receptors determine TGF-β responsiveness

The TGF-β receptors are glycoproteins, with the ectodomains of TβRI and TβRII containing N-glycosylation on asparagine residues.[67] The translocation of TβRII to the cell surface and subsequent responsiveness to TGF-β was shown to be dependent on N-glycosylation of TβRII.[68,69] The cell also regulates TGF-β receptor availability by ubiquitylation, and subsequent degradation, through cumulative effects of multiple ubiquitylases and de-ubiquitylases.[70] Sumoylation is another means by which the cell regulates TGF-β receptor functionality through post-translational modification.[71,72] Covalent attachment of small ubiquitin-like modifier (SUMO)-1 to TβRI was shown to strongly enhance Smad3 recruitment and activation in

response to TGF-β. Sumoylation of TβRI was found to require both the kinase activity and phosphorylation of TβRI, and impaired TβRI sumoylation was associated with decreased TGF-β-induced Smad activation and gene response.[72] Finally, TβRI ectodomain shedding is another determinant of cell responsiveness to TGF-β. The matrix metalloprotease TACE was shown to directly cleave the ectodomain of TβRI in response to Erk and MAP kinase activation, thus disrupting the formation of the functional TβRI/TβRII complexes and consequently impairing TGF-β-induced Smad activation and signaling.[73]

Subcellular compartmentalization of TGF-β receptors

TGF-β receptor internalization occurs through both clathrin- and caveolin-associated mechanisms, and the endosomal compartmentalization of TGF-β receptors plays a role in determining the outcome of receptor activation.[17] Association of Smad2 and Smad3 with TβRI is facilitated by scaffolding proteins including the FYVE-domain protein Smad anchor for receptor activation (SARA).[22,74,75] Smad phosphorylation is generally thought to occur in clathrin-mediated vesicles containing TGF-β receptors and Smads, as TβRI and SARA have been found to interact with β-adaptin.[18,22] Conversely, activation of Erk MAP kinase and PI3 kinase Akt signaling, as well as ubiquitylation and degradation of TGF-β receptors, likely occur in caveolar lipid rafts.[19-21] Indeed, knockdown of caveolin-1, which associates with TGF-β receptors, interferes with Akt activation in response to TGF-β.[21] Interaction of TβRI with activated ShcA, which is a substrate for phosphorylation by TβRI, was recently reported to sequester TβRI to caveolar endosomes, therefore limiting Smad activation.[66] While the distinct signaling outcomes associated with endocytic compartmentalization suggest two distinct populations of TGF-β receptors, TβRI internalization through double-positive endosomes containing both clathrin and caveolin was observed by fluorescent labeling. These vesicles most likely arise from fusion of

the two types of TβRI-containing endosomes underneath the plasma membrane, resulting in a multifunctional compartment containing both Smad- and non-Smad signaling components.[76]

In addition to partitioning between caveolin and clathrin endocytic compartments, TGF-β signaling is regulated through control of cell surface receptor abundance. The majority of TGF-β receptors reside intracellularly, poised for transport to the cell surface.[17] It was recently reported that insulin causes cells to upregulate the levels of cell surface TGF-β receptors via Akt activation, thus increasing sensitivity to TGF-β. In this instance, insulin-induced Akt phosphorylation was shown to drive a rapid increase in TGF-β at the cell surface through regulation of AS160, a RAB GTPase-activating protein involved in regulation of endosomal cycling. The increase in TGF-β receptor at the cell surface conferred increased sensitivity of the cells to autoocrine TGF-β signaling, which in turn resulted in integration of autocrine TGF-β signaling through Smads in insulin-responsive gene expression.[77]

1.4 Rationale for this project

Since TGF-β receptor is known to activate Akt, perhaps similarly but not to the same extent as the insulin receptor, I hypothesized that TGF-β may regulate its own receptor levels at the cell surface as a means of amplifying the TGF-β response after initial ligand binding. My results demonstrate that TβRI and TβRII were rapidly upregulated at the cell surface in response to TGF-β in manner dependent on Akt activation and TβRI kinase activity. Moreover, inhibition of receptor upregulation impaired downstream Smad activation and transcriptional responses to TGF-β. Finally, I found that BMP-4 also induced an increase in cell surface TGF-β receptors, providing context for the crosstalk between TGF-β and BMP signaling that has long been observed.[78-81]

While much is known about ligand-induced internalization of transmembrane receptor proteins, especially in the case of receptor tyrosine kinases such as EGFR, there are no reports to my knowledge of rapid transport of a receptor kinase to the plasma membrane in response to its own ligand. Here I present data that illustrates such novel mechanism by which cells increase their responsiveness to an extracellular ligand, resulting in signal amplification.

Chapter 2. Results

2.1 TGF-β induces a rapid increase in cell surface TGF-β-receptor levels

To determine whether TGF-β directly causes an increase in TGF-β receptors at the cell surface, I examined cell surface TGF-β receptors in three mammalian cell lines: HaCaT, A549, and NMuMG cells, which are stable immortalized human keratinocyte, human lung carcinoma, and mouse mammary epithelial lineages, respectively. These are well-established models for studying the TGF-β response, exhibiting Smad phosphorylation and associated gene expression changes.[82-84] Cell surface biotinylation analysis was used to visualize proteins that are exposed to the extracellular surface. Briefly, cells were labeled at 4 °C using Sulfo-NHS-LC biotin, a water-soluble biotinylation reagent that is unable to permeate the plasma membrane, then lysed and incubated with NeutrAvidin-conjugated beads to precipitate biotinylated proteins. The resulting fraction, consisting of proteins exposed to the cell surface and co-precipitating complexes, was then visualized by western blotting.

I observed in each of these cell lines a considerable increase of both TβRI and TβRII at the cell surface within 15-30 minutes after stimulation with TGF-β (Figure 1). Cell surface abundance of transferrin receptor (TfR), a transmembrane protein not known to be regulated by TGF-β signaling, was not affected by TGF-β treatment, suggesting that upregulation of TGF-β receptors was specific. Since the overall abundance of TGF-β receptor protein was not affected by TGF-β treatment, and given the rapid kinetics of the increase in receptor, these data likely reflect translocation of receptor to the cell surface. Indeed, rapid redistribution of intracellular TGF-β to the cell surface in response to insulin has been reported.[77]

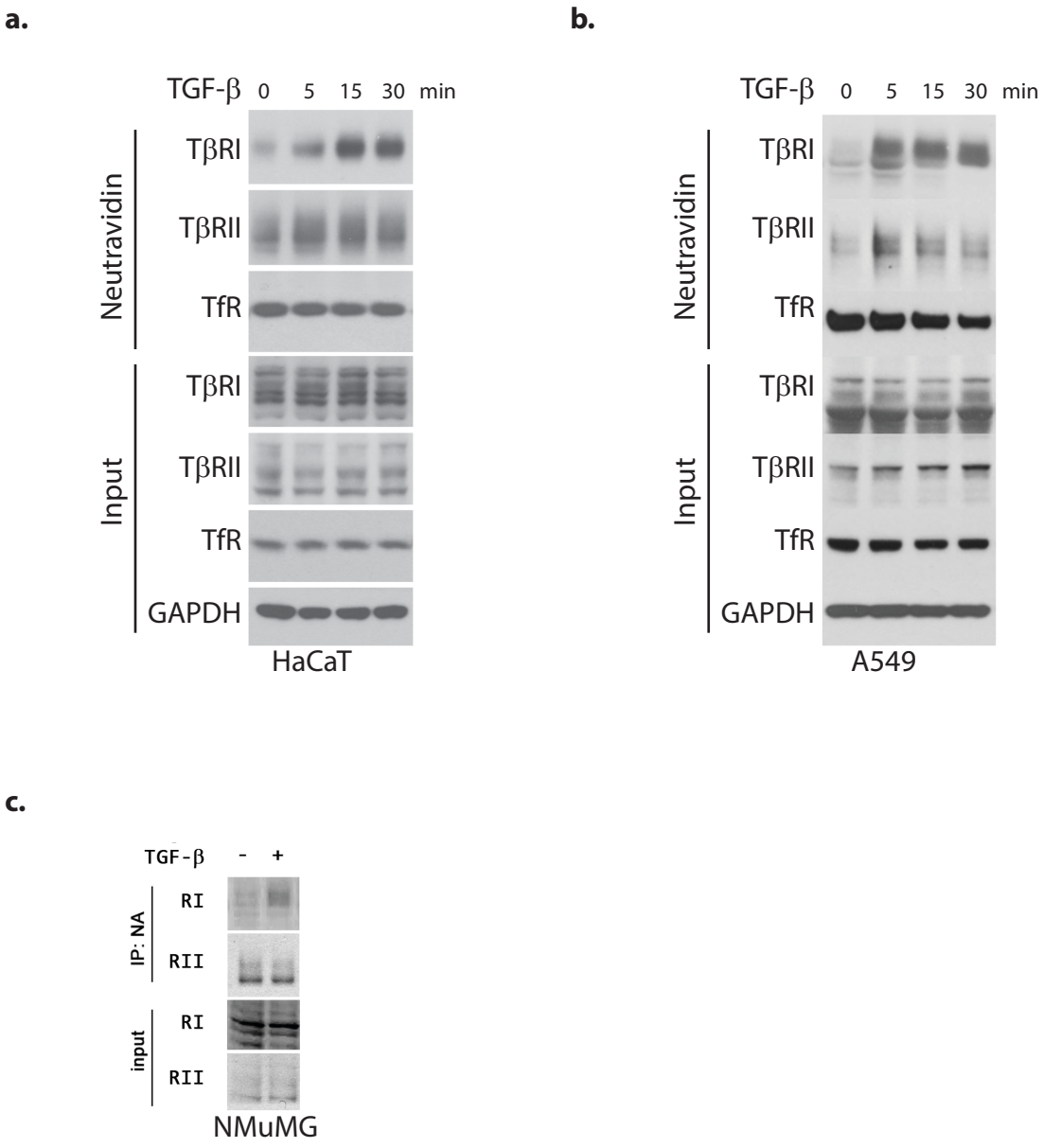

Figure 1. TGF-β induces an increase of type I and type II TGF-β receptors at the cell surface. Cell-surface receptor levels were quantified by selectively cross-linking biotin to proteins exposed to the extracellular surface, followed by immunoprecipitation with neutravidin-conjugated sepharose beads and western blotting. An increase in cell surface TβRI and TβRII was observed within 5-15 minutes after addition of TGF-β, but overall receptor abundance was not affected. This effect was observed in a) human keratinocyte (HaCaT), b) human lung carcinoma (A549), and c) mouse mammary epithelial cells (NMuMG).

2.2 Akt signaling contributes to ligand-induced increase in cell surface receptor presentation

Akt signaling has been shown to mediate insulin-induced TGF-β receptor upregulation at the cell surface, through regulation of receptor cycling between the cell surface and the plasma membrane.[77] I therefore tested whether Akt plays a role in ligand-induced TGF-β receptor upregulation by inhibiting Akt phosphorylation in cells treated with TGF-β, and evaluating receptor upregulation. Consistent with previous findings, TGF-β caused an increase in phosphorylation of Akt on both Serine 473 and Threonine 308 in HaCaT cells, and Akt activation was fully inhibited by treatment with AktVIII, a specific inhibitor of Akt phosphorylation (Figure 2).[57] By performing cell surface biotinylation analysis in HaCaT and A549 cells treated with AktVIII before addition of TGF-β, I observed significant attenuation of ligand-induced cell surface TGF-β receptor levels (Figure 3). Again, this effect appears to be specific to TGF-β receptors as cell surface transferrin receptor levels were not affect. These data highlight the importance of Akt phosphorylation in regulation of cell surface TGF-β receptors. However, AktVIII only partially inhibited receptor induction, despite fully preventing Akt activation, suggesting involvement of other mechanisms.

2.3 TβRI kinase activity contributes to receptor upregulation

TGF-β is known to activate PI3K-Akt signaling through non-Smad pathways in multiple epithelial cell types. While the exact mechanism of Akt activation by TGF-β is not known, it has been reported to require type I receptor kinase activity.[56,57] Because Akt phosphorylation contributes to the ligand-induced increase in TGF-β receptor presentation, I evaluated whether the TβRI kinase activity is necessary. Therefore I performed a cell surface biotin labeling assay

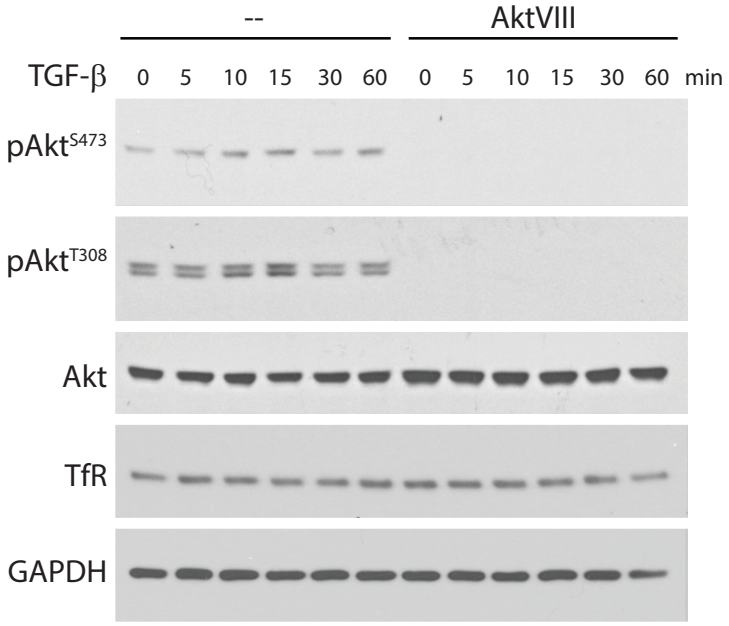

Figure 2. Akt activation in response to TGF-β is inhibited by AktVIII. HaCaT cells were treated with 5 μM AktVIII 30 minutes prior to addition of 0.25 ng/mL TGF-β. Akt phosphorylation on Serine 473 and Threonine 308 was measured by immunoblotting. Although Akt phosphorylation is low compared to cells treated with insulin, there is significant Akt activation within one hour of TGF-β treatment. AktVIII completely blocks this induction and prevents basal levels of Akt phosphorylation.

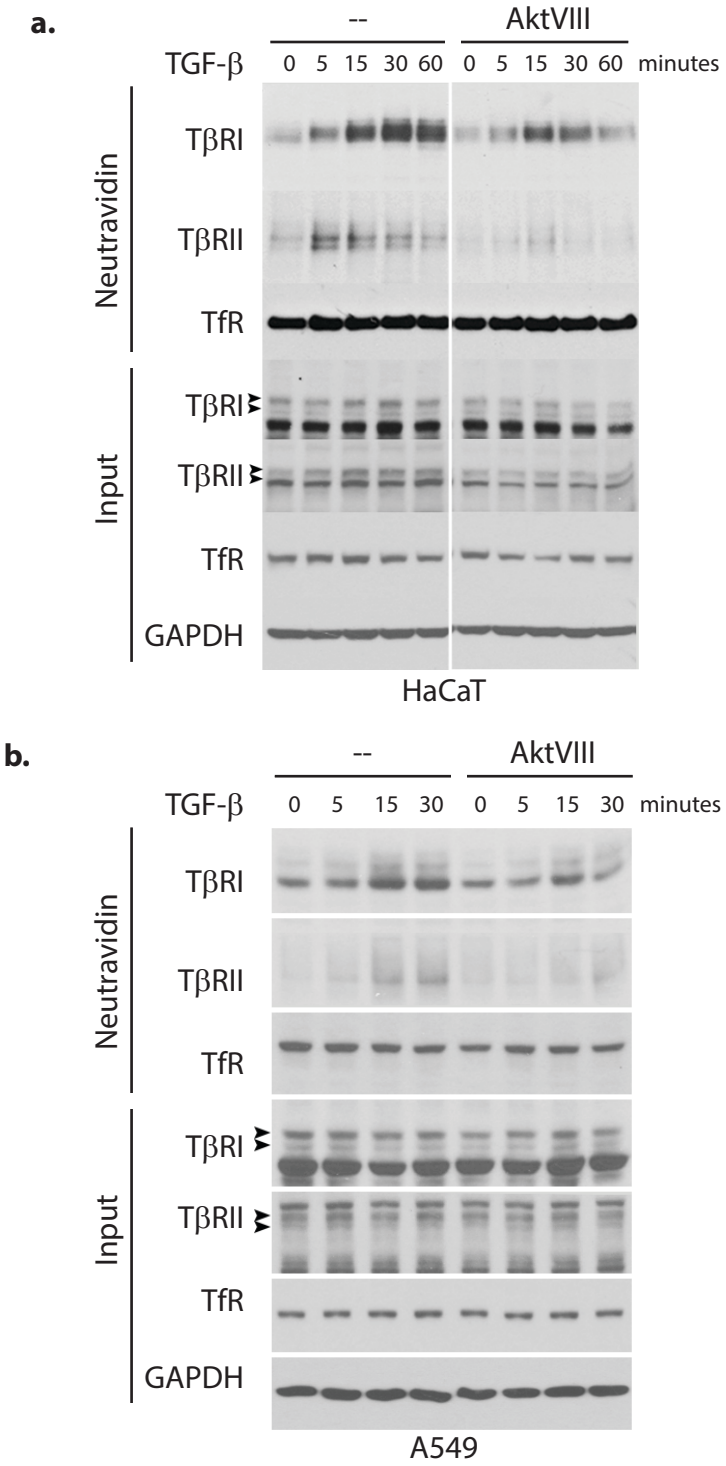

Figure 3. Cell surface TGF-β receptor upregulation requires Akt activation. Akt phosphorylation in response to TGF-β leads to upregulation of the TGF-β receptors at the cell surface. Treatment with AktVIII partially prevented TGF-β-induced increase in cell surface type I and type II receptors, as detected by cell-surface biotinylation. Inhibition was seen in both a) HaCaT and b) A549 cells. Total TβRI and TβRII protein levels were unaffected by AktVIII.

in cells treated with TGF-β in the presence of SB431542, a specific inhibitor of TβRI kinase activity.[85] Interestingly, SB431542 caused decreased induction of both TβRI and TβRII, possibly through inhibition of phospho-Akt (Figure 4). Consistent with prior reports, treating cells with SB431542 resulted in attenuation of TGF-β-induced Akt phosphorylation. As expected, activation of Smad2 and Smad3 was blocked (Figure 5). Additionally, I measured TGF-β receptor induction in the presence of corilagin, a small molecule recently reported to inhibit the TβRI kinase.[86] (See Section II of this dissertation for a description of my work characterizing corilagin as a TβRI kinase inhibitor.) In both HaCaT and A549 cells, corilagin decreased TGF-β-induced receptor presentation without affecting total TGF-β receptor protein levels or cell surface induction of TfR (Figure 6).

Taken together, these data suggest that cell surface TGF-β receptor upregulation requires Akt phosphorylation in response to activation of TβRI kinase. In the context of reported findings that increased TGF-β receptor presentation, as a result of Akt activation through insulin signaling, amplifies the cells' responsiveness to TGF-β, it seemed likely that upregulation of TβRI and TβRII at the cell surface functions to sensitize the cell to TGF-β following initial exposure to ligand.[77]

2.4 Increased availability of receptor allows for increased receptor- and Smad activation

Upon ligand binding, stabilization of the interaction between TβRI and TβRII allows for activation of the TβRI kinase, which then phosphorylates intracellular Smad proteins associated with the receptor complex.[38] To address whether receptor upregulation plays a role in initiation of Smad signaling, I evaluated the formation of the TβRI/RII complex and association of Smad3 with activated TGF-β receptors. Using cells treated with TGF-β and AktVIII, I performed co-

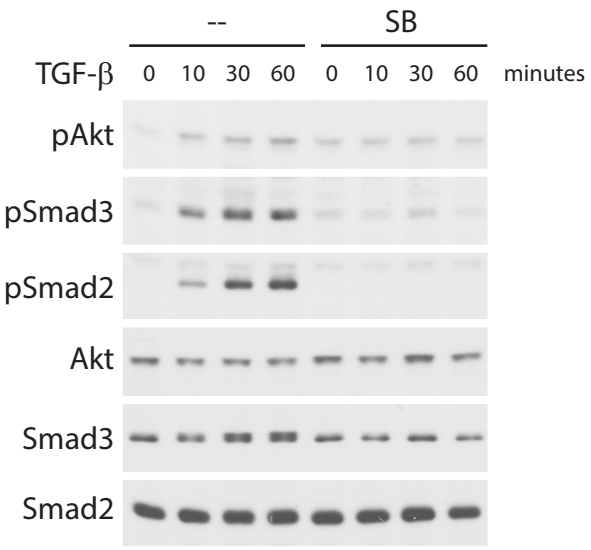

Figure 4. Akt activation in response to TGF-β requires type I receptor kinase activity. HaCaT cells treated with the TβRI kinase inhibitor SB431542 did not show increased Akt phosphorylation in response to TGF-β as measured by immunoblotting. Total Akt levels were not affected. As expected, SB431542 prevented activation of Smad2 and Smad3.

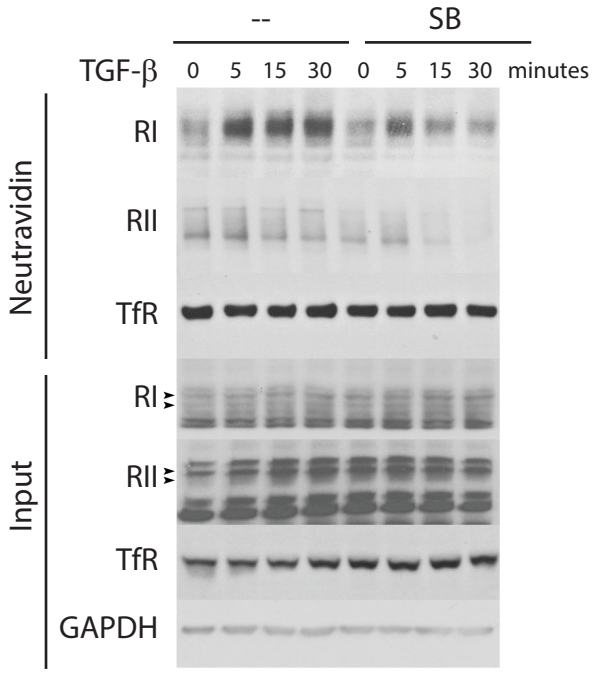

Figure 5. TGF-β type I receptor kinase activity promotes ligand-induced translocation of TGF-β receptors to the cell surface. In HaCaT cells in which TβRI kinase activity was blocked using the specific inhibitor SB431542, induction of type I receptor to the cell surface in response to TGF-β, evaluated by cell surface biotinylation analysis, was significantly decreased. Whole cell abundance of TβRI and TβRII were not affected by inhibitor.

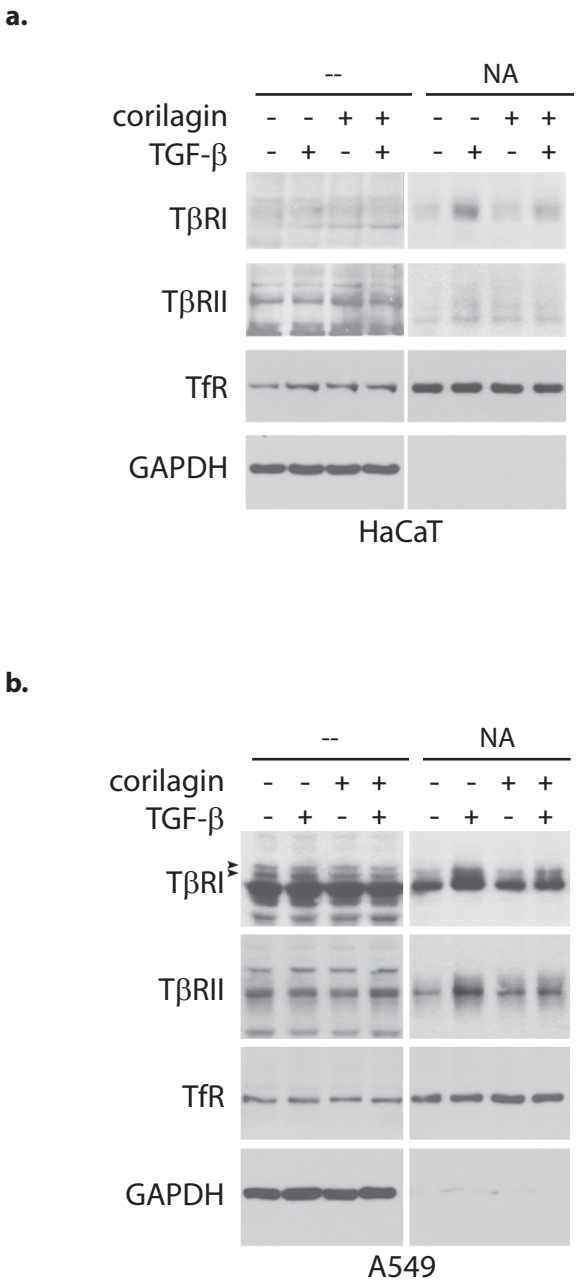

Figure 6. Corilagin pretreatment inhibits cell surface receptor induction. Corilagin, a small molecule inhibitor of TGF-β signaling, has been shown to prevent TβRI kinase activity. Pretreatment for 6 hours with corilagin prevents ligand induced cell surface presentation of both TβRI and TβRII in both HaCaT a) and b) A549 cells, without affecting overall TGF-β receptor abundance.

immunoprecipitation of endogenous RI with RII, and measured Smad-receptor interaction through cell-surface biotinylation.

To assess the ligand-induced interaction of TβRI with TβRII, I immunoprecipitated endogenous TβRI and performed immunoblotting to detect interacting TβRII. Following TGF-β treatment, I observed increased association of TβRII with TβRI, which was prevented in the presence of AktVIII (Figure 7). The inhibition of TβRI/TβRII interaction may be a direct result of decreased cell surface receptor availability. I also observed that TGF-β induced a rapid increase of Smad3 in the membrane-associated protein fraction when performing cell surface biotinylation assays (Figure 8). Presumably this is due to increased Smad3 in transmembrane protein complexes following TGF-β treatment, consistent with interaction of TGF-β receptors and Smad3 in response to ligand. This effect is likely a consequence of receptor upregulation in response to TGF-β. Furthermore, AktVIII, which I earlier showed to inhibit ligand-induced TGF-β receptor presentation, decreased the amount of Smad3 associated with cell-surface proteins. The observed decrease in cell-surface-associated Smad3 is likely due to decreased cell surface TGF-β receptor complexes.

These results are consistent with the notion that Akt activation drives receptor upregulation, leading to increase in heterotypic TGF-β receptor interactions and association of Smad3 receptor complexes at the cell-surface. However, these data do not rule out the possibility that the binding affinity of TβRI and TβRII, or of Smad3 and receptor complex, are affected by the phosphorylation state of Akt.

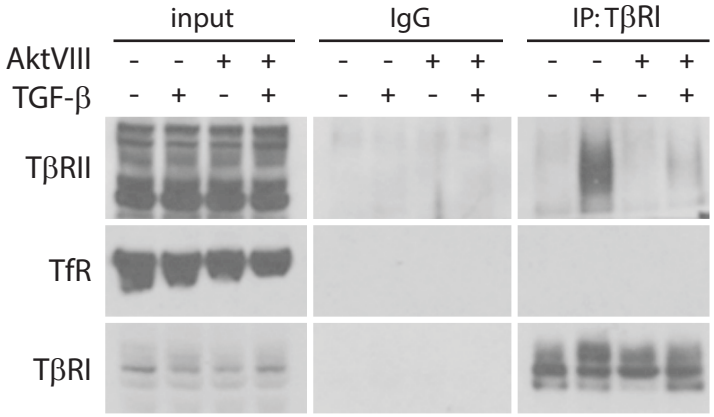

Figure 7. Increased availability of receptor at the cell surface amplifies formation of the TβRI/RII complex upon ligand binding. Coimmunoprecipitation of endogenous TβRII with endogenous TβRI in HaCaT cells demonstrates association of the two receptor types upon stimulation with TGF-β. This interaction is inhibited by AktVIII, suggesting decreased receptor activation due to fewer available receptors at the cell surface when Akt phosphorylation is inhibited.

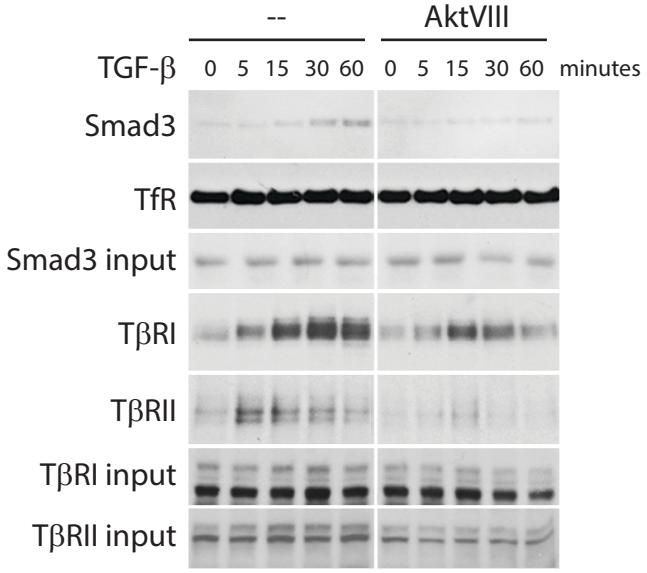

Figure 8. AktVIII prevents ligand-induced interaction of Smad3 with the TGF-β receptor complex. An increase in association of intracellular Smad3 with membrane-bound proteins upon TGF-β stimulation was observed in HaCaT cells. Smad3 was detected in neutravidin enrichment fraction of cell-surface biotinylated cell lysates following addition of TGF-β, presumably due to interaction of Smad3 with TGF-β receptor complexes. This was attenuated by treatment with AktVIII.

Note: Figure 8 presents data from the same experiment as shown in Figure 3a.

2.5 Ligand-induced receptor upregulation at the cell surface results in amplification of Smad activation and transcriptional responses

Phosphorylation of TβRI by TβRII results in activation of TβRI kinase domain, which activates Smad2 and Smad3, which then mediate downstream gene expression changes. Because I observed a decreased receptor-associated Smad3 in conjunction with attenuated TGF-β receptor cell surface presentation, I next determined whether Smad activation and subsequent gene activation was affected by inhibition of receptor induction by AktVIII. Smad phosphorylation was detected by immunoblotting, and Smad-responsive gene activation was examined using reporter assays as well as qRT-PCR of endogenous gene expression.

In a timeframe consistent with the inhibition of rapid receptor induction shown in Figure 2, AktVIII treatment decreased TGF-β-induced Smad2 and Smad3 phosphorylation while the overall Smad2 and Smad3 protein levels remained unchanged (Figure 9). These data are consistent with amplified Smad signaling as a result of receptor upregulation.

Phosphorylated Smad2 and/or Smad3 dissociate from the receptor complex and localize to the nucleus with Smad4, where they modulate gene expression by interacting with DNA at Smad-binding elements (SBE). As a direct readout of transcription regulation by activated Smads, I performed reporter assays using SBE-Luc, a plasmid containing a gene encoding firefly luciferase downstream of multiple SBEs.[87] After 3.5 hours TGF-β induced a four- to fivefold increase in expression of luciferase protein in cells expressing SBE-Luc. Reporter activation was decreased by roughly half in the presence of AktVIII. As expected, luciferase expression was fully inhibited by SB431542, which blocks Smad activation (Figure 10).

I also quantified early expression of the endogenous genes encoding PAI-1, Slug, and Smad7, known to be regulated by TGF-β-activated Smads. I observed induction of these genes in

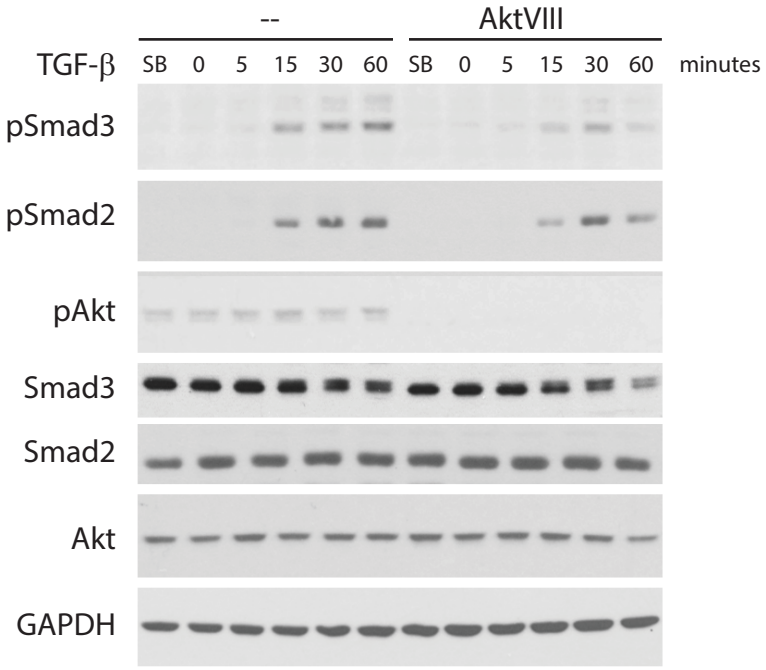

Figure 9. Inhibition of Akt phosphorylation leads to a decrease in Smad2 and Smad3 activation in response to TGF-β. In conjunction with the effect of Akt inhibition on TGF-β-induced receptor presentation, these data suggest a decrease in cellular response to TGF-β when cell surface receptor translocation is impaired. Total Smad3 and Smad2 protein levels were not affected. As expected, AktVIII fully inhibits Akt phosphorylation.

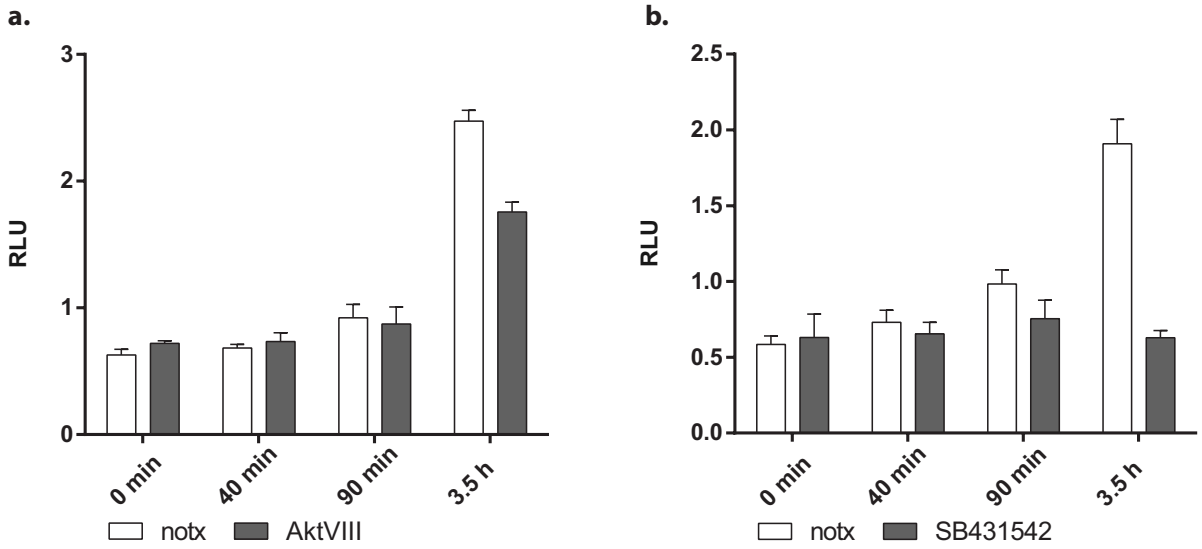

Figure 10. AktVIII inhibits expression of a Smad luciferase reporter. Early gene expression under the transcriptional control of activated Smads was evaluated using a Smad-binding element (SBE) luciferase reporter in HaCaT cells. Luciferase readout, quantified by luminescence, was observed as early as 3.5 h in response to TGF-β. Reporter expression was a) partially inhibited by AktVIII and b) fully blocked by SB431542.

less than 4 hours following TGF-β treatment, and AktVIII partially blocked activation of all three genes while SB431542 inhibited transcription in response to TGF-β (Figure 11).

These data support a model in which TGF-β receptor upregulation increases Smad2- and Smad3 activation and Smad-mediated gene expression, thereby amplifying the cell's responsiveness to TGF-β. Inhibition of TGF-β response in the presence of AktVIII is consistent with the notion that receptor upregulation requires Akt activation.

2.6 Inhibition of ligand-induced cell surface receptor by AktVIII is due to impaired receptor cycling

To study whether receptor internalization was affected by inhibition of Akt signaling, I measured receptor endocytosis by pulse-labeling cell surface proteins with a reversible biotinylation reagent. After the cells were incubated under growth conditions to allow endocytosis, biotin label was removed from proteins remaining at the cell surface using a reducing buffer, while internalized proteins were protected from stripping. Thus, proteins that retained the biotin tag, as detected by NeutrAvidin pulldown, represent the endocytosed fraction (Figure 12a).

I observed an accumulation of intracellular receptor after 20 minutes, which was amplified in the presence of TGF-β. Interestingly, adding AktVIII, after biotinylation but prior to exposing the cells to conditions permissive to endocytosis, inhibited both the basal rate of receptor internalization as well as the increase in receptor internalization seen in response to TGF-β. The rate of internalization of transferrin receptor was not affected by either TGF-β treatment or AktVIII, suggesting specific regulation of TGF-β receptor cycling rather than an overall effect on endocytosis (Figure 12b).

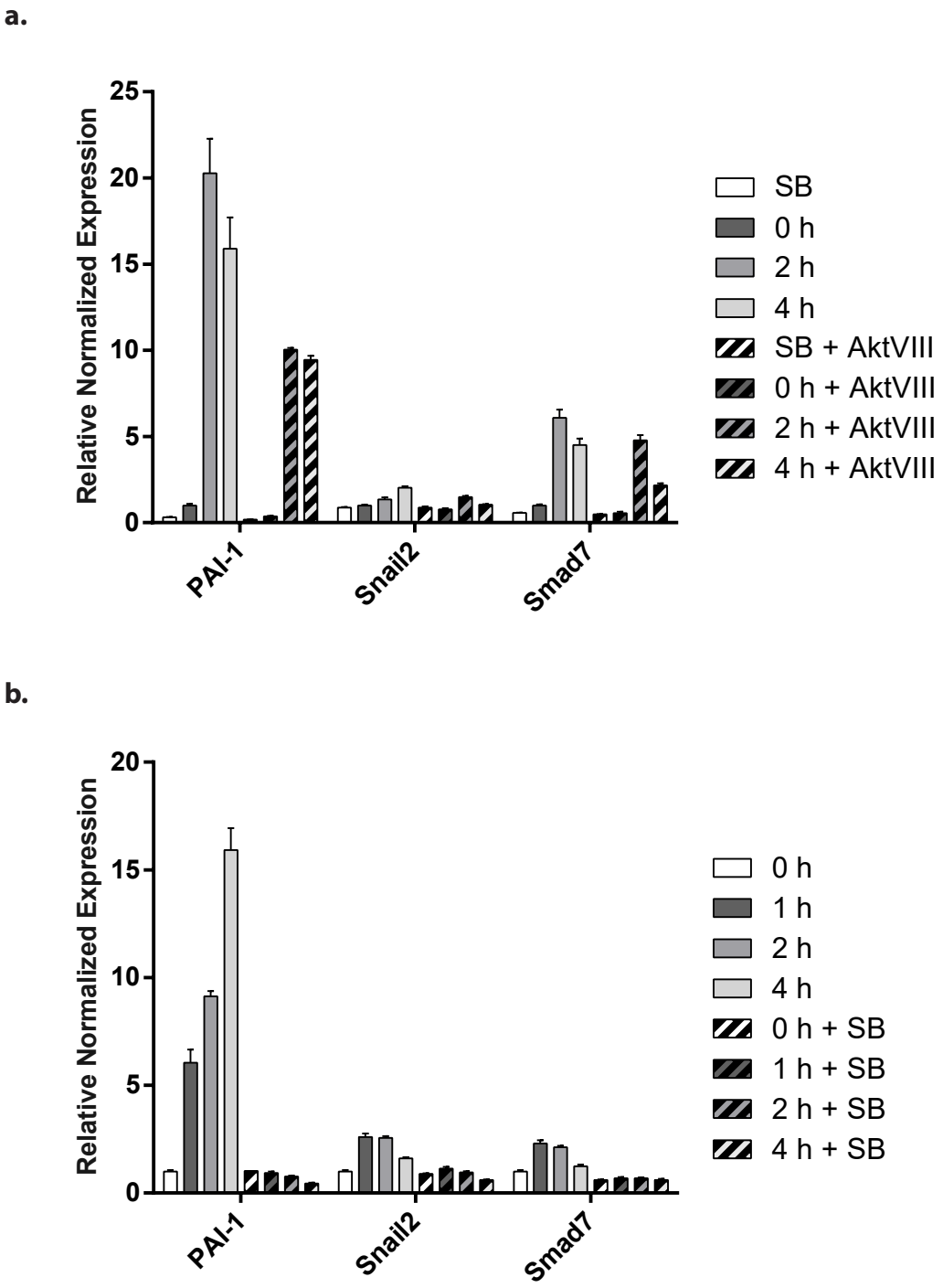

Figure 11. AktVIII partially blocks expression of TGF-β responsive genes. Early expression of *PAI-1*, *Snail2*, and *Smad7*, genes known to be directly regulated by TGF-β-activated Smads, was quantified by qRT-PCR in HaCaT cells treated with TGF-β and AktVIII or TGF-β and SB431542. Normalized expression of all three genes was a) partially inhibited by AktVIII and b) fully blocked by SB431542.

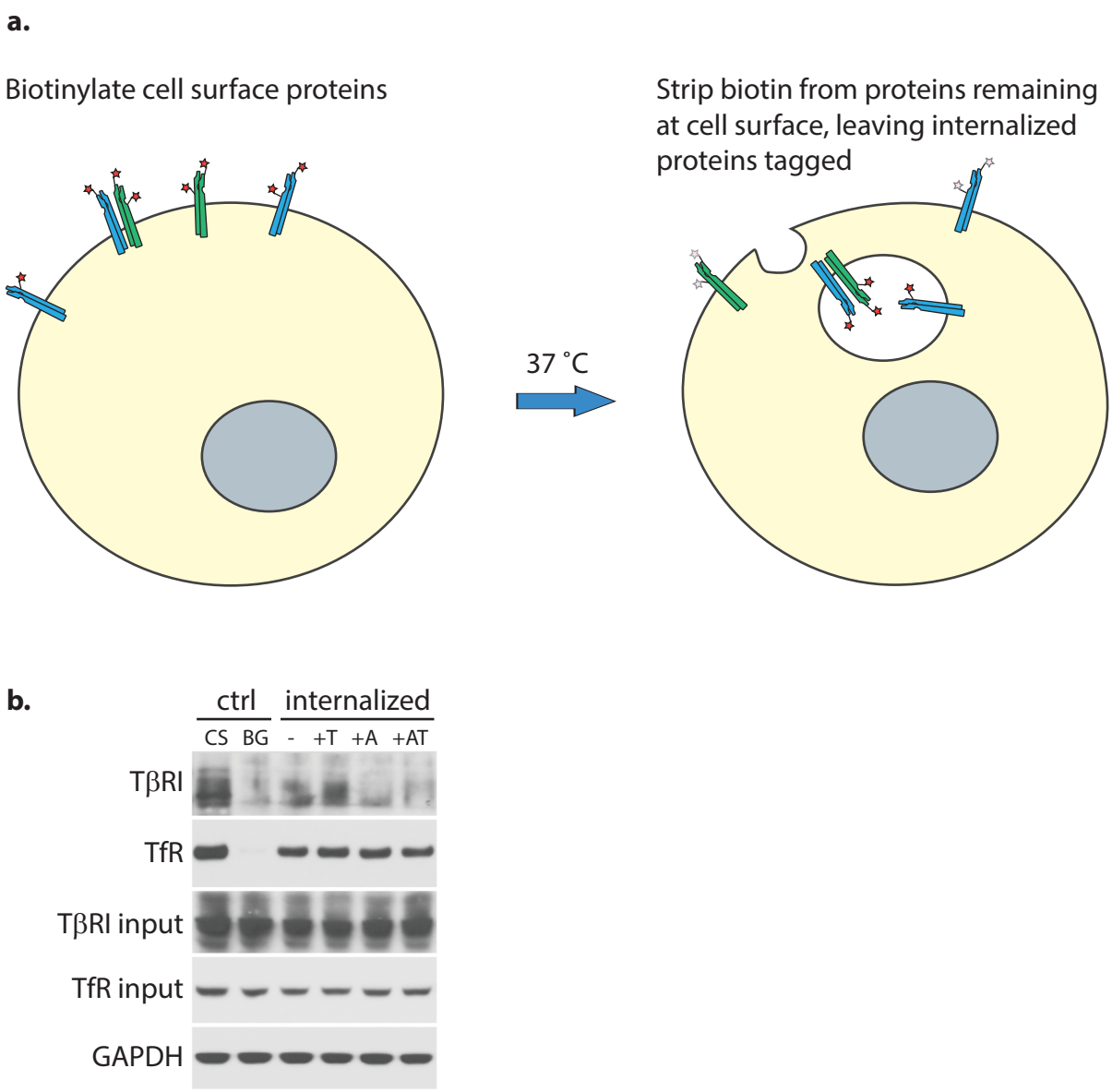

Figure 12. AktVIII inhibits ligand-responsive internalization of TGF- receptors. TGF-β increases rate of receptor trafficking between the cell surface and intracellular vessicles. a) Receptor endocytosis in HaCaT cells was measured using a cleavable biotinylation reagent to selectively tag cell surface proteins. Endocytosis occurred when cells were returned to growth media at 37 ˚C for 20 minutes. Cells were then washed with a reducing buffer to strip the biotin tag from proteins remaining at the cell surface. Internalized tagged proteins protected from stripping buffer were quantified to reflect rate of endocytosis. b) Compared with total cell surface labeled protein (CS) controls and background (BG), stimulation with TGF-β (T) caused an increase in the basal rate of receptor internalization (-). Addition of AktVIII after biotinylation but before returning cells to warm growth media had an inhibitory effect on receptor internalization, both in samples treated with Akt alone (+A) and with TGF-β (+AT).

These results may explain the partial, rather than complete, reduction of TGF-β-induced receptor presentation upon Akt inhibition. A scenario in which AktVIII treatment blocks the phospho-Akt-dependent increase in receptor translocation to the cell surface but also prevents receptor internalization would result in retention of cell surface receptors and thus partially offset the inhibition of the TGF-β receptor response.

2.7 BMP-4 regulates cells surface levels of TGF-β receptor

The interaction between BMP and TGF-β signaling pathways has been previously observed; however, the mechanism by which BMPs activate TGF-β signaling is not well understood. Regulation of cell surface receptor levels occurs within minutes of exposure to TGF-β, and thus represents a very early step in TGF-β signal transduction, raising the question of whether receptor upregulation could be a node of crosstalk between TGF-β and BMP signaling pathways. To address this, I treated cells with BMP-4 and assessed TGF-β receptor induction by cell surface biotinylation. I also evaluated activation of TGF-β-responsive Smad signaling by measuring phospho-Smad2 and -Smad3, and quantifying expression of TGF-β-responsive genes.

I observed an increase in cell surface TβRI and TβRII within 60 minutes of treatment with BMP-4 (Figure 13). This induction was inhibited by AktVIII in a similar manner as in cells treated with TGF-β (Figure 14). I also observed corresponding Smad2 and Smad3 phosphorylation, although at lower levels and with slower kinetics than normally observed in response to TGF-β. Activation of Smad2 and Smad3 was inhibited by SB431542, which blocks the TβRI kinase and does not affect the BMP type I receptors, thus implicating TβRI kinase in BMP-induced phosphorylation of Smad2 and Smad3 (Figure 15). These findings are consistent

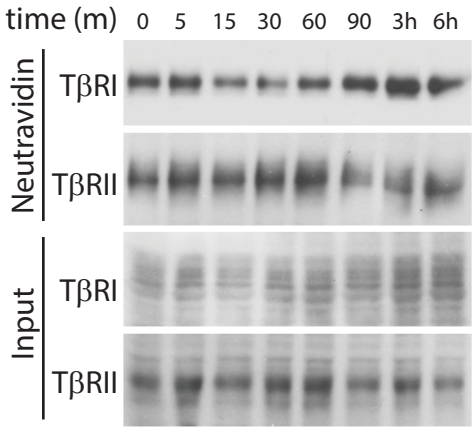

Figure 13. BMP regulates cell surface levels of TGF-β receptors. HaCaT cells were treated with 5 ng/mL BMP-4 and subjected to cell surface biotinylation analysis. Addition of BMP-4 resulted in an initial decrease followed by an increase in available type I TGF-β receptor at the cell surface. Total TβRI and TβRII protein levels are not affected.

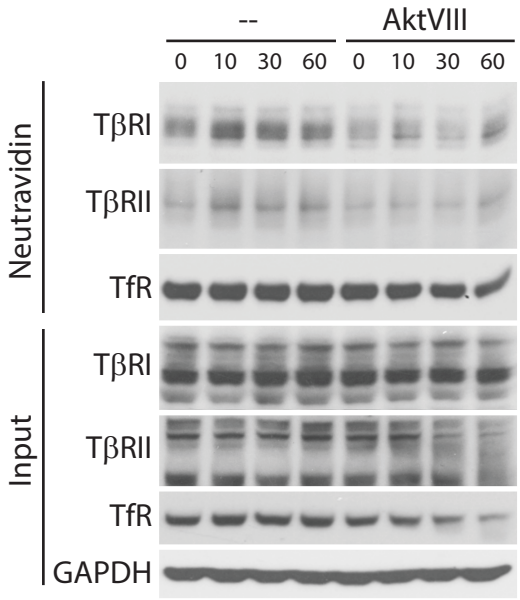

Figure 14. AktVIII downregulates induction of cell surface TGF-β receptors by BMP. Prior to BMP-4 stimulation and cell surface biotinylation analysis, HaCaT cells were treated with 5 μM AktVIII for 30 minutes. The initial increase in both TβRI and TβRII following stimulation with BMP-4 was inhibited when cells were pre-treated with AktVIII. Total TGF-β receptor protein levels were not affected by addition of BMP or AktVIII.

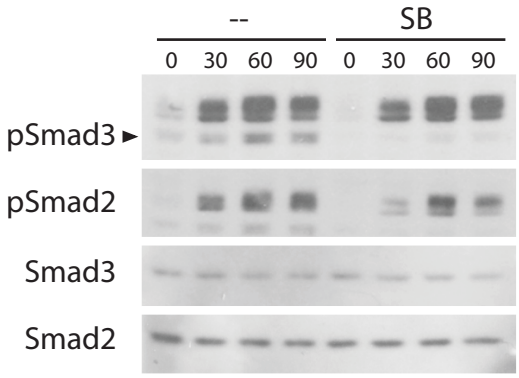

Figure 15. BMP stimulation activates the TGF-β effectors Smad2 and Smad3. HaCaT cells were treated with the TβRI kinase inhibitor SB431542 for 1 hour prior to addition of 5 ng/mL BMP-4. Phosphorylation of Smad2 and Smad3 was observed in response to BMP-4, while total Smad2 and Smad3 protein levels were unchanged. SB431542 fully blocked Smad3 activation and partially inhibited phospho-Smad2 response to BMP-4, implicating TGF-β receptors in activation of TGF-β signaling by BMP-4.

with BMP mediating activation of Smad2 and Smad3 through upregulation of cell surface TGF-β receptors.

Looking further downstream in the TGF-β signaling pathway, I performed qRT-PCR targeting the genes encoding PAI-1, Slug, and Smad7, which are known to be transcriptionally activated by Smad2 and/or Smad3, and not by BMP-activated Smad1 and/or Smad5. All three genes were upregulated in response to BMP-4, and this was partially inhibited in cells treated with SB431542, consistent with activation of TGF-β receptor in response to BMP. In comparison, induction of genes encoding Id1 and Id3, which are directly activated by BMP signaling through Smad1 and/or Smad5, was not significantly affected by SB431542. Smad6, whose expression can be activated in response to both BMP and TGF-β, was inhibited in the presence of SB431542 (Figure 16).

Inhibition of phospho-Akt using AktVIII also attenuated BMP-induced expression of TGF-β-responsive genes, in agreement with TGF-β signal amplification through receptor upregulation in response to TGF-β. Expression of Smad6, Id1, and Id3 was partially repressed in the presence of AktVIII as well. However, both Id1 and Id3 have been reported to be regulated by Akt signaling (Figure 17).

Taken together, the data support a model of amplified TGF-β responsiveness as a result of receptor upregulation in cells treated with BMP. In conjunction with autocrine signaling, BMP-induced sensitization of cells to TGF-β could lead to activation of Smad2 and/or Smad3, and subsequent gene expression changes associated with TGF-β signaling.

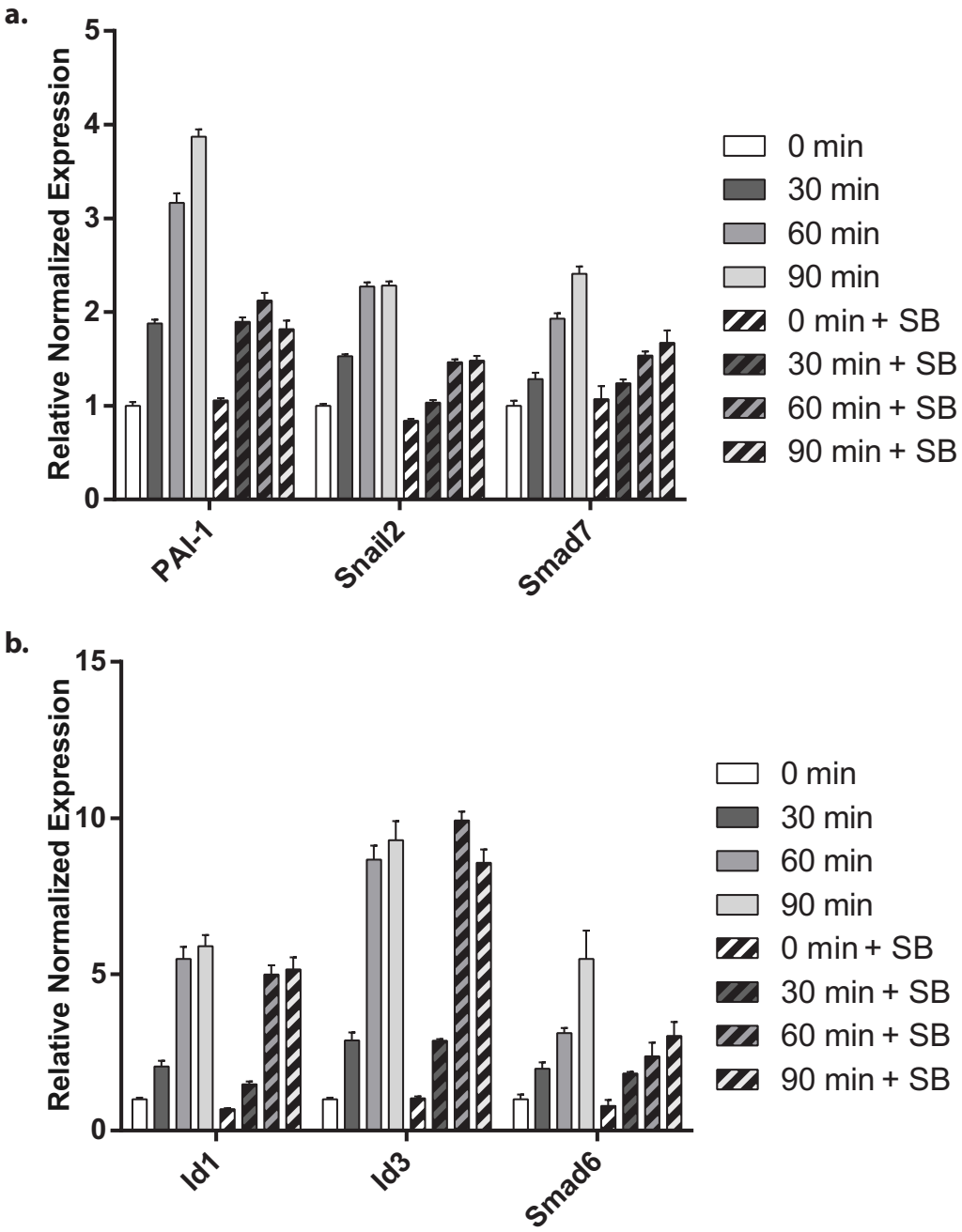

Figure 16. BMP-induced expression of genes known to be regulated by TGF-β is inhibited by SB431542. a) BMP-4 treatment of HaCaT cells resulted in expression of *PAI-1*, *Snail2*, and *Smad7*, genes known to be regulated by TGF-β through Smads as quantified by qRT-PCR. The TβRI kinase inhibitor SB431542 partially blocked this induction, suggesting that TGF-β receptor activation is involved in transcription of TGF-β-regulated genes in response to BMP. b) In contrast, induction of *Id1* and *Id3*, whose expression is regulated by BMP-responsive Smad1/5 but is not known to be controlled by TGF-β-responsive Smad2/3, was not inhibited by SB431542. *Smad6*, which has been reported to be regulated by both BMP and TGF-β signaling, was induced by BMP and its expression was attenuated by SB431542.

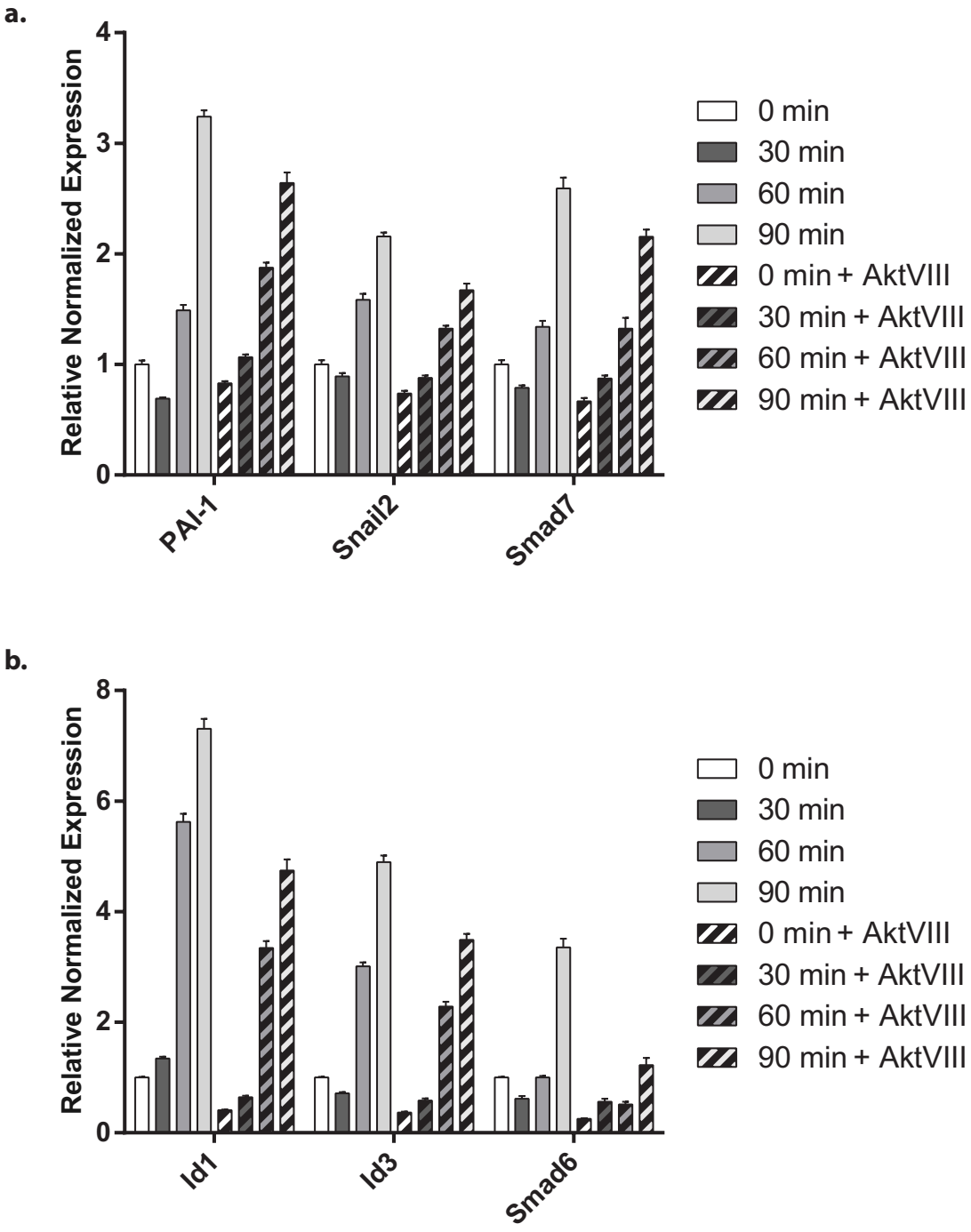

Figure 17. AktVIII partially blocks induction of TGF-β-regulated genes in response to BMP. mRNA transcripts were quantified by qRT-PCR in HaCaT cells treated with 5 ng/mL BMP-4 for the time specified. AktVIII was added 30 min prior to BMP stimulation. a) BMP-mediated expression *PAI-1*, *Snail2*, and *Smad7*, genes known to be directly regulated by TGF-β-activated Smad2 and Smad3, was partially inhibited by AktVIII. b) Expression of *Id1*, *Id3*, and *Smad6* was also inhibited by treatment with AktVIII.

Chapter 3. Discussion

Post-translational modifications and internalization of transmembrane receptor proteins have been well documented to control and define the cellular response to extracellular ligands. My findings reveal a novel regulatory mechanism in which an extracellular signaling protein stimulates mobilization of its own transmembrane receptor to the cell surface. Specifically, my results demonstrate a rapid increase in cell surface levels of TGF-β receptors in response to TGF-β, which requires the TβRI kinase activity and Akt phosphorylation, and this response serves to amplify the sensitivity of cells to TGF-β. Additionally, I found that this upregulation of TGF-b responsiveness can be activated by BMP. Of note is the discovery that while TGF-β signals an overall increase of cell surface TGF-β receptor abundance, it also mediates increased endocytosis of TGF-β receptors, suggesting an increased rate of TGF-β receptor cycling between endosomes and the cell membrane.

3.1 Increased receptor presentation and endocytic cycling in response to TGF-β

In the case of receptor tyrosine kinases, regulation of endocytosis is seen to play a significant role in determining the amplitude and nature of cell response. Ligand-induced internalization of EGF, insulin, VEGF, PDGF receptors is necessary for appropriate signaling, with disruption of endocytosis causing alteration or attenuation of response in each of these pathways.[3] Likewise, abnormal routing of RTKs contributes to disease progression. For example, in acute myeloid leukemia, internal tandem duplications in the transmembrane domain of the hematopoietic RTK Flt3 leads to prolonged cytosolic residence and, consequently, to constitutive activation of Flt3.[88] Hyperphosphorylation of EGFRvIII, a deletion mutant occurring in glioblastomas, attenuates

receptor internalization and appropriate sorting to proteasomal compartments, resulting in oncogenic signaling.[89,90]

Much less is known with regards to spatial regulation of TGF-β receptors. Like the RTKs, the TGF-β receptors remain catalytically active in endocytic compartments, where colocalization with downstream Smad and non-Smad effector proteins mediates downstream signaling.[17,22] Moreover, endosomal sorting plays a determining role in the nature of the TGF-β response, with clathrin-associated vesicles favoring Smad activation, while non-Smad signaling and receptor degradation are associated with caveolar endosomes.[17]

My data revealed an increased net abundance of TGF-β signaling at the cell surface, which accordingly resulted in amplified sensitivity to TGF-β. However, my results demonstrate that TGF-β stimulated an increase in TGF-β receptor endocytosis as well, implying a generally increased rate of receptor recycling. TGF-β receptors are constitutively endocytosed and recycled, providing signaling specificity through directed compartmentalization with downstream signaling effectors and proteins that catalyze post-translational modifications on the TGF-β receptors. Given that both Smad and non-Smad TGF-β signaling initiate with ligand binding at the cell surface and proceed in endocytic vesicles, one might surmise that increased receptor presentation allows for a greater initial response by permitting increased ligand binding, and that a concurrent faster rate of TGF-β receptor recycling results in further signal amplification. Thus, while the ligand-induced upregulation of transmembrane receptors decreases the threshold of signal activation, the increased rate of receptor recycling not only confers greater sensitivity to ligand, but most likely allows finely tuned responsiveness to regulatory inputs as well. Additionally, TGF-β receptor-expressing cells often secrete TGF-β and are competent for autocrine TGF-β signaling, allowing for receptor upregulation to mediate

TGF-β signaling in the absence of added ligand, as is seen in activation of TGF-β response through increased autocrine TGF-β signaling in the presence of insulin or high glucose conditions.[77,91] In view of this, I speculated that transport of the receptor to the cell surface may provide a means of integration of TGF-β with other signaling pathways, and therefore investigated the relevance of receptor cell surface regulation in crosstalk between BMP and TGF-β.

3.2 BMP induces increased sensitivity to TGF-β

My findings revealed a previously undescribed regulation of TGF-β receptor, and therefore the TGF-β response, through modulation of cell surface receptor presentation in response to BMP. I found that stimulation of cells with BMP-4 resulted in upregulation of the cell surface TGF-β receptors and, subsequently, activation of TGF-β-responsive Smads and expression of genes normally induced by TGF-β. Additionally, inhibition of Akt activation abrogated the upregulation of TGF-β receptor. Moreover, blocking the TβRI kinase prevented activation of Smad2 and Smad3 in response to BMP and partially inhibited the expression of genes thought to be regulated by TGF-β but not genes controlled directly by BMP signaling. These results support the notion that BMPs activate the TGF-β response through upregulation of TGF-β receptors, thereby increasing sensitivity to autocrine TGF-β signaling. This finding complements the previously observed interplay between TGF-β and BMP signaling in developmental and disease contexts.

During development and in somatic tissue homeostasis, BMP and TGF-β have been observed to exhibit antagonistic effects in some instances while acting synergistically in others, depending on cell type and environment. For example, BMP-7 opposes the effects of TGF-β

signaling in a mouse model of kidney disease and in collagen production by pulmonary myofibroblasts.[92,93] In endochondral bone formation, BMPs are generally seen as promoting differentiation during chondrogenesis and osteogenesis, while TGF-β is thought to inhibit the osteogenic response to BMP.[94-96] Additionally, the balance between TGF-β and BMP regulates the homeostatic cycle of regeneration, quiescence, and degeneration of the hair follicle. In the transition to the hair follicle's growth phase, production of TGF-β2 in the dermal papillae promotes hair follicle stem cell activation by inhibiting response to BMP, which is thought to negatively regulate stem cell activation for tissue regeneration.[97]

However, synergistic effects of TGF-β on BMP signaling have been reported as well, with TGF-β inducing Smad1 activation in chondrocyte, myoblast, keratinocyte, fibroblast, and liver carcinoma cell models.[78,79] Additionally, BMP-4, TGF-β, and estrogen receptor were found to act in concert at the promoter of the gene encoding prolactin.[81] In a cell culture model of insulin-positive cell differentiation, acquisition of β-cell characteristics in response to exendin-4 (glucagon-like peptide 1) was found to be mediated by TGF-β through Smad2 and Smad3.[98] Furthermore, inhibition of BMP ligands prevented exendin-4-mediated upregulation of Smad3 and as a result blocked insulin-induced differentiation.[80] These findings support a scenario in which exendin-4 promotes differentiation of β-cells through BMP signaling, which then activates TGF-β-associated Smad3, that may be mechanistically explained by my results described in this section.

In this study, I presented a novel mechanism for activation of TGF-β response by BMP, which may shed light on the closely intertwined nature of BMP and TGF-β signaling. During development, TGF-β is often seen as providing permissive environment for cell fate specification, while BMPs generally initiate differentiation processes. In this context, the

activation of TGF-β responses by BMPs could allow BMPs to signal permissiveness to cell differentiation, and enable cell fate decisions.

3.3 Akt signaling regulates TGF-β responsiveness

In agreement with the notion that regulation of TGF-β receptor translocation serves as a potential point of cross-regulation of TGF-β response by other signaling proteins, insulin and high-glucose were shown to mobilize intracellular TGF-β receptors to the cell surface. The work of *Budi et al* defined Akt as a mediator of rapid translocation of cytosolic TGF-β to the cell surface, thus promoting increased responsiveness and autocrine TGF-β signaling.[77] In fact, those findings, in combination with the knowledge that TGF-β induces Akt activation, inspired the initial hypothesis for my research presented in this section.

There are many additional examples of crosstalk between the PI3K-Akt and TGF-β signaling pathways. Direct interaction of Akt with Smad3 inhibits TGF-β response, independently of Akt kinase activity, by preventing Smad3 nuclear translocation and regulation of transcription.[58,99] More recently, expression of pluripotency genes mediated by Smad2 and Smad3 was shown to be regulated by the level of PI3K-Akt signaling. In the presence of Akt activation, low Erk MAPK signaling was permissive for cooperative regulation of gene expression by Smad2 and/or Smad3, and Wnt. Under conditions of low Akt signaling, Erk-dependent inactivation of Gsk3β prevented this Smad-Wnt coregulation from promoting pluripotency, thus illustrating a scenario in which the Akt phosphorylation status determines whether Smad activation drives pluripotency or differentiation.[100,101] Akt activation was also found to induce Smad2 and Smad3 activation and to direct the cytostatic effects of Smad activation through the tuberous sclerosis protein TSC1.[102]

My findings reveal that in addition to promoting accumulation of cell surface TGF-β receptors, Akt activation also contributes to TGF-β receptor internalization, leading to an overall increase in endosomal recycling of TβRI. Together, my study and those mentioned above illustrate the complex interaction between PI3K-Akt and TGF-β signaling. Akt is normally seen as a cell survival factor, stimulating cell growth and proliferation, whereas TGF-β/Smad signaling is known to function as a pro-metastatic driver of EMT.[103,104] Therefore, understanding the interaction between TGF-β and Akt signaling is of potential clinical importance with regards to cancer progression and metastasis. Accordingly, Akt was found to upregulate the levels of TβRI, effecting TGF-β signaling in multiple breast cancer cell models, through increased expression of a deubiquitylase targeting TβRI.[105] In addition, increased expression of TβRII mediated by Akt-activated Twist-1 was shown to promote tumor metastasis in a mouse injection model.[106]

3.4 Conclusion

The data presented in this section provide a novel view of TGF-β receptor regulation, in which mobilization of intracellular stores of TGF-β provide an efficient mechanism regulating sensitivity of cells to TGF-β ligand. The induction of cell surface TGF-β receptors functions to enhance the TGF-β response shortly after initiation of signaling, serving as a positive feedback mechanism whose biological function may be to poise the cell for rapid response to external signals. Importantly, regulation of cell surface TGF-β receptor abundance describes a node of regulation by other signaling molecules such as BMP and Akt, providing precise response coordination of multiple signaling pathways. It is worth noting that transcription regulation by Smads, which bind weakly to DNA, requires interaction with cooperating transcription factors

with higher DNA or chromatin binding affinity, thus positioning the TGF-β-induced Smad response as "parasitic" upon other signal pathways. Likewise, it appears that although TGF-β controls cell surface presentation of its own receptor, an interesting and unusual phenomenon in itself, the importance of this regulatory mechanism is all the more apparent as a means of integrating TGF-β with other signaling modalities. So far, my findings and a recent study demonstrating insulin-induced TGF-β receptor upregulation are the only two reports of amplification of TGF-β signaling through receptor transport to the membrane, despite establishing an important new mode of TGF-β signaling regulation and crosstalk. Thus I anticipate cell surface regulation of TGF-β to be an exciting field of future research.

MATERIALS AND METHODS

Cell culture and transfection

Cells were cultured in a humidified incubator at 37 °C and 5% CO_2. HaCaT cells were cultured in Dulbecco's modified Eagle's medium (DMEM) with 4.5 mM glucose and 10% fetal bovine serum (FBS). A549 cells were maintained in Rosewell Park Memorial Institute (RPMI) 1640 medium with 10% FBS. For assays involving TGF-β treatment, cells were rinsed twice in phosphate buffered saline (PBS) then serum-starved for 6 hours prior to addition of TGF-β unless otherwise specified. HaCaT cells were starved in serum-free DMEM with 4.5 mM glucose and A549 in Small Airway Epithelial Cell Basal Medium (SABM) (Lonza). Transfections were performed in Opti-MEM minimal media (Thermo-Fisher) using TurboFect (Thermo Fisher) in A549 cells or Lipofectamine 2000 (Life Technologies) in HaCaT cells, as specified by the manufacturers.

Growth factors, inhibitors, and antibodies

TGF-β1 and BMP-4 purchased from HumanZyme were used at concentrations of 0.25 ng/mL and 5 ng/mL, respectively. The phospho-Akt inhibitor AktVIII (EMD Millipore) and the TβRI kinase inhibitor SB431542 (Sigma) were used at a concentration of 5 μM. AktVIII and SB431542 were added to cells 20 minutes and 2 hour prior to addition of TGF-β, respectively. For immunostaining, I used rabbit anti-TβRII and mouse anti-transferrin receptor purchased from Santa Cruz Biotechnology. Rabbit anti-TβRI and anti-phospho-Smad3 were from Abcam. Rabbit anti-Smad2, anti-phospho-Smad2, anti-Smad3, anti-phospho-Akt (Ser473), anti-phospho-Akt (Thr308), were from Cell Signaling.

Cell lysis, immunoprecipitation, and western blotting

For TGF-β stimulation assays without immunoprecipitation, cells were rinsed twice with PBS and lysed at in ice cold RIPA buffer [10 mM Tris-HCl pH 7.6, 1 mM EDTA, 1% NP-40, 0.25% sodium deoxycholate, 0.1% SDS, 150 mM NaCl, 10 mM NaF, 1 mM Na_3VO_4, and cOmplete Protease Inhibitor cocktail (Roche)]. Lysates were cleared by centrifugation for 10 minutes at 14,000 rcf at 4 °C and protein concentration was quantified using Protein Assay Dye Reagent (Bio-Rad). Total protein was normalized between samples before denaturing with LDS sample buffer (Invitrogen) at 95 °C for 2 minutes before being subjected to SDS-PAGE and immunoblotting. For immunoprecipitation of endogenous TβRI, cells were washed twice following appropriate treatment and harvested by scraping in pre-chilled lysis buffer containing 25 mM Tris-HCl pH 7.6, 150 mM NaCl, 1 mM EDTA, 0.75% Triton X-100, 7% glycerol, 10 mM NaF, 1 mM Na_3VO_4, and cOmplete Protease Inhibitor cocktail (Roche) and incubated for 10 minutes on ice. Lysates were cleared as described above, then immunoprecipitated with anti-TβRI overnight. The antibody-lysate solution centrifuged for 10 minutes at 14,000 rcf and incubated with Protein G Sepharose beads (GE Healthcare) for 2 hours. The beads were washed 3 times for 10 minutes with lysis buffer, eluted with LDS sample buffer (Invitrogen), and subjected to SDS-PAGE and immunoblotting. All steps until elution were performed at 4 °C.

Cell surface biotinylation assay

Cells were washed twice with cold PBS and incubated for 20 minutes with EZ Link Sulfo-NHS-LC-Biotin (Thermo Scientific) at a concentration of 0.25 mg/mL in PBS. The biotinylation reaction was quenched by washing the cells twice with PBS and incubating for 15 minutes with 0.1 M glycine in PBS. Cells were then harvested by scraping in a mild lysis buffer (MLB)

containing 20 mM Tris pH 7.6, 200 mM NaCl, 1% NP-40, 10 mM NaF, 1 mM Na_3VO_4, and cOmplete Protease Inhibitor cocktail (Roche), and incubated for 10 minutes. Lysates were cleared by centrifugation at 14,000 rcf for 10 minutes then incubated with NeutrAvidin beads (Thermo Scientific) overnight. Beads were washed three times in MLB, eluted with LDS sample buffer (Invitrogen), and subjected to SDS-PAGE and immunoblotting. All steps until elution were performed at 4 °C.

Protein endocytosis assay

Following serum starvation, cells were washed twice with cold PBS and incubated for 20 minutes with 0.4 mg/mL EZ Link Sulfo-NHS-SS-Biotin (Thermo Scientific) in PBS, and quenched washing twice with PBS and incubating for 15 minutes with 0.1 M glycine in PBS at 4 °C. After rinsing with pre-warmed PBS, cells were returned to warm serum free media containing growth factors and inhibitors, and incubated for 20 minutes at 37 °C. Endocytosis was stopped by washing twice with cold PBS on ice, and biotin was stripped from proteins at the extracellular surface by incubating twice for 15 minutes with ice-cold reducing buffer containing 50 mM reduced glutathione, 75 mM NaCl, 75 mM NaOH, and 10% fetal bovine serum, followed by 30 minutes incubation with a solution of 50 mM sodium iodoacetamide and 1% BSA in PBS. Cells were then harvested by scraping in ice-cold MLB buffer [20 mM Tris pH 7.6, 200 mM NaCl, 1% NP-40, 10 mM NaF, 1 mM Na_3VO_4, and cOmplete Protease Inhibitor cocktail (Roche)]. Lysates were cleared by centrifugation at 14,000 rcf for 10 minutes then incubated with NeutrAvidin beads (Thermo Scientific) overnight. Beads were washed three times in MLB, eluted with LDS sample buffer (Invitrogen), and subjected to SDS-PAGE and immunoblotting.

Luciferase reporter assay

Cells were transfected with the plasmid SBE-Luc, which contains the firefly luciferase gene under control of four repeated Smad binding elements (SBE), and a Renilla luciferase reporter downstream of the thymidine kinase promoter (Promega), 20 hours prior to serum starvation. After stimulation with the appropriate growth factors and inhibitors, cells were rinsed with PBS, and after aspirating liquid from the monolayer, frozen at -80 °C and thawed on ice before lysis. Relative luciferase activity was quantified using Dual Luciferase Assay System (Promega) according to the manufacturer's protocol. Readout was normalized to Renilla luciferase as an internal control.

RNA preparation and quantitative real-time PCR

RNA was purified from cells using the RNEasy Mini Kit (QIAGEN). Total RNA (1 μg per sample) was used as a template for reverse transcription with iScript (Bio-Rad) according to the manufacturer's protocol. *PAI-1, Snail2, Smad7, Smad6, Id1,* and *Id3* mRNA were quantified by RT-PCR using IQ SYBR-Green Supermix (Bio-Rad) and normalized against *RPL19* mRNA. The primers used were as follows:

PAI-1	5′-GGCTGACTTCACGAGTCTTTCA-3′ (forward)
	5′-ATGCGGGCTGAGACTATGACA-3′ (reverse)
Snail2	5′-TGTGACAAGGAATATGTGAGCC-3′ (forward)
	5′-TGAGCCCTCAGATTTGACCTG-3′ (reverse)
Smad7	5′-TGCTGTGAATCTTACGGGAAG-3′ (forward)
	5′-AATCCATCGGGGTATCTGGAG-3′ (reverse)

Smad6	5′-GCTGCAACCCCTACCACTTC-3′ (forward)
	5′-AGACAATGTGGAATCGGACAG-3′ (reverse)
Id1	5′-CTGCTCTACGACATGAACGG-3′ (forward)
	5′-GAAGGTCCCTGATGTAGTCGAT-3′ (reverse)
Id3	5′-CATTCGTCTACATTCTCGACCTG-3′ (forward)
	5′-TCCTTTTGTCGTTGGAGATGAC-3′ (reverse)
RPL19	5′-ATGTATCACAGCCTGTACCTG-3′ (forward)
	5′-TTCTTGGTCTCTTCCTCCTTG-3′ (reverse)

REFERENCES

1. Lemmon, M.A. & Schlessinger, J. Cell signaling by receptor tyrosine kinases. *Cell* **141**, 1117-34 (2010).

2. Tomas, A., Futter, C.E. & Eden, E.R. EGF receptor trafficking: consequences for signaling and cancer. *Trends Cell Biol* **24**, 26-34 (2014).

3. Casaletto, J.B. & McClatchey, A.I. Spatial regulation of receptor tyrosine kinases in development and cancer. *Nat Rev Cancer* **12**, 387-400 (2012).

4. Lai, W.H., Cameron, P.H., Doherty, J.J., 2nd, Posner, B.I. & Bergeron, J.J. Ligand-mediated autophosphorylation activity of the epidermal growth factor receptor during internalization. *J Cell Biol* **109**, 2751-60 (1989).

5. Cohen, S. & Fava, R.A. Internalization of functional epidermal growth factor:receptor/kinase complexes in A-431 cells. *J Biol Chem* **260**, 12351-8 (1985).

6. Wang, Z., Tung, P.S. & Moran, M.F. Association of p120 ras GAP with endocytic components and colocalization with epidermal growth factor (EGF) receptor in response to EGF stimulation. *Cell Growth Differ* **7**, 123-33 (1996).

7. Fukazawa, T., Miyake, S., Band, V. & Band, H. Tyrosine phosphorylation of Cbl upon epidermal growth factor (EGF) stimulation and its association with EGF receptor and downstream signaling proteins. *J Biol Chem* **271**, 14554-9 (1996).

8. Levkowitz, G. et al. c-Cbl/Sli-1 regulates endocytic sorting and ubiquitination of the epidermal growth factor receptor. *Genes Dev* **12**, 3663-74 (1998).

9. Vieira, A.V., Lamaze, C. & Schmid, S.L. Control of EGF receptor signaling by clathrin-mediated endocytosis. *Science* **274**, 2086-9 (1996).

10. Maudsley, S. et al. The beta(2)-adrenergic receptor mediates extracellular signal-regulated kinase activation via assembly of a multi-receptor complex with the epidermal growth factor receptor. *J Biol Chem* **275**, 9572-80 (2000).

11. Burgess, J.W. et al. Decrease in beta-subunit phosphotyrosine correlates with internalization and activation of the endosomal insulin receptor kinase. *J Biol Chem* **267**, 10077-86 (1992).

12. Ceresa, B.P., Kao, A.W., Santeler, S.R. & Pessin, J.E. Inhibition of clathrin-mediated endocytosis selectively attenuates specific insulin receptor signal transduction pathways. *Mol Cell Biol* **18**, 3862-70 (1998).

13. Lampugnani, M.G., Orsenigo, F., Gagliani, M.C., Tacchetti, C. & Dejana, E. Vascular endothelial cadherin controls VEGFR-2 internalization and signaling from intracellular compartments. *J Cell Biol* **174**, 593-604 (2006).

14. Wang, Y. et al. Ephrin-B2 controls VEGF-induced angiogenesis and lymphangiogenesis. *Nature* **465**, 483-6 (2010).

15. Sawamiphak, S. et al. Ephrin-B2 regulates VEGFR2 function in developmental and tumour angiogenesis. *Nature* **465**, 487-91 (2010).

16. Wang, Y., Pennock, S.D., Chen, X., Kazlauskas, A. & Wang, Z. Platelet-derived growth factor receptor-mediated signal transduction from endosomes. *J Biol Chem* **279**, 8038-46 (2004).

17. Budi, E.H., Duan, D. & Derynck, R. Transforming Growth Factor-beta Receptors and Smads: Regulatory Complexity and Functional Versatility. *Trends Cell Biol* **27**, 658-672 (2017).

18. Yao, D., Ehrlich, M., Henis, Y.I. & Leof, E.B. Transforming growth factor-beta receptors interact with AP2 by direct binding to beta2 subunit. *Mol Biol Cell* **13**, 4001-12 (2002).

19. Shapira, K.E. et al. Dab2 inhibits the cholesterol-dependent activation of JNK by TGF-beta. *Biomed Res Int* **25**, 1620-8 (2014).

20. Zuo, W. & Chen, Y.G. Specific activation of mitogen-activated protein kinase by transforming growth factor-beta receptors in lipid rafts is required for epithelial cell plasticity. *Mol Biol Cell* **20**, 1020-9 (2009).

21. Meyer, C., Liu, Y., Kaul, A., Peipe, I. & Dooley, S. Caveolin-1 abrogates TGF-beta mediated hepatocyte apoptosis. *Cell Death Dis* **4**, e466 (2013).

22. Le Roy, C. & Wrana, J.L. Clathrin- and non-clathrin-mediated endocytic regulation of cell signalling. *Nat Rev Mol Cell Biol* **6**, 112-26 (2005).

23. Di Guglielmo, G.M., Le Roy, C., Goodfellow, A.F. & Wrana, J.L. Distinct endocytic pathways regulate TGF-beta receptor signalling and turnover. *Nat Cell Biol* **5**, 410-21 (2003).

24. Bertelsen, V. et al. A chimeric pre-ubiquitinated EGF receptor is constitutively endocytosed in a clathrin-dependent, but kinase-independent manner. *Traffic* **12**, 507-20 (2011).

25. Madshus, I.H. & Stang, E. Internalization and intracellular sorting of the EGF receptor: a model for understanding the mechanisms of receptor trafficking. *J Cell Sci* **122**, 3433-9 (2009).

26. Lonardo, F. et al. The normal erbB-2 product is an atypical receptor-like tyrosine kinase with constitutive activity in the absence of ligand. *New Biol* **2**, 992-1003 (1990).

27. Weiner, D.B., Liu, J., Cohen, J.A., Williams, W.V. & Greene, M.I. A point mutation in the neu oncogene mimics ligand induction of receptor aggregation. *Nature* **339**, 230-1 (1989).

28. Guo, G. et al. Ligand-Independent EGFR Signaling. *Cancer Res* **75**, 3436-41 (2015).

29. Di Fiore, P.P. et al. erbB-2 is a potent oncogene when overexpressed in NIH/3T3 cells. *Science* **237**, 178-82 (1987).

30. Hudziak, R.M., Schlessinger, J. & Ullrich, A. Increased expression of the putative growth factor receptor p185HER2 causes transformation and tumorigenesis of NIH 3T3 cells. *Proc Natl Acad Sci U S A* **84**, 7159-63 (1987).

31. Couet, J., Sargiacomo, M. & Lisanti, M.P. Interaction of a receptor tyrosine kinase, EGF-R, with caveolins. Caveolin binding negatively regulates tyrosine and serine/threonine kinase activities. *J Biol Chem* **272**, 30429-38 (1997).

32. Engelman, J.A. et al. Reciprocal regulation of neu tyrosine kinase activity and caveolin-1 protein expression in vitro and in vivo. Implications for human breast cancer. *J Biol Chem* **273**, 20448-55 (1998).

33. Wang, Y. et al. Hypoxia promotes ligand-independent EGF receptor signaling via hypoxia-inducible factor-mediated upregulation of caveolin-1. *Proc Natl Acad Sci U S A* **109**, 4892-7 (2012).

34. Morikawa, M., Derynck, R. & Miyazono, K. TGF-beta and the TGF-beta Family: Context-Dependent Roles in Cell and Tissue Physiology. *Cold Spring Harb Perspect Biol* **8**(2016).

35. Massague, J. TGFbeta in Cancer. *Cell* **134**, 215-30 (2008).

36. Leask, A. & Abraham, D.J. TGF-beta signaling and the fibrotic response. *Faseb j* **18**, 816-27 (2004).

37. de Caestecker, M. The transforming growth factor-beta superfamily of receptors. *Cytokine Growth Factor Rev* **15**, 1-11 (2004).

38. Massague, J. TGFbeta signalling in context. *Nat Rev Mol Cell Biol* **13**, 616-30 (2012).

39. Massague, J. TGF-beta signaling in development and disease. *FEBS Lett* **586**, 1833 (2012).

40. Dickson, M.C. et al. Defective haematopoiesis and vasculogenesis in transforming growth factor-beta 1 knock out mice. *Development* **121**, 1845-54 (1995).

41. Oshima, M., Oshima, H. & Taketo, M.M. TGF-beta receptor type II deficiency results in defects of yolk sac hematopoiesis and vasculogenesis. *Dev Biol* **179**, 297-302 (1996).

42. Gordon, K.J. & Blobe, G.C. Role of transforming growth factor-beta superfamily signaling pathways in human disease. *Biochim Biophys Acta* **1782**, 197-228 (2008).

43. Blobe, G.C., Schiemann, W.P. & Lodish, H.F. Role of transforming growth factor beta in human disease. *N Engl J Med* **342**, 1350-8 (2000).

44. Oft, M., Heider, K.H. & Beug, H. TGFbeta signaling is necessary for carcinoma cell invasiveness and metastasis. *Curr Biol* **8**, 1243-52 (1998).

45. Portella, G. et al. Transforming growth factor beta is essential for spindle cell conversion of mouse skin carcinoma in vivo: implications for tumor invasion. *Cell Growth Differ* **9**, 393-404 (1998).

46. Seth, P. et al. Development of oncolytic adenovirus armed with a fusion of soluble transforming growth factor-beta receptor II and human immunoglobulin Fc for breast cancer therapy. *Hum Gene Ther* **17**, 1152-60 (2006).

47. Welch, D.R., Fabra, A. & Nakajima, M. Transforming growth factor beta stimulates mammary adenocarcinoma cell invasion and metastatic potential. *Proc Natl Acad Sci U S A* **87**, 7678-82 (1990).

48. Horiguchi, M., Ota, M. & Rifkin, D.B. Matrix control of transforming growth factor-beta function. *J Biochem* **152**, 321-9 (2012).

49. Heldin, C.H. & Moustakas, A. Signaling Receptors for TGF-beta Family Members. *Cold Spring Harb Perspect Biol* **8**(2016).

50. Hata, A. & Chen, Y.G. TGF-beta Signaling from Receptors to Smads. *Cold Spring Harb Perspect Biol* **8**(2016).

51. Feng, X.H. & Derynck, R. Specificity and versatility in tgf-beta signaling through Smads. *Annu Rev Cell Dev Biol* **21**, 659-93 (2005).

52. Hill, C.S. Transcriptional Control by the SMADs. *Cold Spring Harb Perspect Biol* **8**(2016).

53. Mullen, A.C. et al. Master transcription factors determine cell-type-specific responses to TGF-beta signaling. *Cell* **147**, 565-76 (2011).

54. Moustakas, A. & Heldin, C.H. Non-Smad TGF-beta signals. *J Cell Sci* **118**, 3573-84 (2005).

55. Zhang, Y.E. Non-Smad pathways in TGF-beta signaling. *Cell Res* **19**, 128-39 (2009).

56. Bakin, A.V., Rinehart, C., Tomlinson, A.K. & Arteaga, C.L. p38 mitogen-activated protein kinase is required for TGFbeta-mediated fibroblastic transdifferentiation and cell migration. *J Cell Sci* **115**, 3193-206 (2002).

57. Lamouille, S. & Derynck, R. Cell size and invasion in TGF-beta-induced epithelial to mesenchymal transition is regulated by activation of the mTOR pathway. *J Cell Biol* **178**, 437-51 (2007).

58. Conery, A.R. et al. Akt interacts directly with Smad3 to regulate the sensitivity to TGF-beta induced apoptosis. *Nat Cell Biol* **6**, 366-72 (2004).

59. Wrighton, K.H., Lin, X. & Feng, X.H. Phospho-control of TGF-beta superfamily signaling. *Cell Res* **19**, 8-20 (2009).

60. Luo, K. & Lodish, H.F. Positive and negative regulation of type II TGF-beta receptor signal transduction by autophosphorylation on multiple serine residues. *Embo j* **16**, 1970-81 (1997).

61. Wieser, R., Wrana, J.L. & Massague, J. GS domain mutations that constitutively activate T beta R-I, the downstream signaling component in the TGF-beta receptor complex. *Embo j* **14**, 2199-208 (1995).

62. Manning, G., Whyte, D.B., Martinez, R., Hunter, T. & Sudarsanam, S. The protein kinase complement of the human genome. *Science* **298**, 1912-34 (2002).

63. Lawler, S. et al. The type II transforming growth factor-beta receptor autophosphorylates not only on serine and threonine but also on tyrosine residues. *J Biol Chem* **272**, 14850-9 (1997).

64. Lee, M.K. et al. TGF-beta activates Erk MAP kinase signalling through direct phosphorylation of ShcA. *Embo j* **26**, 3957-67 (2007).

65. Ravichandran, K.S. Signaling via Shc family adapter proteins. *Oncogene* **20**, 6322-30 (2001).

66. Muthusamy, B.P. et al. ShcA Protects against Epithelial-Mesenchymal Transition through Compartmentalized Inhibition of TGF-beta-Induced Smad Activation. *PLoS Biol* **13**, e1002325 (2015).

67. Wells, R.G., Yankelev, H., Lin, H.Y. & Lodish, H.F. Biosynthesis of the type I and type II TGF-beta receptors. Implications for complex formation. *J Biol Chem* **272**, 11444-51 (1997).

68. Kim, Y.W., Park, J., Lee, H.J., Lee, S.Y. & Kim, S.J. TGF-beta sensitivity is determined by N-linked glycosylation of the type II TGF-beta receptor. *Biochem J* **445**, 403-11 (2012).

69. Goetschy, J.F., Letourneur, O., Cerletti, N. & Horisberger, M.A. The unglycosylated extracellular domain of type-II receptor for transforming growth factor-beta. A novel assay for characterizing ligand affinity and specificity. *Eur J Biochem* **241**, 355-62 (1996).

70. Liu, S., de Boeck, M., van Dam, H. & Ten Dijke, P. Regulation of the TGF-beta pathway by deubiquitinases in cancer. *Int J Biochem Cell Biol* **76**, 135-45 (2016).

71. Zhou, X. & Gao, C. High glucose induces sumoylation of Smad4 via SUMO2/3 in mesangial cells. **2014**, 782625 (2014).

72. Kang, J.S., Saunier, E.F., Akhurst, R.J. & Derynck, R. The type I TGF-beta receptor is covalently modified and regulated by sumoylation. *Nat Cell Biol* **10**, 654-64 (2008).

73. Liu, C., Xu, P., Lamouille, S., Xu, J. & Derynck, R. TACE-mediated ectodomain shedding of the type I TGF-beta receptor downregulates TGF-beta signaling. *Mol Cell* **35**, 26-36 (2009).

74. Tsukazaki, T., Chiang, T.A., Davison, A.F., Attisano, L. & Wrana, J.L. SARA, a FYVE domain protein that recruits Smad2 to the TGFbeta receptor. *Cell* **95**, 779-91 (1998).

75. Miura, S. et al. Hgs (Hrs), a FYVE domain protein, is involved in Smad signaling through cooperation with SARA. *Mol Cell Biol* **20**, 9346-55 (2000).

76. He, K. et al. Internalization of the TGF-beta type I receptor into caveolin-1 and EEA1 double-positive early endosomes. *Cell Res* **25**, 738-52 (2015).

77. Budi, E.H., Muthusamy, B.P. & Derynck, R. The insulin response integrates increased TGF-beta signaling through Akt-induced enhancement of cell surface delivery of TGF-beta receptors. *Sci Signal* **8**, ra96 (2015).

78. Keller, B. et al. Interaction of TGFbeta and BMP signaling pathways during chondrogenesis. *PLoS One* **6**, e16421 (2011).

79. Wrighton, K.H., Lin, X., Yu, P.B. & Feng, X.H. Transforming Growth Factor {beta} Can Stimulate Smad1 Phosphorylation Independently of Bone Morphogenic Protein Receptors. *J Biol Chem* **284**, 9755-63 (2009).

80. Yew, K.H. et al. Cross-talk between bone morphogenetic protein and transforming growth factor-beta signaling is essential for exendin-4-induced insulin-positive differentiation of AR42J cells. *J Biol Chem* **280**, 32209-17 (2005).

81. Giacomini, D., Paez-Pereda, M., Stalla, J., Stalla, G.K. & Arzt, E. Molecular interaction of BMP-4, TGF-beta, and estrogens in lactotrophs: impact on the PRL promoter. *Mol Endocrinol* **23**, 1102-14 (2009).

82. Zavadil, J. et al. Genetic programs of epithelial cell plasticity directed by transforming growth factor-beta. *Proc Natl Acad Sci U S A* **98**, 6686-91 (2001).

83. Xi, Y. et al. Inhibition of epithelial-to-mesenchymal transition and pulmonary fibrosis by methacycline. *Am J Respir Cell Mol Biol* **50**, 51-60 (2014).

84. Miettinen, P.J., Ebner, R., Lopez, A.R. & Derynck, R. TGF-beta induced transdifferentiation of mammary epithelial cells to mesenchymal cells: involvement of type I receptors. *J Cell Biol* **127**, 2021-36 (1994).

85. Inman, G.J. et al. SB-431542 is a potent and specific inhibitor of transforming growth factor-beta superfamily type I activin receptor-like kinase (ALK) receptors ALK4, ALK5, and ALK7. *Mol Pharmacol* **62**, 65-74 (2002).

86. Wei, Y. et al. Fibroblast-specific inhibition of TGF-beta1 signaling attenuates lung and tumor fibrosis. *J Clin Invest* **127**, 3675-3688 (2017).

87. Zawel, L. et al. Human Smad3 and Smad4 are sequence-specific transcription activators. *Mol Cell* **1**, 611-7 (1998).

88. Choudhary, C. et al. Mislocalized activation of oncogenic RTKs switches downstream signaling outcomes. *Mol Cell* **36**, 326-39 (2009).

89. Grandal, M.V. et al. EGFRvIII escapes down-regulation due to impaired internalization and sorting to lysosomes. *Carcinogenesis* **28**, 1408-17 (2007).

90. Han, W., Zhang, T., Yu, H., Foulke, J.G. & Tang, C.K. Hypophosphorylation of residue Y1045 leads to defective downregulation of EGFRvIII. *Cancer Biol Ther* **5**, 1361-8 (2006).

91. Wu, L. & Derynck, R. Essential role of TGF-beta signaling in glucose-induced cell hypertrophy. *Dev Cell* **17**, 35-48 (2009).

92. Wang, S. & Hirschberg, R. BMP7 antagonizes TGF-beta -dependent fibrogenesis in mesangial cells. *Am J Physiol Renal Physiol* **284**, F1006-13 (2003).

93. Izumi, N. et al. BMP-7 opposes TGF-beta1-mediated collagen induction in mouse pulmonary myofibroblasts through Id2. *Am J Physiol Lung Cell Mol Physiol* **290**, L120-6 (2006).

94. Spinella-Jaegle, S. et al. Opposite effects of bone morphogenetic protein-2 and transforming growth factor-beta1 on osteoblast differentiation. *Bone* **29**, 323-30 (2001).

95. Faucheux, C., Ulysse, F., Bareille, R., Reddi, A.H. & Amedee, J. Opposing actions of BMP3 and TGF beta 1 in human bone marrow stromal cell growth and differentiation. *Biochem Biophys Res Commun* **241**, 787-93 (1997).

96. Mehlhorn, A.T. et al. Differential effects of BMP-2 and TGF-beta1 on chondrogenic differentiation of adipose derived stem cells. *Cell Prolif* **40**, 809-23 (2007).

97. Oshimori, N. & Fuchs, E. Paracrine TGF-beta signaling counterbalances BMP-mediated repression in hair follicle stem cell activation. *Cell Stem Cell* **10**, 63-75 (2012).

98. Yew, K.H. et al. Interplay of glucagon-like peptide-1 and transforming growth factor-beta signaling in insulin-positive differentiation of AR42J cells. *Diabetes* **53**, 2824-35 (2004).

99. Remy, I., Montmarquette, A. & Michnick, S.W. PKB/Akt modulates TGF-beta signalling through a direct interaction with Smad3. *Nat Cell Biol* **6**, 358-65 (2004).

100. Singh, A.M. et al. Signaling network crosstalk in human pluripotent cells: a Smad2/3-regulated switch that controls the balance between self-renewal and differentiation. *Cell Stem Cell* **10**, 312-26 (2012).

101. Chen, Y.G., Li, Z. & Wang, X.F. Where PI3K/Akt meets Smads: the crosstalk determines human embryonic stem cell fate. *Cell Stem Cell* **10**, 231-2 (2012).

102. Thien, A. et al. TSC1 activates TGF-beta-Smad2/3 signaling in growth arrest and epithelial-to-mesenchymal transition. *Dev Cell* **32**, 617-30 (2015).

103. Zhang, L., Zhou, F. & ten Dijke, P. Signaling interplay between transforming growth factor-beta receptor and PI3K/AKT pathways in cancer. *Trends Biochem Sci* **38**, 612-20 (2013).

104. Siegel, P.M. & Massague, J. Cytostatic and apoptotic actions of TGF-beta in homeostasis and cancer. *Nat Rev Cancer* **3**, 807-21 (2003).

105. Zhang, L. et al. USP4 is regulated by AKT phosphorylation and directly deubiquitylates TGF-beta type I receptor. *Nat Cell Biol* **14**, 717-26 (2012).

106. Xue, G. et al. Akt/PKB-mediated phosphorylation of Twist1 promotes tumor metastasis via mediating cross-talk between PI3K/Akt and TGF-beta signaling axes. *Cancer Discov* **2**, 248-59 (2012).

SECTION II.

Characterization of ellagic acid and corilagin as inhibitors of TGF-β type I receptor kinase

Chapter 1. Introduction

This section describes some of my work on a project in collaboration with the laboratory of Dr. Hal Chapman at UCSF. As a result of a high throughput screen of small molecules that prevent epithelial-mesenchymal transition (EMT) in cultured immortalized human lung cells, the Chapman lab discovered that ellagic acid (EA) and its derivatives, a class of compounds called ellagitannins, are potent inhibitors of EMT in cell culture and fibrosis in an animal model. In addition, their data suggested that EA prevented the gene expression changes associated with TGF-β-induced EMT and fibrosis. At this point nothing else was known about the mechanistic effect of EA on TGF-β signaling, and this collaboration was initiated as a result of the Derynck lab's expertise in studying signal transduction mechanisms and TGF-β. Thus my aim going into this project was to determine the cellular mechanism by which EA and corilagin, a similar and more potent ellagitannin that functions otherwise identically to EA, ultimately affect regulation of gene expression by TGF-β.

The collaboration resulted in the publication of "Fibroblast-specific inhibition of TGF-β1 signaling attenuates lung and tumor fibrosis," The Journal of Clinical Investigation 2017, 127(10):3675-3688, which is presented in Section III. However, I also generated a substantial amount of data regarding the inhibition of cell surface receptor induction by both EA and corilagin that did not fit in the already extensive body of data in the publication, which was the culmination of work by multiple cooperating labs.

Here I present briefly my unpublished data on the effect of ellagitannins on TGF-β receptor activation and Smad signaling. I also include some supplemental data on inhibition of TβRI kinase activity by corilagin, a discovery that was published in the JCI paper. A more

detailed presentation of the scientific background of TGF-β and Smad pathways can be found in the previous section of this manuscript, and the role of TGF-β in fibrosis is discussed in depth in the published material quoted in Section III.

Chapter 2. Results and discussion

2.1 Ellagic acid inhibits epithelial-mesenchymal transition in response to TGF-β

One of the hallmarks of EMT is the dissolution of cell-cell junctions as cells gain fibroblast-like morphology and increased motility.[1,2] Multiple epithelial cell types have been reported to respond to TGF-β by downregulating the cell adhesion protein E-cadherin, a structural component of adherens junctions.[3,4] From a human lung carcinoma-derivePd immortalized line, A549 cells were cultured for a maximum of 20 passages after having been FACS sorted for high E-cadherin expression. Using these cells I performed immunofluorescence staining of E-cadherin in response to stimulation with TGF-β and treatment with EA. I observed downregulation of E-cadherin 24 hours after addition of TGF-β, which was prevented when EA was added to the media with TGF-β (Figure 18a). Interestingly, while addition of EA alone caused the cells to adopt a more epithelial phenotype, addition of EA with TGF-β did not prevent the cells from developing the more fibroblast-like morphology characteristic of EMT.

Cultured cells that undergo EMT in the presence of TGF-β have been observed to revert back to more epithelial characteristics when TGF-β is removed. To test the effect of EA on the ability of cells stimulated to undergo EMT, I cultured A549 cells for 48 h with TGF-β before switching cells to either basal growth media or media containing EA, TGF-β, or both, for 24 hours before staining and imaging. Cells partially reverted to epithelial characteristics in the presence of EA and TGF-β, similarly to cells switched to media without TGF-β, further suggesting inhibition of TGF-β signaling (Figure 18b).

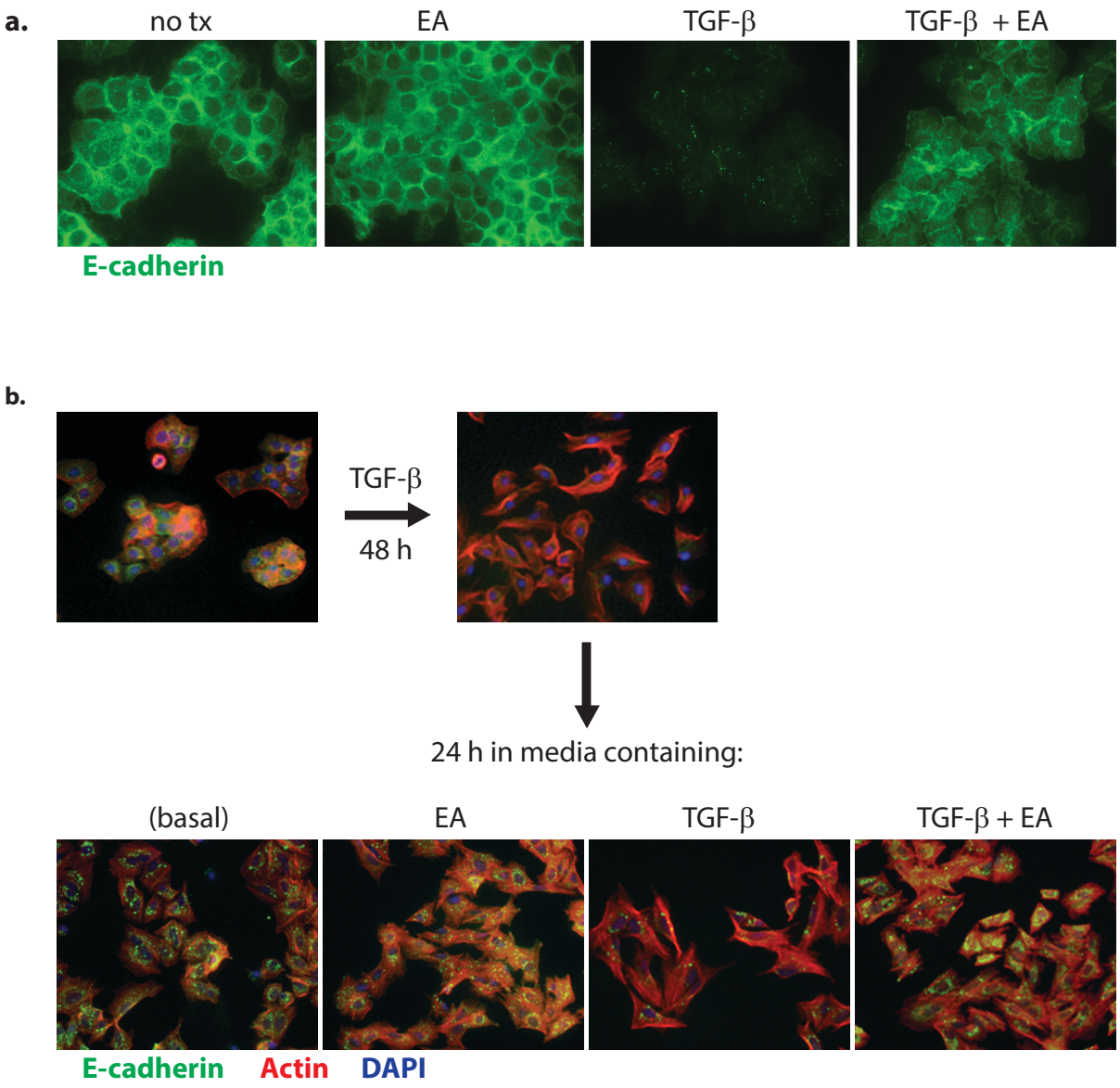

Figure 18. Ellagic acid inhibits epithelial-mesenchymal transition in response to TGF-β. Ellagic acid (EA) prevented downregulation of E-cadherin protein levels in A549 cells in response to TGF-β, and maintenance of mesenchymal characteristics in TGF-β-containing medium. a) Immunofluorescence microscopy showed a decrease of E-cadherin 24 hours after stimulation with 1 ng/mL TGF-β, but this downregulation was abolished in the presence of 1 μM ellagic acid. However, cells still underwent morphological changes associated with TGF-β-induced epithelial-mesenchymal transition (EMT). b) Cells stimulated with TGF-β were allowed to undergo EMT, marked by cell morphology and E-cadherin expression, and then maintained for 24 hours in basal media or media containing EA, TGF-β, or EA plus TGF-β. Cells remained mesenchymal in media containing TGF-β but in the absence of TGF-β the cells partially reverted to epithelial characteristics. Cells were unable to maintain mesenchymal traits in TGF-β containing media in the presence of EA.

2.2 EA and corilagin prevent activation of Smad2 and Smad3 in a manner independent of new protein synthesis

Although our collaborators' initial data demonstrated that treating A549 cells with EA along with TGF-β did not prevent Smad activation, I discovered that pre-incubating cells with EA-containing media for 5-6 hours prior to stimulation with TGF-β was necessary to see strong inhibition of Smad3 phosphorylation, as detected by immunoblotting (Figure 19). This effect was seen in other lung carcinoma (H358, H1299) and lung fibroblast (MRC-5) cell lines as well (Figure 20). The related ellagitannin compound corilagin behaved similarly in preventing Smad activation in a manner dependent on pre-incubation time (Figure 21). Because both EA and corilagin were initially inactive in preventing TGF-β signaling, I hypothesized that the delayed activity was due to either metabolism of the compounds into an active form, or inhibition of Smad activation was occurring through an indirect process requiring new protein synthesis, for which a 3-6 hour incubation would have been sufficient.

To investigate whether new protein synthesis was required for inhibition of Smad signaling by EA, I treated A549 cells with varying concentrations of the translation elongation inhibitor cycloheximide.[5] Inhibition of Smad2 and Smad3 activation, detected by immunostaining, in the presence EA was not affected by cycloheximide (Figure 22a). As a positive control, I showed that cycloheximide treatment effectively blocked expression of a luciferase reporter under control of a Smad binding sequences (SBE-Luc), as described in more detail below, demonstrating its effectiveness at preventing protein synthesis in A549 cells at the concentrations used (Figure 22b.) This experiment suggested direct inhibition of Smad activation, leading to the hypothesis that a metabolic derivative of EA and corilagin was the active compound (detailed in Section III).

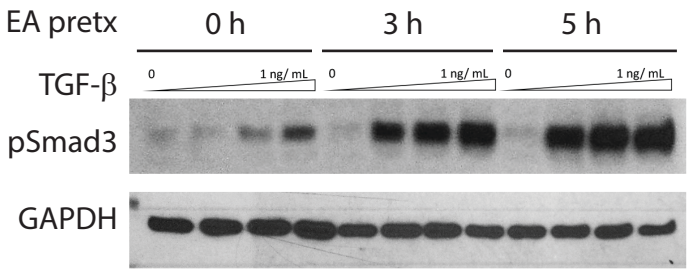

Figure 19. Pre-incubation with EA is necessary for inhibition of Smad activation. A549 cells were serum-starved and incubated with 1 μM EA for the time specified prior to stimulation with 0, 0.2, 0.5, or 1 ng/mL TGF-β for 30 minutes then subjected to immunoblot analysis. Normal Smad3 activation occurred in cells in which EA and TGF-β were added simultaneously ("0 h" pre-treatment), but pre-treating the cells with EA for 5 hours inhibited Smad phosphorylation.

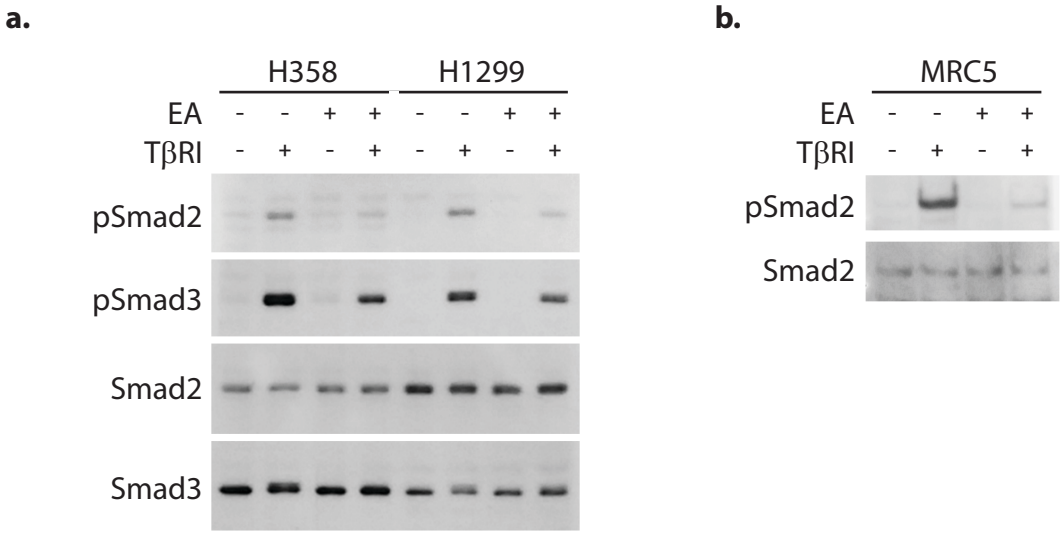

Figure 20. EA pre-treatment prevents Smad activation in multiple human lung cell lines. a) Phosphorylation of Smad2 and Smad3 was inhibited in cells derived from non-small cell lung carcinoma (H358 and H1299), and b) phospho-Smad2 inhibition was seen in cells from normal lung fibroblast (MRC-5). Cells were serum-starved and pre-treated with 1 μM EA for 6 hours prior to addition of 0.25 ng/mL TGF-β for 30 minutes.

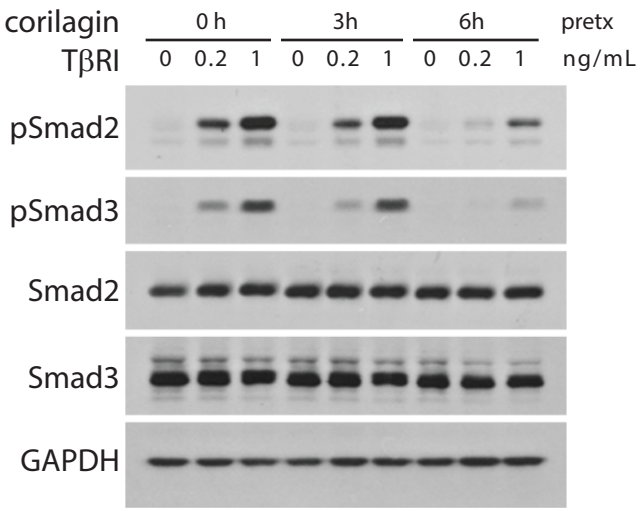

Figure 21. Inhibition of Smad2 and Smad3 by corilagin is dependent upon pre-incubation. Serum-starved A549 cells were exposed to 0.1 μM corilagin for the time specified prior to treatment with varying concentrations of TGF-β for 30 minutes and phosphorylation of Smad2 and Smad3 was evaluated by immunoblotting. Pre-incubation for 6 hours was required for inhibition of Smad activation.

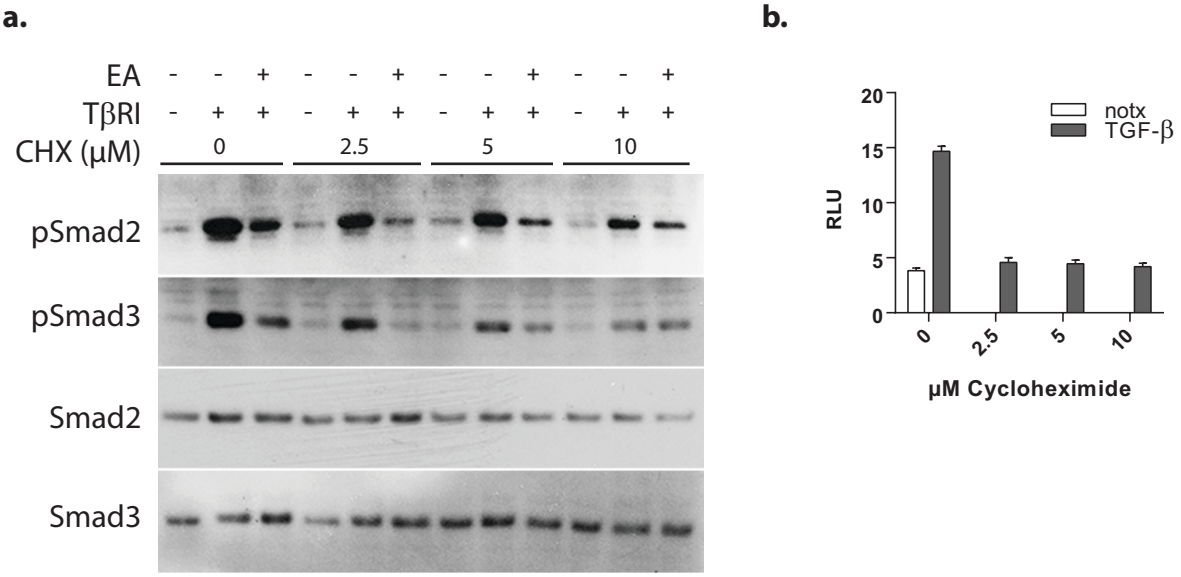

Figure 22. New protein synthesis is not required for inhibition of Smad activation in the presence of ellagic acid. A549 cells were treated with varying concentrations of the translation elongation inhibitor cycloheximide in addition to EA prior to stimulation with TGF-β. a) Addition of cycloheximide did not prevent inhibition of Smad2 and Smad3 phosphorylation by EA, demonstrating that new protein synthesis is not required. b) The concentrations of cycloheximide used in a) were sufficient to prevent protein synthesis as measured by expression of luciferase in a SBE-Luc reporter assay.

2.3 Smad-mediated gene expression is inhibited by EA and corilagin

To further assess the effect of EA and corilagin on Smad signaling, I performed luciferase reporter assays to measure transcriptional activation by Smad2 and Smad3. Activated Smad2 and/or Smad3 in complex with Smad4 regulate transcription of TGF-β-responsive genes by interacting with a motif known as a Smad-binding element (SBE), and gene expression as a direct result of Smad activation can be evaluated using a luciferase reporter gene under the control of repeated SBE sequences (SBE-Luc).[6,7] Therefore, I transfected A549 cells with SBE-Luc and measured luciferase expression in response to TGF-β with EA. I found that EA reduced SBE-Luc expression in response to TGF-β by approximately half (Figure 23). The partial inhibition could be explained by the fact that EA and TGF-β were added simultaneously, potentially allowing for some level of early expression of luciferase that persisted through the 24 hours until the point of assay. My data in the previous section demonstrate that measurable luciferase expression occurs within the first 3.5 hours after TGF-β stimulation.

In addition to downregulation of epithelial genes such as E-cadherin, EMT in response to TGF-β involves expression of the master transcription regulator Snail, and upregulation of the adhesion proteins N-cadherin and fibronectin. I performed quantitative reverse-transcription PCR (qRT-PCR) to measure mRNA encoding Snail1, N-cadherin, and fibronectin in A549 cells treated with TGF-β in the presence or absence of EA. Pre-treatment with EA effectively prevented downregulation of genes encoding E-cadherin and expression of genes encoding fibronectin and Snail1, and partially inhibited N-cadherin gene expression (Figure 24a). Smad7 and PAI-1 are also expressed from genes known to be induced by TGF-β, and I found that corilagin inhibited upregulation of fibronectin, Smad7, and PAI-1 mRNA by TGF-β (Figure 24b). These results demonstrated that EA and corilagin suppressed activation of Smad2 and

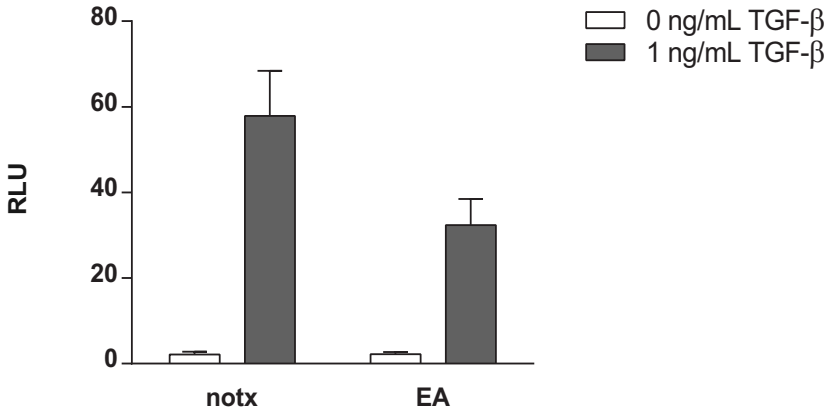

Figure 23. EA partially inhibits expression of a Smad luciferase reporter. Gene expression under the transcriptional control of activated Smads was evaluated using a Smad-binding element (SBE) luciferase reporter in A549 cells. Firefly luciferase expression, quantified by luminescence, was measured after 24 hours stimulation with 0.25 ng/mL TGF-β in the presence of 1 μM EA. Reporter expression was partially inhibited by EA.

Smad3, directly prevented transcriptional activation by Smad2 and/or Smad3, and thus ultimately impaired gene expression changes in response to TGF-β.

2.4 EA and corilagin impair TGF-β-induced receptor upregulation

At this point, it was still unclear how EA and corilagin prevented Smad activation. This work was conducted simultaneously with the project described in Section I, in which I found that TGF-β receptor upregulation played a role in activation of Smad signaling, leading me to hypothesize that EA/corilagin may inhibit Smad activation by interfering with ligand-induced TGF-β receptor presentation. Thus I performed cell surface biotinylation analysis to measure cell surface TGF-β receptor levels in A549 cells that had been pretreated with EA before stimulation with TGF-β. I found that EA prevented upregulation of both TβRI and TβRII, and also significantly inhibited association of Smad2 and Smad3 with cell surface protein complexes (Figure 25). In addition, corilagin pretreatment similarly blocked TGF-β induced receptor presentation (Figure 26a). Furthermore, this phenomenon was seen in human keratinocyte (HaCaT) and mouse mammary epithelial (NMuMG) cells as well, suggesting a general mechanism by which corilagin prevents Smad activation (Figure 26b, 26c).

Since Akt activation contributes to TGF-β receptor upregulation, I tested whether EA and corilagin affect phosphorylation of Akt. Pre-incubation with EA for 6 hours prevented Akt activation in response to TGF-β in A549 and H358 cells, as detected by immunoblotting (Figure 27a). Corilagin also prevented TGF-β-induced Akt signaling in HaCaT cells (Figure 27b).

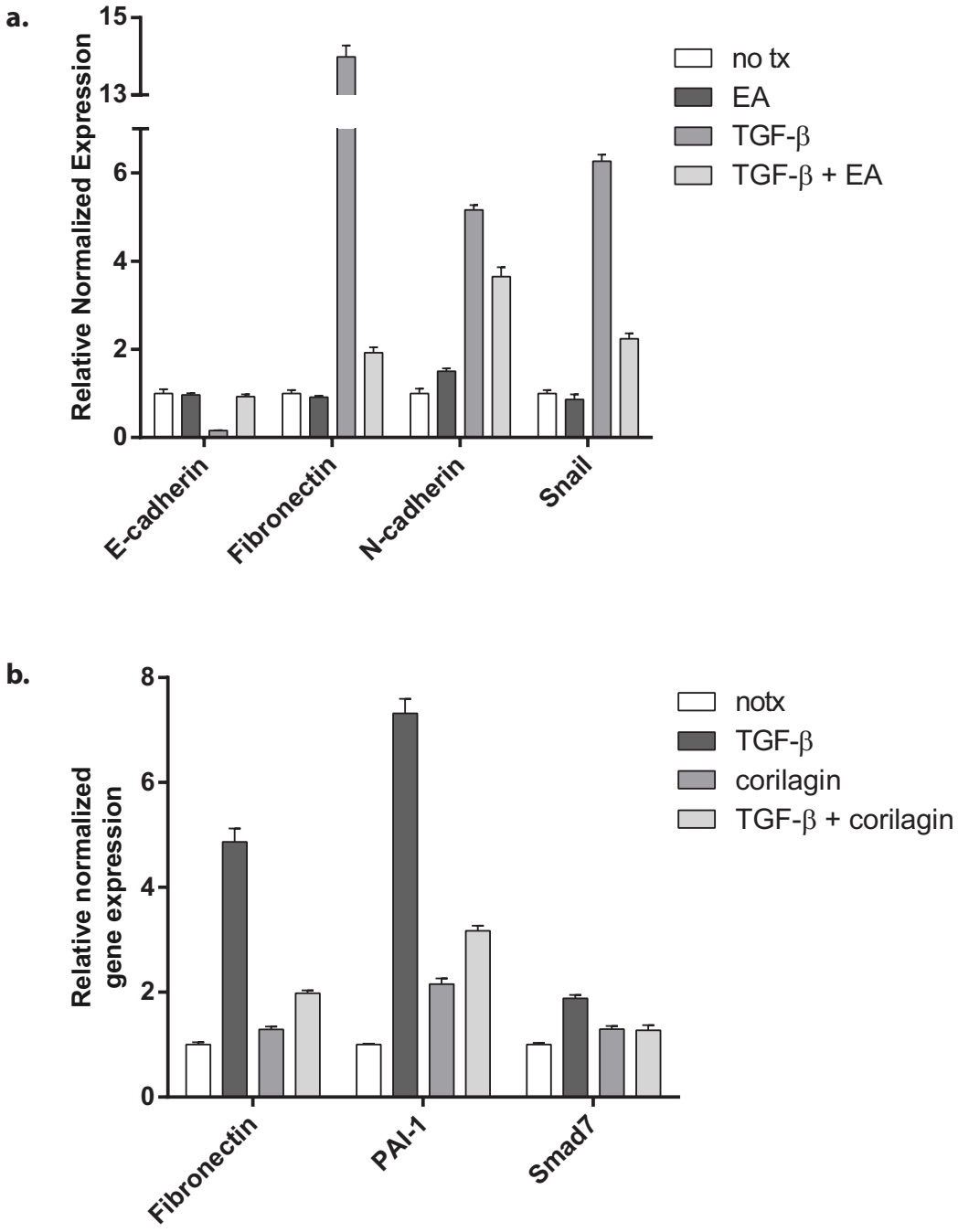

Figure 24. EA and corilagin prevents gene expression changes associated with EMT in response to TGF-β. mRNA was quantified by qRT-PCR and normalized to expression of RPL19 in A549 cells treated with TGF-β and 1 μM EA or 0.1 μM corilagin for 24 hours in serum-free medium. a) Expression of the EMT marker genes *E-cadherin*, *Fibronectin*, *N-cadherin*, and *Snail1* was modulated by TGF-β. Downregulation of *E-cadherin* and expression of *Fibronectin* and *Snail1* were inhibited and *N-cadherin* induction was partially blocked in the presence of EA. b) *Fibronectin*, *Smad7*, and *PAI-1* expression was inhibited by corilagin.

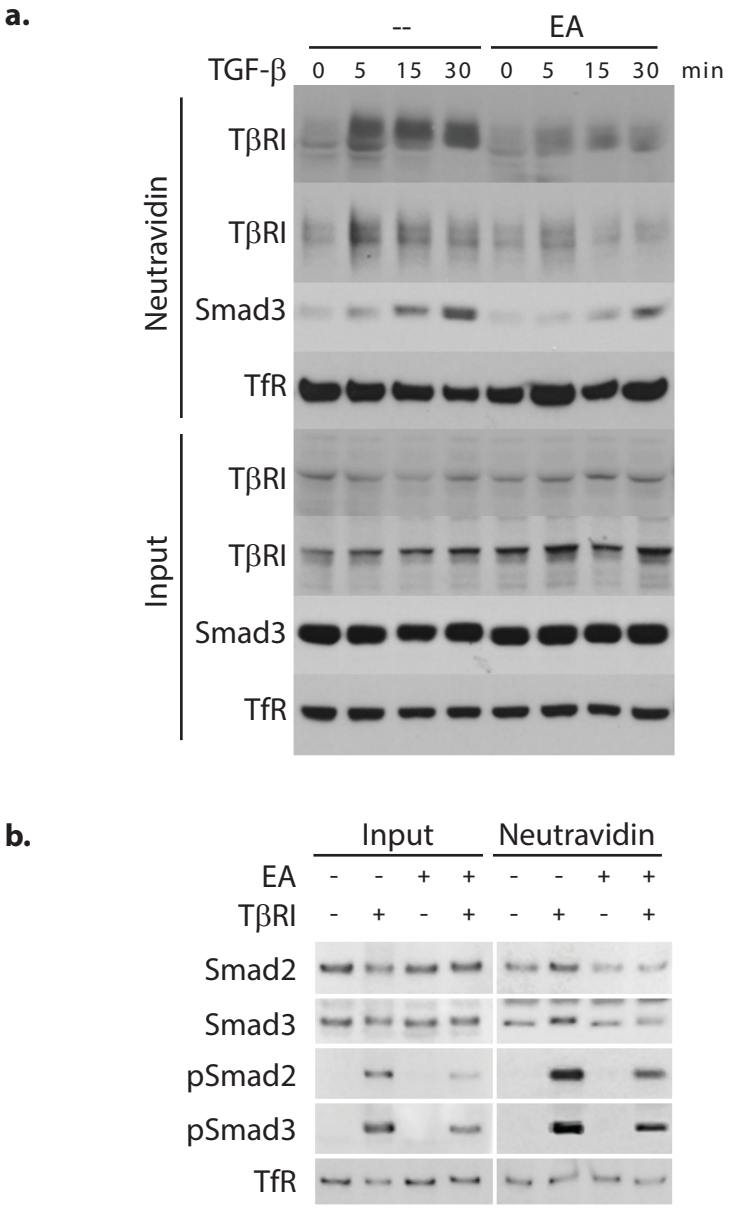

Figure 25. EA inhibits TGF-β-induced increase of cell surface type I and type II TGF-β receptor levels. Cell-surface protein-associated Smad3 in response to TGF-β was decreased in the presence of EA. A549 cells were serum-starved and pretreated with 1 μM EA for 6 hours prior to addition of 0.25 ng/mL TGF-β for the time specified. Cell-surface receptor levels were quantified by selectively cross-linking biotin to proteins exposed to the extracellular surface, followed by immunoprecipitation with neutravidin-conjugated sepharose beads and immunoblotting. b) A549 cells treated with DSP to stabilize protein interactions followed by cell surface biotinylation and neutravidin enrichment. TGF-β induced an increased association of Smad2 and Smad3 with cell-surface proteins, presumably the TGF-β receptor complex, and this interaction was decreased with EA treatment.

Note: The data shown in a) is from the experiment presented in Section I as Figure 1b.

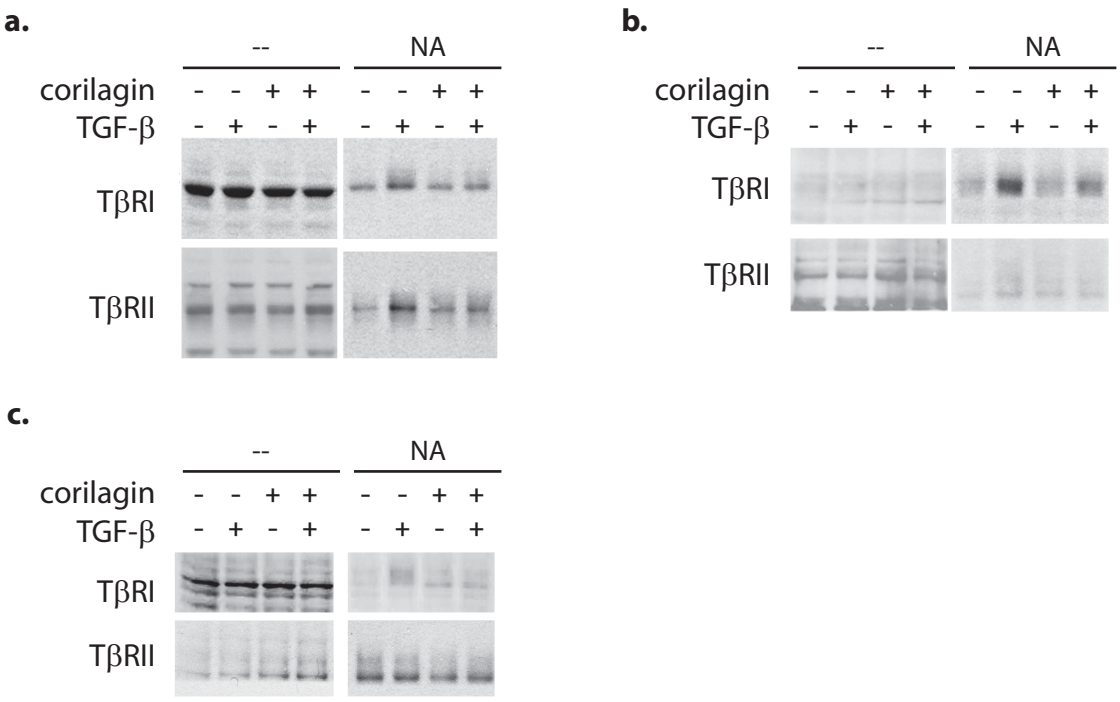

Figure 26. Corilagin prevents TGF-β receptor upregulation in multiple cell lines. Cell surface biotinylation analysis was performed in a) A549, b) HaCaT, and c) NMuMG cells that were pre-treated with 0.1 μM corilagin for 6 hours before stimulation with 0.25 ng/mL TGF-β for 30 minutes. Corilagin inhibited cell surface TβRI induction in all three cell lines. TβRII upregulation was inhibited in A549 and HaCaT cells, but was not observed in NMuMG.

Note: The data shown in a) and b) are from the experiments presented in Section I in Figures 6b and 6a, respectively.

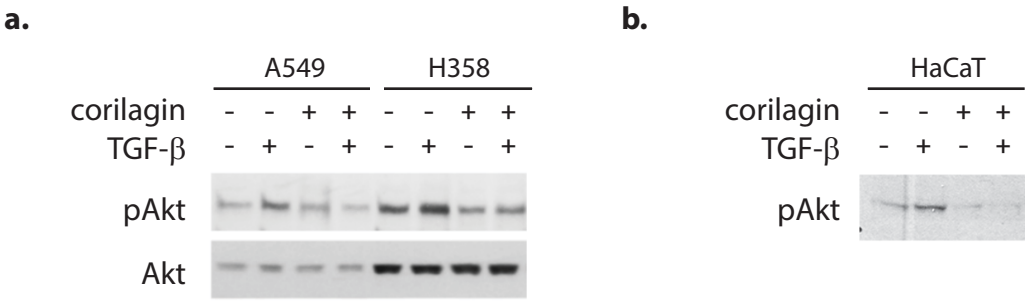

Figure 27. EA inhibits Akt phosphorylation in response to TGF-β. a) A549, H358, and b) MRC-5 cells were serum starved for 6 h with 1 μM EA, then stimulated with TGF-β for 30 min before lysis and immunoblotting. Akt phosphorylation was inhibited in the presence of EA in all three cell types.

2.5 Corilagin is an inhibitor of TβRI kinase

At this time, my research on TGF-β receptor induction had revealed that the TβRI kinase inhibitor SB431542 inhibits receptor upregulation (Section I), and another researcher in this lab had observed that TβRI kinase activity was required for Akt activation by TGF-β (data not published). Taken together, these results lead me to question whether EA or corilagin similarly affects TGF-β receptor kinase activity. To address this, I performed in vitro tyrosine kinase assays using TβRI and TβRII purified from A549 cells. In brief, I co-transfected cells with C-terminally flag-tagged TβRI and TβRII and immuno-precipitated the overexpressed receptors using flag antibody bound to protein G Sepharose beads. Incubation of the TβRI/TβRII-enriched beads with a kinase reaction buffer resulted in ATP-dependent tyrosine phosphorylation on TβRI, which was inhibited by addition of SB431542 (Figure 28). Since TβRI has been reported to auto-phosphorylate on tyrosine residues,[8] and tyrosine phosphorylation was prevented by the TβRI kinase inhibitor SB431542, I concluded that this assay was a viable readout of TβRI kinase activity.

Because a pre-incubation period was necessary for inhibition of Smad activation in live cells, I did not expect that adding EA or corilagin directly to the kinase reaction would inhibit TβRI auto-phosphorylation, and indeed corilagin added directly to the in vitro kinase reaction did not affect levels of tyrosine-phosphorylated TβRI (data not shown). Therefore, I treated serum-starved A549 cells with DMSO (vehicle control) or corilagin for 6 hours and lysed the cells immediately before use in the TβRI/RII in vitro kinase assay. The data from this series of in vitro kinase experiments was included in the manuscript presented in the next section, but I will highlight the results here briefly: TβRI tyrosine phosphorylation in the presence of ATP was observed in the reactions containing DMSO-treated cell lysates but inhibited in the presence of

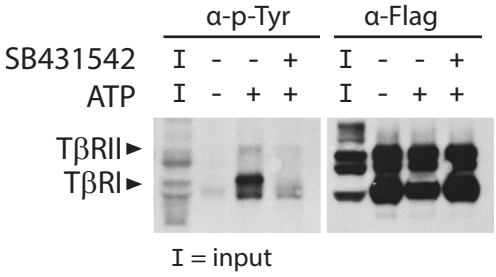

Figure 28. SB431542 prevents tyrosine phosphorylation on TβRI. Phosphorylation of tyrosine residues on TβRI in the presence of ATP was detected in an in vitro kinase reaction containing TβRI and TβRII purified from A549 cells. Addition of the TβRI kinase inhibitor SB5431542 prevented TβRI phosphorylation, suggesting tyrosine autophosphorylation.

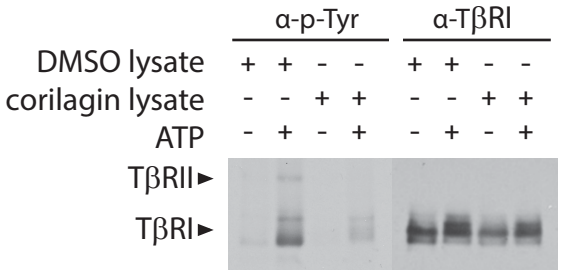

Figure 29. Lysate from corilagin-treated cells inhibits TβRI tyrosine auto-phosphorylation. Lysates from A549 cells treated with 0.1 μM corilagin or DMSO for 6 hours was added to in vitro kinase assays using flag-tagged TβRI and TβRII purified from A549 cells.

Note: This data is included in the manuscript presented in the Section III.

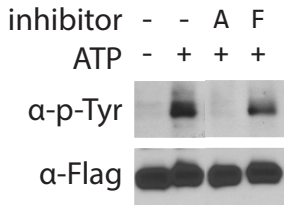

Figure 30. The corilagin derivative 3Abd directly inhibits tyrosine phosphorylation on TβRI. Addition of 3Abd (A), a compound that is likely a metabolic derivative of corilagin, to the in vitro kinase reaction blocked TβRI auto-phosphorylation compared with the control compound 3Fc (F).

Note: This data is included in the supplemental figures of the manuscript presented in Section III.

corilagin-treated cell lysates (Figure 29). Additionally, 3-aminobenzene-1,2-diol (3Abd), a biologically active structural derivative of corilagin, inhibited tyrosine phosphorylation when directly added to the in vitro kinase reaction, while the control compound 3-fluorocatechol (3Fc) did not (Figure 30). In this instance, addition of N-acetylcysteine was necessary to prevent formation of high-molecular-weight protein aggregates that prevented detection of phosphorylated TβRI.

Chapter 3. Conclusion

In the previous section, I presented the results of my studies on TGF-β-induced receptor presentation and concluded that both Akt phosphorylation and TβRI kinase activity contribute to upregulation of receptors. Here I demonstrate that EA and the related compound corilagin inhibit the TβRI kinase activity and, possibly as a result of impaired TβRI kinase activity, Akt phosphorylation, providing a likely mechanism by which EA and corilagin prevent ligand-induced cell-surface TβRI and TβRII, further amplifying inhibition of Smad phosphorylation by these compounds. It remains to be addressed whether the ellagitanins inhibit the kinase activity of TβRII or phosphorylation of TβRII by TβRI, since the kinase reactions were performed with both receptor types combined. This would be an interesting future study as there are currently no known small molecule inhibitors of TβRII kinase.

MATERIALS AND METHODS

Cell culture and transfection

Cells were cultured in a humidified incubator at 37 °C and 5% CO_2. HaCaT cells were cultured in Dulbecco's modified Eagle's medium (DMEM) with 4.5 mM glucose and 10% fetal bovine serum (FBS). A549, H358, and H-1299 cells were maintained in Rosewell Park Memorial Institute (RPMI) 1640 medium with 10% FBS. NMuMG cells were cultured in DMEM (high glucose) supplemented with 10 μg/mL insulin (Sigma-Aldrich) and 10% FBS. MRC-5 cells were grown in Eagle's Minimal Essential Medium (MEM) with 10% FBS.

For assays involving TGF-β treatment, cells were rinsed twice in phosphate buffered saline (PBS) then serum-starved for 6 hours prior to addition of TGF-β unless otherwise specified. HaCaT cells were starved in serum-free DMEM with 4.5 mM glucose and A549 in Small Airway Epithelial Cell Basal Medium (SABM) (Lonza). Transfections were performed in Opti-MEM minimal media (Thermo-Fisher) using TurboFect (Thermo Fisher) in A549 cells or Lipofectamine 2000 (Life Technologies) in HaCaT cells, as specified by the manufacturers.

Growth factors, inhibitors, and antibodies

TGF-β1 from HumanZyme was used at a concentration of 0.25 ng/mL. The phospho-Akt inhibitor AktVIII (EMD Millipore) and the TβRI kinase inhibitor SB431542 (Sigma) were used at a concentration of 5 μM. AktVIII and SB431542 were added to cells 20 minutes and 2 hour prior to addition of TGF-β, respectively. Ellagic acid (EA) (Sigma-Aldrich) and corilagin (BOC Sciences) were added 6 hours prior to addition of TGF-β at final concentrations of 1 μM and 100 nM, respectively. Cycloheximide was used at concentrations of 0, 2.5, 5, and 10 μM and was

added to cells 6 hours prior to stimulation with TGF-β. For prevention of protein aggregation, N-acetylcysteine (Sigma-Aldrich) was added to in vitro kinase reactions at a final concentration of 10 mM. 3-aminobenzene-1,2-diol and 3-fluorocatechol were provided by Dr. Hal Chapman and used in in vitro kinase assays at a concentration of 20 μM.

For immunostaining, I used rabbit anti-TβRII and mouse anti-transferrin receptor purchased from Santa Cruz Biotechnology. Rabbit anti-TβRI and anti-phospho-Smad3 were from Abcam. Rabbit anti-Smad2, anti-phospho-Smad2, anti-Smad3, anti-phospho-Akt (Ser473), anti-phospho-Akt (Thr308), and mouse phospho-Tyr-100 (pY-100) were from Cell Signaling. Mouse anti-Flag was from Sigma. 4G10 mouse anti-phospho-tyrosine antibody was from EMD-Millipore. Mouse anti-E-cadherin was from BD Biosciences, and anti-GAPDH was from Proteintech.

Cell lysis, immunoprecipitation, and western blotting

For TGF-β stimulation assays without immunoprecipitation, cells were rinsed twice with PBS and lysed at in ice cold RIPA buffer [10 mM Tris-HCl pH 7.6, 1 mM EDTA, 1% NP-40, 0.25% sodium deoxycholate, 0.1% SDS, 150 mM NaCl, 10 mM NaF, 1 mM Na_3VO_4, and cOmplete Protease Inhibitor cocktail (Roche)]. Lysates were cleared by centrifugation for 10 minutes at 14,000 rcf at 4 °C and protein concentration was quantified using Protein Assay Dye Reagent (Bio-Rad). Total protein was normalized between samples before denaturing with LDS sample buffer (Invitrogen) at 95 °C for 2 minutes before being subjected to SDS-PAGE and immunoblotting.

For immunoprecipitation of endogenous TβRI, cells were washed twice following appropriate treatment and harvested by scraping in pre-chilled lysis buffer containing 25 mM

Tris-HCl pH 7.6, 150 mM NaCl, 1 mM EDTA, 0.75% Triton X-100, 7% glycerol, 10 mM NaF, 1 mM Na_3VO_4, and cOmplete Protease Inhibitor cocktail (Roche) and incubated for 10 minutes on ice. Lysates were cleared as described above, then immunoprecipitated with anti-TβRI overnight. The antibody-lysate solution centrifuged for 10 minutes at 14,000 rcf and incubated with Protein G Sepharose beads (GE Healthcare) for 2 hours. The beads were washed 3 times for 10 minutes with lysis buffer, eluted with LDS sample buffer (Invitrogen), and subjected to SDS-PAGE and immunoblotting. All steps until elution were performed at 4 °C.

Cell surface biotinylation assay and DSP crosslinking

Cells were washed twice with cold PBS and incubated for 20 minutes with EZ Link Sulfo-NHS-LC-Biotin (Thermo Scientific) at a concentration of 0.25 mg/mL in PBS. The biotinylation reaction was quenched by washing the cells twice with PBS and incubating for 15 minutes with 0.1 M glycine in PBS. Cells were then harvested by scraping in a mild lysis buffer (MLB) containing 20 mM Tris pH 7.6, 200 mM NaCl, 1% NP-40, 10 mM NaF, 1 mM Na_3VO_4, and cOmplete Protease Inhibitor cocktail (Roche), and incubated for 10 minutes. Lysates were cleared by centrifugation at 14,000 rcf for 10 minutes then incubated with NeutrAvidin beads (Thermo Scientific) overnight. Beads were washed three times in MLB, eluted with LDS sample buffer (Invitrogen), and subjected to SDS-PAGE and immunoblotting. All steps until elution were performed at 4 °C.

Dithiobis succinimidyl propionate (DSP), purchased from Thermo Scientific, was used to covalently crosslink proteins in order to stabilize transient interactions. For biotinylation analysis in combination with DSP, cells were first subjected to cell surface biotinylation as described above. Before quenching with glycine, the cells were washed twice with ice cold PBS, incubated

with 1 mM DSP in PBS for 30 minutes at 4 ˚C, washed twice with PBS, then excess biotinylation reagent and DSP were quenched for 15 minutes with 0.1 M glycine in PBS at 4 ˚C. Cells were lysed and biotinylated protein complexes precipitated with NeutrAvidin beads as described above.

Luciferase reporter assay

Cells were transfected with the plasmid SBE-Luc, which contains the firefly luciferase gene under control of four repeated Smad binding elements (SBE), and a Renilla luciferase reporter downstream of the thymidine kinase promoter (Promega), 20 hours prior to serum starvation. After stimulation with the appropriate growth factors and inhibitors, cells were rinsed with PBS, and after aspirating liquid from the monolayer, frozen at -80 °C and thawed on ice before lysis. Relative luciferase activity was quantified using Dual Luciferase Assay System (Promega) according to the manufacturer's protocol. Readout was normalized to Renilla luciferase as an internal control.

RNA preparation and quantitative real-time PCR

RNA was purified from cells using the RNEasy Mini Kit (QIAGEN). Total RNA (1 μg per sample) was used as a template for reverse transcription with iScript (Bio-Rad) according to the manufacturer's protocol. *PAI-1, Snail2, Smad7, Smad6, Id1,* and *Id3* mRNA were quantified by RT-PCR using IQ SYBR-Green Supermix (Bio-Rad) and normalized against *RPL19* mRNA. The primers used were as follows:

Human Primers:

E-cadherin	5′-TGCACCAACCCTCATGAGTG-3′ (forward)
	5′-GTCAGTATCAGCCGCTTTCAG-3′ (reverse)
Fibronectin	5′-TCCCTCGGAACATCAGAAAC-3′ (forward)
	5′-CAGTGGGAGACCTCGAGAAG-3′ (reverse)
N-cadherin	5′-ACAGTGGCCACCTACAAAGG-3′ (forward)
	5′-CCGAGATGGGGTTGATAATG-3′ (reverse)
Snail1	5′-CCTCCCTGTCAGATGAGGAC-3′ (forward)
	5′-CCAGGCTGAGGTATTCCTTG-3′ (reverse)
PAI-1	5′-GGCTGACTTCACGAGTCTTTCA-3′ (forward)
	5′-ATGCGGGCTGAGACTATGACA-3′ (reverse)
Smad7	5′-TGCTGTGAATCTTACGGGAAG-3′ (forward)
	5′-AATCCATCGGGGTATCTGGAG-3′ (reverse)
RPL19	5′-ATGTATCACAGCCTGTACCTG-3′ (forward)
	5′-TTCTTGGTCTCTTCCTCCTTG-3′ (reverse)

Mouse Primers

E-cadherin	5′-CAGGTCTCCTCATGGCTTTGC-3′ (forward)
	5′-CTTCCGAAAAGAAGGCTGTCC-3′ (reverse)
Fibronectin	5′-GCAGTGACCACCATTCCTG-3′ (forward)
	5′-GGTAGCCAGTGAGCTGAACAC-3′ (reverse)
N-cadherin	5′-AGCGCAGTCTTACCGAAGG-3′ (forward)
	5′-TCGCTGCTTTCATACTGAACTTT-3′ (reverse)

Snail1 5′-AAGATGCACATCCGAAGC-3′ (forward)

5′-ATCTCTTCACATCCGAGTGG-3′ (reverse)

Immunofluorescence Microscropy

Epithelial cells were cultured on glass coverslips that had been coated with 0.1% gelatin. Following appropriate treatment with growth factors and inhibitors, cells were washed twice with PBS and fixed in 3.7% paraformaldehyde in PBS for 15 minutes at room temperature. Cells were then permeabilized by incubating with a solution of 0.3% Triton X-100 in PBS for 10 minutes at room temperature, then blocked for 2 hours at room temperature in 3% BSA in PBS that had been passed through a 0.2 μm filter. The coverslips were incubated overnight at 4 °C with anti-E-cadherin at a dilution of 1:300 in 3% BSA/PBS and stained for 2 hours at room temperature with secondary antibody conjugated to Alexa Fluor-488 (Life Technologies) at a dilution of 1:400, along with Alexa Fluor 546 Phalloidin (Life Technologies) at a dilution of 1;100 to stain for actin. Coverslips were mounted on slides with Prolong Gold with DAPI anti-fade reagent (Life Technologies) according to manufacturer's protocol, and visualized using an inverted light microscope. Images were processed with Leica microscopy software (Leica Microsystems).

In vitro kinase assay

A549 cells were co-transfected with a pRK5 plasmids encoding C-terminally flag-tagged rat TβRI and C-terminally flag-tagged TβRII, which were previously generated in this lab.[9] 24 hours after transfection, overexpressed flag-tagged TGF-β receptor proteins were purified by immunoprecipitation with flag antibody and immobilized on Protein G sepharose beads as

follows: Cells were washed twice with ice cold PBS, harvested by scraping in pre-chilled lysis buffer containing 25 mM Tris-HCl pH 7.6, 150 mM NaCl, 1 mM EDTA, 0.75% Triton X-100, 7% glycerol, 10 mM NaF, 1 mM Na_3VO_4, and cOmplete Protease Inhibitor cocktail (Roche), and incubated for 10 minutes on ice. Lysates were cleared by centrifugation at 14,000 rcf for 10 minutes and immunoprecipitated overnight at 4 °C with anti-flag. Following immunoprecipitation, the antibody-lysate solution was incubated with Protein G Sepharose beads (GE Healthcare) for 2 hours. The beads were washed 3 times for 10 minutes with lysis buffer and liquid was removed from the bead bed by aspiration with a 30 x gauge needle.

The beads containing TβRI, TβRII, and associated proteins in the receptor complex, were then incubated with in a total volume of 50 µL kinase reaction buffer (25 mM HEPES, 2 mM MnCl2, 10 mM MgCl2, 0.01% Triton X 100, 20 uM DTT, 100 uM Na3VO4, 100 uM NaF), as well as 5 µL of lysate from A549 cells that had been pre-treated for 6 hours with DMSO or inhibitors. ATP (200 µM), N-acetylcysteine (10 mM), and SB5431542 (10 µM) were added where appropriate. After incubation for 30 minutes at 37 °C, the kinase reaction was stopped by addition of LDS sample buffer and boiling for 2 minutes at 95 °C. Tyrosine phosphorylation was detected by SDS-PAGE and immunoblotting with phospho-Tyr-100 and 4G10 phospho-tyrosine antibodies.

REFERENCES

1. Lamouille, S., Xu, J. & Derynck, R. Molecular mechanisms of epithelial-mesenchymal transition. *Nat Rev Mol Cell Biol* **15**, 178-96 (2014).

2. Thiery, J.P., Acloque, H., Huang, R.Y. & Nieto, M.A. Epithelial-mesenchymal transitions in development and disease. *Cell* **139**, 871-90 (2009).

3. Moustakas, A. & Heldin, C.H. Induction of epithelial-mesenchymal transition by transforming growth factor beta. *Semin Cancer Biol* **22**, 446-54 (2012).

4. Katsuno, Y., Lamouille, S. & Derynck, R. TGF-beta signaling and epithelial-mesenchymal transition in cancer progression. *Curr Opin Oncol* **25**, 76-84 (2013).

5. Ennis, H.L. & Lubin, M. Cycloheximide: aspects of inhibition of protein synthesis in mammalian cells. *Science* **146**, 1474-6 (1964).

6. Zawel, L. et al. Human Smad3 and Smad4 are sequence-specific transcription activators. *Mol Cell* **1**, 611-7 (1998).

7. Feng, X.H. & Derynck, R. Specificity and versatility in tgf-beta signaling through Smads. *Annu Rev Cell Dev Biol* **21**, 659-93 (2005).

8. Wrighton, K.H., Lin, X. & Feng, X.H. Phospho-control of TGF-beta superfamily signaling. *Cell Res* **19**, 8-20 (2009).

9. Feng, X.H., Filvaroff, E.H. & Derynck, R. Transforming growth factor-beta (TGF-beta)-induced down-regulation of cyclin A expression requires a functional TGF-beta receptor complex. Characterization of chimeric and truncated type I and type II receptors. *J Biol Chem* **270**, 24237-45 (1995).

Section III.

Attenuation of lung and tumor fibrosis by fibroblast-specific inhibition of TGFβ1 signaling

Introduction

This section quotes the following published manuscript as it appears in The Journal of Clinical Investigation:

> Wei, Y. et al. Fibroblast-specific inhibition of TGF-beta1 signaling attenuates lung and tumor fibrosis. *J Clin Invest* **127**, 3675-3688 (2017).

The work included here was the result of a collaborative effort between myself and researchers in the lab of Dr. Hal Chapman, who directed this project, and other labs here at University of California at San Francisco, as well as researchers at The University of Texas MD Anderson Cancer Center, University of North Carolina at Chapel Hill, and University of Texas Health Science Center at San Antonio. The research was headed by Dr. Ying Wei at UCSF.

This report details the discovery and characterization of a novel class of inhibitors of TGF-β signaling and their physiological effects in a mouse model of lung fibrosis. My contribution was toward delineation of the molecular mechanism by which these compounds prevent the TGF-β response in the cell. Specifically, I showed that pretreatment of cells with ellagic acid or corilagin resulted in inhibition of TGF-beta-induced Smad activation, while co-administration of either compound with TGF-beta did not affect Smad activation. Further, I showed that this pretreatment inhibited the kinase activity of the TGF-beta type I receptor, and then focused on the activities of several derivative compounds on its kinase activity in vitro. A more detailed description of the background and development of this project can be found in the included introduction.

Attenuation of lung and tumor fibrosis by fibroblast-specific

inhibition of TGFβ1 signaling

Ying Wei[1], Thomas J. Kim[1], David H. Peng[2], Dana Duan[3], Don L. Gibbons[2], Mitsuo Yamauchi[4], Julia R. Jackson[1], Claude J. Le Saux[1,5], Cheresa Calhoun[5], Jay Peters[5], Rik Derynck[3], Bradley J. Backes[1] and Harold A. Chapman[1].

[1]Department of Medicine, University of California at San Francisco, Cardiovascular Research Institute, San Francisco, California 94143, USA. [2]Departments of Thoracic/Head and Neck Medical Oncology, Molecular and Cellular Oncology, The University of Texas MD Anderson Cancer Center, Houston, Texas 77030, USA. [3]Department of Cell and Tissue Biology, University of California at San Francisco, San Francisco, California 94143, USA. [4]Oral and Craniofacial Health Sciences, University of North Carolina at Chapel Hill, Chapel Hill, North Carolina 27599, USA. [5]Dept of Pulmonary and Critical Care, University of Texas Health Science Center at San Antonio, San Antonio, Texas 78249, USA.

Address correspondence to:

Ying Wei, M.D. or Harold A. Chapman, M.D.

Pulmonary and Critical Care Division

University of California at San Francisco

513 Parnassus Avenue

San Francisco, CA 94143-0130

FAX: 415-502-4995

Tel: 415-514-1210

Emails: ying.wei@ucsf.edu
hal.chapman@ucsf.edu

Conflict of interest: The authors have declared that no conflict of interest exists.

Abstract

TGFβ1 signaling is a critical driver of collagen accumulation and fibrotic disease but also a vital suppressor of inflammation and epithelial cell proliferation. The nature of this multi-functional cytokine has limited development of global TGFβ1 signaling inhibitors as therapeutic agents. We conducted phenotypic screens for small molecules that inhibited TGFβ1-induced epithelial-mesenchymal transition without immediate TGFβ1 receptor (TβR) kinase inhibition. We identified trihydroxyphenolic compounds as potent (IC50 ~ 50 nM) blockers of TGFβ1 responses, Snail1 expression, and collagen deposition in vivo in models of pulmonary fibrosis and collagen-dependent lung cancer metastasis. Remarkably, the functional effects of trihydroxyphenolics required the presence of active lysyl oxidase-like 2 (LOXL2) thereby limiting effects to fibroblasts or cancer cells, the major LOXL2 producers. Mechanistic studies revealed the trihydroxyphenolics to induce auto-oxidation of a LOXL2/3-specific lysine (K731) in a time-dependent reaction that irreversibly inhibits LOXL2 and converts the trihydrophenolic to a novel metabolite directly inhibiting TβRI kinase. Combined inhibition of LOXL2 and TβRI activities by trihydrophenolics results in potent blockade of pathological collagen accumulation in vivo without the toxicities associated with global inhibitors. These findings elucidate a therapeutic approach to attenuate fibrosis and the disease promoting effects of tissue stiffness by specifically targeting TβRI kinase in LOXL2-expressing cells.

Introduction

Tissue fibrosis is a major cause of human morbidity and mortality worldwide (1, 2). TGFβ1 signaling through its heterotetrameric receptor complex of two receptor types, TβRII and TβRI, is a well-known driver of collagen expression and tissue accumulation important to wound repair (3). Exaggerated TGFβ1 signaling is also strongly implicated in numerous fibrotic diseases including those involving liver, heart, and lung (4-7). For example, ~80% of the upregulated genes in lungs of patients with Idiopathic Pulmonary Fibrosis (IPF) are reported to be direct or indirect TGFβ1 target genes (8). Pathological collagen accumulation, and its promoting effects on tissue stiffness, is also strongly implicated in cancer progression (9-11). TGFβ1 signaling is both an initiator and driver of tissue stiffness because accumulation of collagen and other matrix proteins promotes integrin-dependent latent TGFβ1 activation and further extracellular matrix deposition (12). Enhanced stiffness is thought to promote tumor cell β1 integrin activation leading to more invasive tumor phenotypes and metastasis, consistent with the strong correlation of TGFβ1 signaling with poor cancer prognosis (9, 13, 14). For these and other reasons there has been much interest in TGFβ1 signaling as a therapeutic target (15-17).

Although attractive as a target, the critical roles of TGFβ1 in suppressing inflammation and epithelial proliferation give pause to the idea of global inhibition of TGFβ1 signaling (18). Indeed, systemic inhibition of TGFβ1 can lead to the development of squamous skin tumors and autoreactive immunity (18-21). In addition, chronic administration of several small molecule inhibitors of TGFβ1 receptor kinases have led to enhanced skin and colonic inflammation and abnormalities in cardiac valves (22, 23). To minimize adverse consequences, an approach of blocking TGFβ1 activation in specific cell types using the unique pathway of $\alpha_v\beta_6$-dependent latent TGFβ1 activation has developed and is currently in clinical trial (24). But this integrin is primarily expressed in epithelia of lung, kidney, and skin (25). In an attempt to develop a more circumscribed inhibitor of TGFβ1 signaling centered on suppression of collagen accumulation we undertook a high-throughput, image-based phenotypic screen of small molecules that could block TGFβ1-induced epithelial-mesenchymal transition (EMT) in vitro but not

directly inhibit TβRI kinase itself. We identified compounds of the ellagitannin and catechin families that met these criteria and then explored the underlying mechanisms, ultimately revealing a novel approach to fibroblast-selective inhibition of TGFβ1 signaling.

Results

Phenotypic screen identifies small molecules with anti-fibrotic activity in vivo. We took advantage of the dramatic phenotypic switch in A549 lung adenocarcinoma cells upon TGFβ1 stimulation resulting in loss of E-cadherin expression and induction of fibronectin (26). Several small molecule libraries totaling ~ 40,000 compounds comprised of both diverse and bioactive compounds were screened. We identified ellagic acid (EA) as one compound meeting our criteria (Figure 1, A-C and Supplemental Figure 1A). We next examined the structural determinants of TGFβ1-induced EMT suppression in A549 cells by other polyphenol family members and found only polyphenols with at least one trihydroxyphenolic motif in their primary structure inhibited Snail1 expression and their potency of inhibition correlated with the number of trihydroxyphenolic units (Supplemental Figure 1, B-D). This point is best illustrated by a comparison of epicatechin (EC) and epigallocatechin (EGC) which are structurally identical aside from a dihydroxy- rather than the trihydroxyphenolic motif in EC (Supplemental Figure 1C). EC had no activity in our in vitro assays whereas EGC was a potent inhibitor of Snail1 and fibronectin in TGFβ1 stimulated A549 cells.

EA was then tested for its anti-fibrotic activity in vivo by either ad libitum feeding of chow comprised of 2% w/w raspberry extract rich in EA and EA precursors given to mice or by administering EA using osmotic pump (Day10-17) after intratracheal bleomycin (Figure 1D). We found that either treatment substantially improved survival (Table 1) and inhibited collagen accumulation (Figure 1, E and F). Because EA is poorly soluble, a more soluble trihydroxyphenolic-containing compound, corilagin with an IC50 for EMT of ~50 nM (Figure 1, G and H), was given daily by gavage beginning 10 days after intratracheal bleomycin (Figure 1I). At day 21 these mice exhibited marked attenuation of bleomycin-induced total lung collagen, fibronectin, Snail1, and p-Smad3 (Figure 1, J and K). The average

circulating level of corilagin 2 hours after the last dose was ~80 nM (Supplemental Figure 1E). EA-rich chow and corilagin had no effect on immune cell numbers or markers of injury (Supplemental Figure 2). Collectively, these findings demonstrate that trihydroxyphenolic compounds attenuate TGFβ1-induced Snail1 and EMT markers in vitro as well as collagen accumulation in vivo and do so at low nM levels. Members of this polyphenol family have previously been shown to inhibit TGFβ1 signaling at μM levels in vitro and fibrosis in vivo but by unclear mechanisms (27, 28).

To test the efficacy of ellagic acid in a second in vivo model of tissue fibrosis, we examined the occurrence of metastatic lung nodules in mice injected subcutaneously 5 weeks earlier with syngeneic KrasG12D/p53R172H metastatic lung cancer cells (344SQ), known to metastasize as a function of the cross-linked fibrillar collagen content of the primary tumors (Figure 2A) (29). Consumption of EA-rich chow following tumor implantation markedly reduced the numbers of metastatic lung nodules (Figure 2, B and C). Although primary tumor volume or weight was unchanged (Figure 2, D and E), immunohistochemistry showed significantly reduced collagen I expression within the primary tumors treated with EA chow (Figure 2F). Furthermore, immunoblotting of these tumor extracts also revealed attenuated total fibronectin and collagen I expression, and decreased Smad activation, assessed by p-Smad3 (Figure 2G). Interestingly, visualizing collagen in situ by second harmonics microscopy, we observed that the primary tumor collagen in mice fed EA chow is not only reduced but also exhibits more curved structures, suggesting less cross-linking (Figure 2, H and I) (9).

LOXL2 is identified as the target of trihydroxyphenolic-containing compounds. We next turned to underlying mechanisms that could account for the activities and potency of the polyphenolic compounds. Because of the striking inhibition of Snail1 expression by several trihydroxyphenolic compounds (Figure 1H and Supplemental Figure 1B), as well as the altered collagen cross-linking structure in primary 344SQ tumors (Figure 2I), we explored the hypothesis that LOXL2 was their target. LOXL2 has previously been linked to Snail1 accumulation in tumor cells (30) and its expression is potently induced by both hypoxia and TGFβ1 (31, 32). LOXL2, like all mammalian copper-dependent

LOX enzymes, utilizes an intrinsically generated quinone, termed LTQ, to mediate oxidation of lysine primary amines (33, 34) (Figure 3A). The catalytic site quinone oxidizes the primary amines of collagen lysine (Lys) and hydroxylysine (Hyl) residues releasing the respective aldehydes, i.e. Lys^{ald} and Hyl^{ald}, creating an intermediate aminophenol followed by release of H_2O_2 and NH_3 completing the LTQ cycle. Lys^{ald} and Hyl^{Ald} in monomeric collagens then undergo a series of spontaneous condensation reactions that result in the formation of intra- and inter-molecular covalent collagen cross-links (35).

We first established an assay of collagen cross-linking induced by recombinant LOXL2 (36, 37) and found corilagin and all other trihydroxyphenolics tested prevented cross-linking (IC50 = 10 nM, Supplemental Figure 3, A-C) whereas an inhibitor of TGFβ1 signaling (SB, SB431542) and an antioxidant (NAC, N-acetylcysteine) had no effect (Figure 3B). LOXL2 enzymatic activity toward a model substrate was assessed monitoring H_2O_2 release. Corilagin blocked this activity with an IC50 of ~50 nM (Figure 3C). LOXL2-induced stabilization of Snail1 protein was also blocked by corilagin (Figure 3D). To test the possibility that the putative anti-oxidant activity of trihydrophenolics could account for either the observed inhibition of TGFβ1 signaling (38) or directly neutralize H_2O_2 in our LOXL2 enzyme assay, we defined the concentrations of corilagin that neutralized H_2O_2 activity in vitro (Supplementary Figure S4). We observed no inhibition of H_2O_2 interaction with a reporter substrate by corilagin at ≤ 10 μM whereas Vitamin C neutralized H_2O_2 at sub μM concentrations, confirming that direct anti-oxidant scavenging activity could not account for our corilagin findings.

To assess inhibition of LOXL2 activity in vivo we performed biochemical analyses of collagens obtained from primary 344SQ tumors of mice treated with EA or control chow (35, 39) (Figure 2A). Accumulation of cross-links including two reducible cross-links, HLNL and DHLNL, and a non-reducible, mature cross-link, deoxypyridinoline (DPD), were all significantly decreased in primary tumors of mice fed EA chow, consistent with the altered collagen organization in the primary tumors demonstrated by quantitative analysis of second harmonic generation (Table 2 and Figure 2I), and confirming inhibition of cross-linking activity by trihydroxyphenolics in vivo. Long-term EA chow

treatment (6 months) did not affect mouse total bone mineral density or collagen content in the aorta (Supplemental Figure 3, D-F), indicating that not all LOX family members were affected by the active compounds.

LOXL2 activity confers inhibition of TGFβ1 signaling by trihydroxyphenolics. To further interrogate the impact of LOXL2 inhibition on TGFβ1 responses we suppressed LOXL2 levels with RNAi in A549 cells. Surprisingly, rather than inhibiting TGFβ1, silencing *LOXL2* completely abrogated the inhibitory effects of corilagin on TGFβ1-induced EMT in A549 cells (Figure 3E). Further, *LOXL2* but not *LOXL1* silencing in fibroblasts completely prevented the corilagin inhibitory effects on TGFβ1-induced mesenchymal proteins N-cadherin, □-SMA and Snail1 (Figure 3F). These findings revealed that the corilagin mechanism of action was not simply LOXL2 inhibition, prompting us to revisit corilagin effects on TGFβ1 signaling.

Because trihydroxyphenolic compounds did not block TGFβ1-induced p-Smad generation in short-term assays (Figure 1C), we considered the possibility that impaired TGFβ1 signaling was due to defective pSmad nuclear import but immunostaining revealed no blockade of Smad2/3 nuclear translocation within 2 hours of compound treatment. However, longer pre-incubation of cells with corilagin (or other trihydroxyphenolics) for several hours completely suppressed Smad activation (Figure 4A and Supplemental Figure 5, A-C), implying a degree of ongoing pSmad generation is required for regulation of the TGFβ1 gene targets studied here (Fig 1H). Similarly, expression of LOXL2 in NMuMG cells that normally express very low levels of LOXL2 conferred corilagin responsiveness and blockage of p-Smad3 following 6-hour pretreatment (Figure 4B). Conversely, silencing *LOXL2* in A549 cells and primary lung fibroblasts completely blocked corilagin effects on p-Smad3 generation (Figure 4, C and D). Consistent with a critical role for LOXL2 in proximal TGFβ1 signaling, a survey of numerous cell lines revealed a direct correlation of LOXL2 mRNA levels with the degree of inhibition of TGFβ1-induced Smad activation by corilagin (Supplemental Figure S6). To further test this principle in vivo, epithelial, fibroblast-rich mesenchymal, and immune cells were isolated by flow cytometry from pools of

normal lungs and lungs of mice exposed 14d earlier to bleomycin, then immediately stimulated with TGFβ1 and tested for their degree of p-Smad accumulation as a marker of TGFβ1 signaling (Figure 4E). There was a marked attenuation of p-Smad3 in the fibroblast-rich lung fraction of bleomycin-exposed mice also given oral EGCG (100 mg/kg qd) but no discernible inhibition of p-Smad3 in either the epithelial or immune cell fractions. A second experimental design in which the isolated fractions from pools of normal lungs and lungs of mice exposed 14d earlier to bleomycin fed with control or EA chow demonstrated the same pattern (Supplementary S7), confirming the cell selectivity of trihydroxyphenolics on TGFβ1 signaling in vivo. Finally, we confirmed that inhibition of active LOXL2 by the copper chelator penacillamine (DPA) also abrogated corilagin effects on Smad activation and Snail1 induction (Figure 4F and Supplemental Figure 5, D-F). Together these data indicate that trihydroxyphenolic compounds selectively target proximal TGFβ1 signaling and Snail1 accumulation only in cells expressing LOXL2 and do so by a mechanism requiring the presence of active LOXL2.

To further investigate the specificity of trihydroxyphenolics for TGFβ1 signaling, we asked whether corilagin inhibited other kinases at 1-10 μM, well above the IC50 for its inhibitory effects on TGFβ1 signaling (Figure 1H). In a screen of 82 purified kinases conducted at the Km for ATP binding for each kinase, only the tyrosine kinases epidermal growth factor receptor (EGFR) and platelet derived growth factor receptor beta (PDGFRβ) were inhibited >50% at 1 μM (Supplemental Figure S8A). However, when we specifically tested the inhibitory effects of corilagin at 1 μM on either EGFR or PDGFRβ activities of intact cells, neither were inhibited by corilagin, implying the cell-free kinase screen is more sensitive than the inhibition of these enzymes in intact cells (Supplemental Figure S8, B and C). These data confirm that corilagin is not a non-specific kinase inhibitor, at least at concentrations ≤ 1μM.

Trihydroxyphenolics induce auto-oxidation of LOXL2 lysine 731. Given the structural similarities between the trihydroxyphenolic motif and LTQ (Figure 3A), the results described above raised the possibility that the trihydroxyphenolic motif operates as a LTQ-like mimic leading to its metabolism by LOXL2 and generating an inhibitor of TGFβ1 signaling. To begin testing this hypothesis we inspected

the LOX catalytic domain for lysines specific to LOXL2 and not found in LOXL1 (Figure 5A), whose silencing had no impact on corilagin responsiveness (Figure 3F and Figure 4D). We then established and expressed flag-tagged point mutants of each of three LOXL2/3 specific lysines, converting each to the corresponding LOXL1 residues: K614N, K731R, and K759R. Each of the point mutants had comparable enzyme activity to wt LOXL2 when expressed in NMuMG cells (Supplemental Figure 9A) and all except the K731 mutant were completely inhibited by corilagin (Figure 5B). Cells expressing K731R LOXL2 were completely resistant to inhibition of TGFβ1 signaling (Figure 5C) and Snail1 stabilization (Figure 5D) by corilagin whereas the other mutants were indistinguishable from wt. Because lysine auto-oxidation by LOX family enzymes is critical to LTQ generation, we asked whether K731 was auto-oxidized to an aldehyde in the presence of corilagin. Incubation of a biotin-hydrazide that covalently links to free aldehydes with immunoprecipitated wt and mutant LOXL2 confirmed that each enzyme except the K731R mutant developed an aldehyde when mixed with corilagin, implying that K731 but not other lysines is converted to an aldehyde during metabolism of corilagin by LOXL2 (Figure 5E).

A novel TβRI kinase inhibitor is generated inside LOXl2-expressing cells. We next screened compounds structurally similar to the intermediate aminophenol known to appear during the LTQ cycle (Figure 3A) for direct TGFβ1 inhibition. A catechol containing an amino group at position 3 (3Abd, 3-aminobenzene-1,2-diol) but not at either position 2 (2Abd) or 4 (4Abd) was found to be a potent inhibitor of TGFβ1-induced Smad3 activation and Snail1 expression without pre-incubation and regardless of LOXL2 expression (Figure 6, A-C and Supplemental Figure 9B). We confirmed that 3Abd, but not control pyrogallol (Pg) or 2Abd, directly blocked the kinase activity of recombinant TβRI catalytic domain with an IC50 ~3 μM (Figure 6D and Supplemental Figure 9C), consistent with the inhibitory profile of 3Abd in cells (Figure 6C). In cells overexpressing TβRI we also observed that 3Abd but not control 3Fc blocked the kinase activity of immunoprecipitated TGFβ receptors (Supplemental Figure 9D). Of note, 3Abd is structurally distinct from any of the known low molecular weight inhibitors of TβRI (18).

To further define the mechanism of TGFβ1 inhibition by trihydroxyphenolic compounds we asked whether secreted LOXL2 generated active 3Abd-like metabolites. Overnight co-culture of corilagin-treated A549 cells with corilagin-nonresponsive NMuMG cells (Figure 4B) expressing a Smad3 reporter (12X CAGA)(40) revealed indistinguishable TGFβ1-induced reporter activation with or without 5-fold excess A549 cells in co-culture, indicating that the generation of a diffusible inhibitor was unlikely (Figure 6E). In addition, lysates of corilagin-treated A549 cells, but not that of untreated cells, inhibited the kinase activity of immunoprecipitated TGF-β receptors (Figure 6F). These results point to an intracellular origin of a trihydroxyphenolic metabolite(s) inhibiting TβRI kinase (Figure 6G). While we demonstrated that the small fragment 3Abd that would result from a trihydroxyphenolic acting through a LTQ-like mechanism (and not pyrogallol) directly inhibits TβRI kinase (Figure 6D), future studies will be needed to isolate the exact inhibitory metabolite(s) present within trihydroxyphenol-treated LOXL2 expressing cells.

Discussion

These studies reveal for the first time a pathway of inhibition of the TGFβ1-induced collagen program selective to the cells that are most accountable for pathological collagen deposition, tissue fibroblasts and fibroblast-like tumor cells. The surprising finding that such selectivity depends on active LOXL2/3 and appears to operate in a cell autonomous manner largely minimizes inhibition by trihydroxyphenolic-containing compounds on TGFβ1 signaling in epithelial or immune cells, avoiding the likely toxicities of general TGFβ1 inhibition for chronic disease processes such as fibrosis and cancer progression. Indeed, we have observed no adverse events in mice on the trihydroxyphenolic-rich diet (EA chow) for at least six months including the absence of skin inflammation and discernible lesions in cardiac valves. Likewise, none of the compounds tested here had any negative effects on cell viability in vitro at concentrations up to 10 μM of trihydroxyphenolics or 50 μM of 3Abd (Supplementary Figure S10). The selective inhibition of intracellular and extracellular LOXL2/3 by trihydroxyphenolics also distinguishes this mechanism of LOX family inhibition from that of previously described extracellular LOXL2

inhibitors as well as global LOX inhibitors, accounting for the lack of negative impact of long term exposure to EA-rich compounds on bone or vascular collagen content (Supplemental Figure 3, D-F) (34, 41). Maintenance of musculoskeletal and vessel wall collagen and elastin integrity depends on LOX and LOXL1, not LOXL2 (42-45). Although selective, the combined inhibition of LOXL2 and TGFβ1 signaling in fibroblast-like cells results in potent in vivo anti-fibrotic activity that has untapped but promising potential as a therapeutic approach for chronic diseases such as pulmonary fibrosis dominated by progressive collagen accumulation.

The combined inhibition of LOXL2 and TGFβ1 signaling in fibroblast-like cells could be expected to impact biomarkers of collagen turnover in vivo. Indeed, we observed urinary levels of the non-reducible end-products of cross-linked collagen metabolism, PYD/DPD, to be increased in mice days 10-21 post bleomycin injection and this increase was suppressed by treatment of the mice with corilagin (Supplemental Figure 11A). Consistent with these findings, we observed increased urinary PYD/DPD mean levels in two cohorts of patients with Idiopathic Pulmonary Fibrosis (Supplemental Figure 11B), suggesting that a signal from fibrotic lungs is present in most of these patients and may enable tracking of collagen turnover and drug responses in vivo.

The biological pathway identified here employs trihydroxy-containing polyphenols at concentrations achievable by dietary ingestion. Indeed, foods rich in this class of compounds, such as epigallocatechin-3-gallate (the major polyphenol in green tea), have been consumed as therapeutics for decades (46). Yet these compounds are not generally thought of as workable drugs because of their potential for pro- and anti-oxidant reactions that could negatively impact pathways, such as drug metabolism, sensitive to such reactions (47). The designation of these polyphenols as anti-oxidants and as reactive compounds however largely stems from prior studies that have employed μM levels of polyphenols to achieve in vitro “anti-oxidant” or signaling inhibition in multiple cell systems (48) even though blood levels above ~150 nM have not been documented for dietary polyphenols consumed by humans (49-53). As well, we observed no neutralization of H_2O_2 oxidant activity by corilagin at

concentrations below 10 μM (Supplemental Figure 4). We believe the LOXL2-dependent interaction with trihydroxyphenolics is a singular example of a relevant protective pathway activated by nM levels of the relevant ellagitannin and catechin subclasses, possibly contributing to the observed beneficial effects of green tea and other trihydroxyphenolic-rich diets in numerous population studies (54-56).

Methods

Reagents. Ellagic acid (E2250), epigallocatechin gallate (E4143), epicatechin gallate (E3893), epigallocatechin (E3768), gallocatechin (E3768), epicatechin (E1753), catechin (C1251), luteolin (L9283), chloramine T (857319), p-dimethylaminobenzaldehyde (156477), bleomycin (B5507), D-penicilamine (P4875), pyrogallol (254002), N-acetylcysteine (A7250), protease inhibitor cocktail (P8340), phosphatase inhibitor cocktail (P5726), fibronectin pAb (F3648), α-SMA mAb (A5228), Flag M2 mAb (F3165), and β-actin mAb (A5441) were purchased from Sigma-Aldrich (St Louis, MO). Corilagin (23094-69-1) was purchased from BOC Sciences (New York, NY). TGFβ type I receptor inhibitor SB431542 (S4317), phospho-Smad2 (Ser 465/467) pAb (566415), EGFR pAb (06-847), and phosphotyrosine mAb 4G10 (05-321) were from EMD Millipore (Billerica, MA). Snail1 mAb (3895), Smad2 mAb (5339), phospho-Smad1/5 (Ser463/465) pAb (9516), Smad1 pAb (9743), phospho-EGFR pAb (2231), phosphor-PDGFRβ pAb (3161), and PDGFRβ Rb mAb (3169) were from Cell Signaling (Beverly, MA). Collagen I pAb (ab292), vimentin mAb (ab45939), LOXL2 pAb (ab96233) for Western blot, and phospho-Smad3 (Ser 423/425) pAb (ab52903) were from Abcam (Cambridge, MA). SiRNAs for human LOXL1 (sc-45220) and LOXL2 (sc-45222), and secondary HRP-conjugated antibodies (mouse, sc-2005; rabbit, sc-2004) were from Santa Cruz Biotechnology (Santa Cruz, CA). Streptavidin-magnetic beads (11205D), TurboFect transfection reagent (R0531), and EZ-Link Hydrazide-LC-Biotin (PI21340) were from Thermo Scientific (Waltham, MA). Protein G-agarose (11719416001) was from Roche (Clovis, CA). E-cadherin (610182) and N-cadherin (610921) antibodies were from BD Biosciences (San Jose, CA). TGFβ1 (100-21) was from PeproTech. 3-aminobenzene-1,2-diol (W4593) is from AURUM Pharmatech Inc. (Franklin Park, NJ). 2-aminobenzene-1,3-diol (23488), 4-aminobenzene-1,2-

diol (31975), and 3-Fluorocatechol (CL8492) were from Astatech Inc. (Bristol, PA). Human recombinant LOXL2 (2639-AO-010) was purchased from R&D Systems (Minneapolis, MN).

Cell culture. Human or mouse cell lines were purchased from ATCC (Manassas, VA, USA) and grown in Dulbecco's Modified Eagle Medium (DMEM) or RPMI1640 medium supplemented with L-glutamine and 10% FBS (Hyclone, Logan, UT, USA). Human and mouse lung fibroblasts were isolated from crude whole lung single-cell suspension cultures on petri dish in DMEM supplemented with L-glutamine and 10% FBS for 2 weeks. Mouse type II alveolar epithelial cells (AECs) isolation and culture was performed as previously described (57) . All the cell lines in the lab are periodically tested for mycoplasma contamination. Only the mycoplasma-free cells are used for experiments.

High throughput screen and high content imaging analysis. A549 cell-based screening of inhibitors to TGFβ1-induced EMT from small molecule libraries was performed in 384-well plate format and the images were captured and analyzed using GE IN Cell 2000 as described previously (26).

Immunofluorescence. Cultured cells and 5-7 μm cryosections were fixed in 4% paraformaldehyde and stained with various antibodies and IgG isotype controls. Where indicated in the figure legends, mosaic images were generated from multiple ×20 images captured on a Zeiss Axio upright fluorescent microscope and tiled using 10% image overlap by Axiovision 4.7 software.

Masson's Trichrome stain. For histological assessment of lung collagen, frozen sections of the left lung were stained using Masson's Trichrome stain kit (22-110-648, Thermo Scientific). The whole section was imaged with a Zeiss Axio upright microscope and tiled using 10% image overlap into a single panoramic by Axiovision 4.7 software (Zeiss).

Immunoblot. Pulverized tissue and cells were lysed in RIPA buffer (150 mM NaCl, 50 mM Tris, pH 8.0, 1% Triton X-100, 0.5% sodium deoxycholate, 0.1% SDS, supplemented with protease and phosphatase inhibitors) and analyzed by immunoblotting. Densitometry was quantified using NIH ImageJ software.

Bleomycin fibrosis model. Eight-week old C57BL/6 mice were intratracheally instilled with saline or 1.9 units/kg of bleomycin (Sigma-Aldrich). Mice were implanted with Alzet osmotic pumps (1007D, DURECT Corporation, Cupertino, CA) loaded with ellagic acid salt (24 mg/kg/day, Day 10-Day 17), fed with red raspberry diet (EA chow, Day 0-Day 21), or gavaged with corilagin (100 mg/kg, Day 10-Day 21). Controls were treated with control pump, control diet, or vehicle in the same formulation. Red raspberry diet (TD.130761) and red control diet (TD.150279) was custom made by Envigo (Indianapolis, IN). The lungs were lavaged and followed by OCT embedding for imaging or snap freezing in liquid nitrogen for protein extraction or hydroxyproline assay.

Syngeneic in vivo tumorigenesis and metastasis assays. KrasG12D/p53R172H metastatic lung cancer cells (344SQ) were subcutaneously injected in the right flanks of male, syngeneic 129/sv mice at 3 months of age and allowed to form tumors for 5 to 6 weeks (29). The mice were fed with red raspberry diet or control diet. After euthanasia, tumors were measured and lung metastatic nodules were quantified. Primary tumor tissues were snap frozen and analyzed by Western blot. Some primary tumors were formalin fixed, paraffin embedded, and sectioned for immunohistochemistry or second harmonic generation imaging. The investigators were completely blinded to drug treatment and outcome assessment.

Immunohistochemistry (IHC) and second harmonics generation (SHG) microscopy. Paraffin embedded tissue sections were rehydrated, blocked with goat serum, and probed for collagen I. Tissues were subsequently washed and probed with HRP-conjugated secondary antibodies and signal was attained by developing with a DAB reagent. Collagen cross-linking alteration was evaluated by SHG microscopy. Tissues stained by H&E were visualized using a Zeiss LSM 7 MP Multiphoton Microscope at an excitation wavelength of 800 nm and collagen fiber signals were detected at 380-430 nm using bandpass filters. Collagen linearity was calculated as a ratio of the total length versus the end-to-end length of the individual collagen fiber.

Collagen content. Lung or aorta collagen content was evaluated using hydroxyproline assay

(58). Briefly, whole left lung tissue or aorta was hydrolyzed in 1 ml 12N HCl at 110 °C for 24 h and the hydroxyproline was detected by incubating with Chloramine T and p-dimethylaminobenzaldehyde and the absorbance was measured at 550 nm. Each sample was run in triplicate. Collagen content in lung or aorta tissues was expressed as micrograms of collagen per lung or aorta and was converted from micrograms of hydroxyproline.

Bronchoalveolar lavage. After the trachea was exposed, a 20-G catheter was inserted into the trachea through a small incision. 1 ml cold PBS was instilled into the mouse lungs followed by gentle aspiration repeated for three times. All the bronchoalveolar lavage fluid (BALF) was centrifuged and cell pellet was re-suspended in erythrocyte (RBC) lysis buffer (Sigma, St. Louis) followed by re-centrifugation. Cell number was counted using hemocytometer. Cell types of BALF were determined by morphology following Diff-quick stain of cytospin slides. About 500 cells were counted for each sample in order to determine the cell types. Macrophages account for more than 80% of the cells in BALF and were collected by centrifugation. After centrifugation, the supernatant was collected to measure total protein content using the BCA assay (23225, Pierce), while the cell pellet was lysed for immunoblotting or RNA isolation. *Plasma level of corilagin – LC/MS analysis.* Plasma level of corilagin in C57BL/6 mice two hours following last oral administration at day 21 was analyzed by Quintara Discovery, South San Francisco, California. Blood samples (~ 500 µL/ sample) were collected via cardiac puncture. Samples were placed in tubes containing heparin sodium and stored on ice until centrifuged for plasma.

Preparation of insoluble cross-linked collagen. Fibroblasts were cultured on 10 cm dish until confluent. The medium was then changed to DMEM containing 5% FBS, 100 µM L-ascorbic acid with 500 kDa Dextran Sulfate at 100 µg/ml, and 50 ng/ml recombinant human LOXL2 (rhLOXL2) for 7 days (36, 37). The cell layer was extracted with 0.5 M acetic acid and 0.1 mg/ml pepsin overnight at 4ºC. The leftover insoluble fraction was further extracted and the insoluble cross-linked collagen measured using

Sircol Insoluble Collagen Assay kit (S1000, Biocolor, Westbury, NY) according to manufacturer's instruction.

LOX activity assay. LOX activity of recombinant human LOXL2 or conditioned medium collected from cells expressing LOXL2 was measured using a Fluorimetric Lysyl Oxidase Activity Assay Kit (ab112139, Abcam, Cambridge, MA) following a protocol provided by the manufacturer. Briefly, 50 µl of sample was mixed with an equal volume of assay reaction mixture containing LOX substrate, horseradish peroxidase (HRP) and HRP substrate in the presence and absence of testing inhibitors and D-penicillamine (DPA), a LOX inhibitor. The mixture was incubated for 30 min at 37 °C in darkness. The fluorescence increase was then measured with a fluorescence plate reader (BMG LabTech FLUOstar) at Ex/Em = 540/590 nm. Sample buffer or medium alone without LOXL2 was used for determination of the background fluorescence.

Collagen crosslink analysis. Snap frozen primary 344SQ tumors were pulverized in liquid nitrogen using a Spex Freezer Mill (Spex, Metuchen, NJ), washed with cold PBS and cold distilled water, lyophilized, and weighed. Aliquots were reduced with standardized NaB3H4 and hydrolyzed with 6 N HCl. The hydrolysates were then subjected to amino acid and cross-linking analyses using LC-MS/MS as described previously (59). The terms DHLNL, HLNL, and HHMD represent both the unreduced and reduced forms. The mature trivalent cross-links, PYD and DPD, were simultaneously analyzed by their fluorescence. All cross-links were quantified as the mol/mol collagen based on the value of 300 residues of hydroxyproline per collagen molecule.

Urinary PYD/DPD measurements. Pooled urine from each of 3-5 mice for each time point after bleomycin in a cohort of mice treated with vehicle or corilagin (100 mg/kg) beginning on day 10 post bleomycin were collected. Urine specimens were also collected from two cohorts of IPF patients and controls at two sites: UT San Antonio Medical Center and UCSF. All consenting patients with physician-established diagnosis of IPF followed in the respective ILD programs were included in sample collection. PYD/DPD levels from all the samples were measured using MicroVue EIA Assay Kit (8010)

and MicroVue Creatinine EIA Kit (8009) (Quidel Corp., San Diego, CA) along with PYD/DPD standards and the results were normalized relative to urinary creatinine. The statistical significance of human urine samples was analyzed using Mann-Whitney U-Test.

Bone mineral density (BMD) measurement. BMD of mice treated with red raspberry diet or control diet up to 6 months was measured using Dual-energy X-ray absorptiometry (DEXA) scan. DEXA scans were performed using the Lunar PIXImus Densitometer (GE Medical Systems, Waukesha, WI) at UCSF animal facility. PIXImus Densitometer was calibrated before each testing using a quality control phantom following the manufacturers' instructions.

Elastic van Gieson stain. Aortas isolated from mice treated with red raspberry diet or control diet up to 6 months were embedded in paraffin (n=3 per group). Sections (5□µm) were cut every 30 µm along the aortas (starting from the proximal end). Selected sections were stained with Miller's Elastica van Gieson stain.

Site-directed mutagenesis of LOXL2. Site-directed mutagenesis was performed to generate K614N, K731R, and K759R point mutations using Phusion Site-Directed Mutagenesis Kit (F541, Thermo Scientific, Waltham, MA) according to manufacturer's instructions. A pcDNA3-hLOXL2-flag plasmid containing the cDNA fragment of wild-type human LOXL2 fused with a flag tag at the C-terminus (gift from Dr. Amparo Cano from Instituto de Investigaciones Biomédicas UAM/CSIC, Madrid, Spain (30), was used as the template DNA (30). Mutations were confirmed by DNA sequencing. The primers and their complementary strands used are: K614N forward 5'- GACTTCCGGCCTAATAATGGCCGC-3', K614N reverse 5'-GGACTGGCCATTGTTGTGGATCTG-3'; K731R forward 5'-ACAACATCATACGATGCAGGAGCC-3', K731R reverse 5'-TGGAGTAATCGGATTCTGCAACCT-3'; K759R forward 5'-ACGGAAAAACGTTTTGAGCACTTCA-3', and K759R reverse 5'-CTCTTCGCTGAAGGAACCACCTAT-3'.

Biotin hydrazide derivatization of carbonylated LOXL2. NMuMG cells were transiently transfected with wild-type or mutant human LOXL2-Flag in 10 cm dish and 24 hours later the cells were treated with 1 μM corilagin for 6 hours at 37 ºC before lysis in 50 mM HEPES, 100 mM NaCl, 2 mM EDTA, 0.5% Triton-100 plus protease inhibitor cocktail, 10 mM NaF, 1 mM Na3VO4. The lysates were incubated with 2.5 mM EZ-Link Hydrazide-LC-Biotin in dark for 2 h at room temperature. Biotin hydrazide bound proteins were captured using streptavidin-magnetic beads (Pierce) on a rotary mixer at 4 °C overnight. The beads were washed three times with lysis buffer and eluted with sample buffer for 10 min at 70 °C. Biotin hydrazide linked carbonylated LOXL2 and total input LOXL2 were detected by LOXL2 polyclonal antibody or Flag monoclonal antibody (M2) blot.

In vitro TGFβ receptor kinase assay. A549 cells were transiently co-transfected with Flag-tagged human TGFbeta receptor I and II. After 24 hours the cells were lysed in 1% NP40 lysis buffer (1% NP40, 20 mM Tris pH7.6, 200 mM NaCl plus protease inhibitor cocktail, 10 mM NaF, 1 mM Na3VO4), and the type I and II receptors were immunoprecipitated using anti-Flag antibody and Protein G-agarose (Roche). The beads were washed three times with kinase buffer (0.01% Triton X-100, 25 mM HEPES, pH 7.4, 2 mM MnCl2, 10 mM MgCl2, 20 μM DTT, 0.1 mM NaF, 0.1 mM Na3VO4). The kinase reactions were initiated by addition of 0.1 mM ATP in the presence or absence of inhibitors or lysate from A549 cells pre-treated with corilagin (1:10 dilution into kinase reaction). The kinase reactions were terminated by addition of an equal volume of 2 × sample buffer. The TGFβ receptor kinase activity was analyzed by SDS-PAGE and immunoblotting with anti-phosphotyrosine monoclonal antibody 4G10 and anti-Flag antibody.

ALK5/TGFβRI catalytic domain kinase assay. ALK5/TGFβRI kinase assays using purified catalytic domain was performed by Reaction Biology Corp., Malvern, Pennsylvania. The reaction buffer contains 20 mM Hepes (pH 7.5), 10 mM $MgCl_2$, 1 mM EGTA, 0.02% Brij35, 0.02 mg/ml BSA, 0.1 mM Na_3VO_4, 2 mM DTT, and 200 μM NAC. In brief, ten 3-fold series dilutions of 3Abd and controls pyrogallol or 2Abd starting at 100 μM was delivered into kinase reaction mixture with kinase, cofactors,

and substrate. After 20 min incubation at room temperature, ^{33}P-ATP was delivered into the mixture to initiate the reaction. Kinase activity was detected 2 h later by P81 filter-binding method.

Co-culture SBE reporter. NMuMG and A549 cells were transiently transfected with pGL(CAGA)$_{12}$Luc by using Turbofect reagent as specified by the manufacturer (Thermo Fisher). The transfected cells were seeded into 96-well plate in triplicates 24 hours after transfection. Co-cultured wells were seeded with transfected NMuMG cells and non-transfected A549 cells (1:5 ratio). The cells were pretreated with or without 1 μM corilagin, 1 μM EGCG, 10 μM 3Abd, or 5 μM SB431542 for 6 hours before stimulating with TGFβ1 overnight. The cells were lysed and luciferase activity was measured using the luciferase assay kit (E4030) from Promega.

qRT-PCR analysis. Total RNA (1 μg of each sample isolated using RNeasy Kit, 74004, Qiagen) was reverse transcribed using Superscript III (18080-051, Invitrogen) and assayed for gene expression using Platinum Quantitative PCR SuperMix-UDG (11730-025, Invitrogen). β-actin, GAPDH and S9 were used as internal controls and all the data were normalized by β-actin. The primer and probe sequences are listed in Supplemental Table 1.

Mouse lung cell sorting and analysis. Mouse lung single cell preparations were performed as previously described(57). Single cells were incubated for 1 hr at 4°C with the following primary antibodies: rat anti-mouse CD45 APC Cy7 (1:100, BD, #557659), rat anti-mouse PeCAM PE (1:100, BD, #553373), rat anti-mouse EpCAM Alexa 488 (1:250, BioLegend, #118210), and viability dye Sytox blue (1:1000, Thermo Fisher #S34857). Cell sorting was performed on BD FACS Aria cytometers. EpCAM+ and CD45+ cells were collected, respectively. EpCAM/CD45/CD31-triple negative cells were collected as mesenchymal cells. Each of the three cell types sorted from saline control, bleomycin control, and bleomycin EGCG groups (n=5) were lysed and blotted for p-Smad3 and total Smad3.

Protein and Lipid kinase screen. Protein kinase assays were conducted using the KinaseProfiler^{TM} service of Eurofins Pharma Discovery Services UK Limited. The kinase of interest was incubated with the test compound in assay buffer containing substrate, 10 mM magnesium acetate and [γ-

^{33}P-ATP]. The reaction was initiated by the addition of the Mg/ATP mix. After incubation at room temperature, the reaction was stopped by the addition of a 3% phosphoric acid solution. An aliquot of the reaction was then spotted onto a filtermat and washed in phosphoric acid followed by a rinse in methanol prior to drying and scintillation counting. Results were expressed in relation to controls containing DMSO only in place of test compound. The ATP concentration in each assay was within 15 μM of the determined apparent K_m for ATP.

Lipid kinase assays were conducted using the KinaseProfiler™ service of Eurofins Pharma Discovery Services UK Limited. The kinase of interest was incubated in assay buffer containing substrate and Mg/ATP. The reaction was initiated by the addition of the Mg/ATP solution. After incubation for 30 minutes at room temperature, the reaction was stopped by the addition of Stop solution containing EDTA and a biotinylated form of the reaction product. Finally, Detection buffer was added, containing europium-labelled anti-GST monoclonal antibody, a GST-tagged lipid binding domain and streptavidin-conjugated allophycocyanin. The plate was then read in time-resolved fluorescence mode and the homogeneous time-resolved fluorescence (HTRF) signal was determined according to the formula HTRF = 10000 x (Em665nm/Em620nm).

H_2O_2 scavenging assay. The oxidant scavenging activity of corilagin and Vitamin C were measured using Amplex Red Hydrogen Peroxide/Peroxidase assay kit (Thermo Fisher # A22188) following manufacturer's instructions. H_2O_2 (0.5 μM) samples were incubated with different concentrations of corilagin (0-100 μM) and Vitamin C (0-10 μM) for 2 h at room temperature before Amplex Red/HRP reaction and the plate read at Ex/Em 540/590 nm with a fluorescence plate reader (BMG LabTech FLUOstar). Compound vehicle was used for determination of the background fluorescence. Experiments were performed in triplicate and data were presented as means ± S.D.

Cell viability assay. AlamarBlue cell viability reagent (Thermo Fisher #DAL1025) was used to access cell viability. A549 or human primary lung fibroblasts (20,000 cells) in complete RPMI or DMEM medium were seeded into 96-well tissue culture plate for overnight, then the cells were exposed to

different compounds for 72 h. AlamarBlue reagent (1:10) was added to the cells followed by 2 h incubation at 37 ºC and absorbance at 570 nm was measured. Experiments were performed in triplicate using different batches of cells and data were presented as means ± S.D.

Statistics. Descriptive statistics are reported as means ± standard deviation (SD). For evaluation of two group differences, the unpaired 2-tailed Student's t-test or Mann-Whitney U-test was used assuming equal variance. Comparisons among multiple treatments were performed via one-way ANOVA for repeated measures. Differences between groups were assessed with Tukey's multiple comparison tests. A *P* value less than 0.05 was accepted as significant. Two-tailed Spearman's Rho Calculation was used to access the correlations. The survival of bleomycin-treated mice was analyzed by Chi test.

Study approval. All mice were maintained under specific pathogen–free conditions at UCSF according to IACUC protocol AN109566 and at MD Anderson Cancer Center according to IACUC protocol 00001271. For human subjects, written informed consent was obtained from each patient in accordance with the ethics guidelines for research in USA (protocols 10-02400 and 12-09662, approved by the IRB Committee of UCSF and protocol HSC20110086H, approved by IRB Committee of UT San Antonio Medical Center).

Figures and Figure Legends

Figure 1

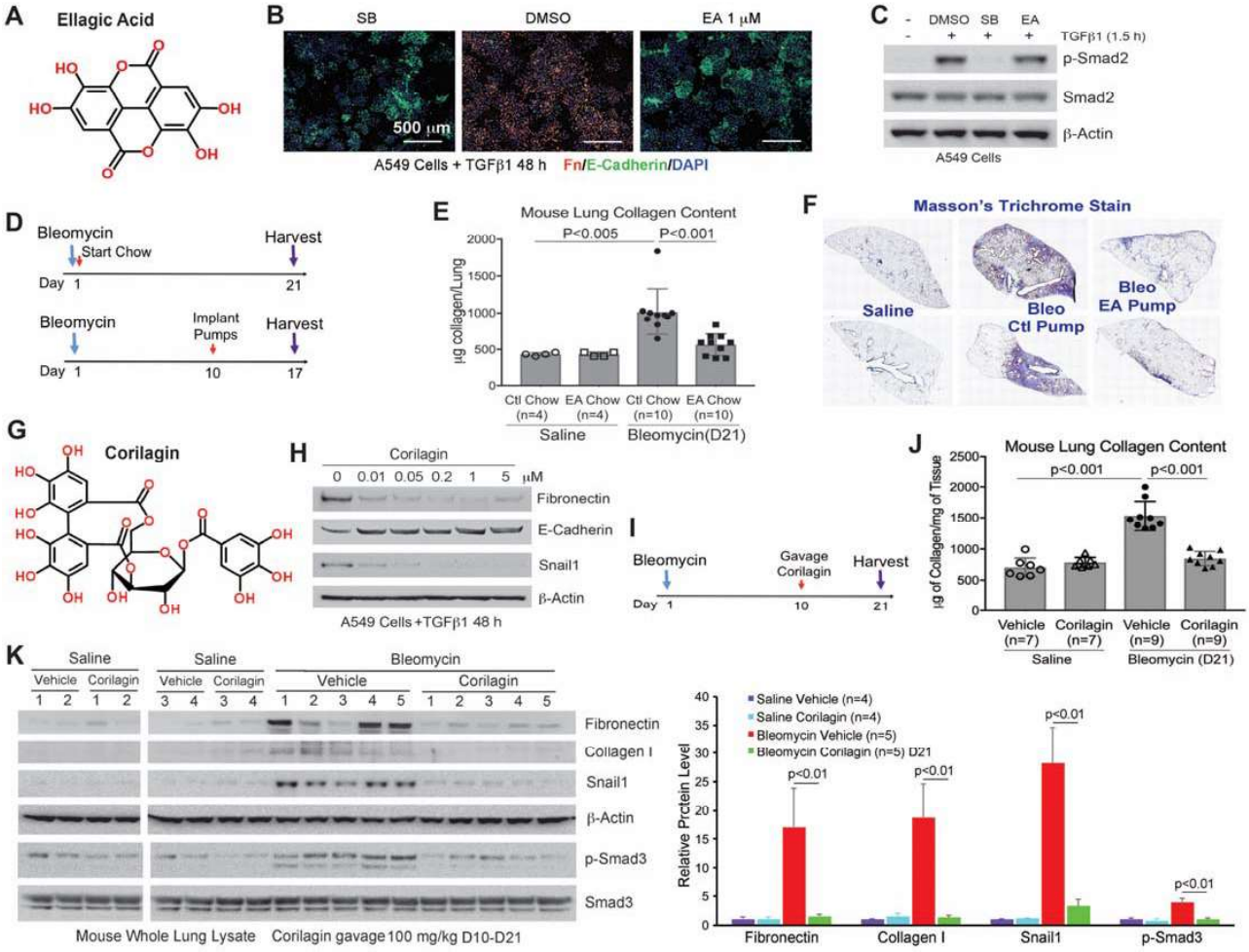

Figure 1. Ellagic acid (EA) and corilagin inhibit TGFβ1-dependent EMT and attenuate bleomycin-induced fibrogenesis. (**A**) Structure of ellagic acid. (**B**) Immunofluorescence of TGFβ1-stimulated A549 cells treated with DMSO, SB431542 (SB), or EA. E-cadherin green, fibronectin orange, and DAPI blue. Scale bar, 500 μm. Repeat=3. (**C**) A549 cells were treated with EA (1 μM) and TGFβ1 for 1.5 h and lysates immunoblotted for p-Smad2, Smad2, and β-actin. Repeat=3. (**D**) EA dosing and treatment in lung fibrosis model. EA and control chow were given to mice for 21 days. Osmotic pumps with EA or PBS were implanted on mice for 7 day at D10 after bleomycin. (**E**) Hydroxyproline analysis of lung tissues from saline ctl chow (n=4), saline EA chow (n=4), bleomycin ctl chow (n=10), and bleomycin EA chow (n=10) treated mice. Data represent mean±SD. (**F**) Masson's Trichrome staining of lung sections from ctl or EA pump-treated mice 17 days after bleomycin. Mosaic images (4x) covering whole lung section are shown. (**G**) Structure of corilagin. (**H**) A549 cells stimulated with TGFβ1 were treated with corilagin (0-5 μM) for 48 h and lysates blotted for fibronectin, E-cadherin, Snail1, and β-actin. Repeat=3. (**I**) Corilagin dosing and treatment in lung fibrosis model. Vehicle or corilagin were given to mice by daily gavage starting from D10 after bleomycin for 11 days. (**J**) Hydroxyproline analysis of lung tissues from saline vehicle (n=7), saline corilagin (n=7), bleomycin vehicle (n=9), and bleomycin corilagin (n=9) treated mice. Data represent mean±SD. (**K**) Whole lung lysates from mice given saline vehicle (n=4), saline corilagin (n=4), bleomycin vehicle (n=5), and bleomycin corilagin (n=5) were blotted for fibronectin, collagen I, Snail1, β-actin, p-Smad3, and total Smad3. Quantification of bands normalized to β-actin are expressed as mean±SD. Data from **F**, **K**, and **L** are analyzed by one-way ANOVA with a Tukey post hoc test.

Figure 2

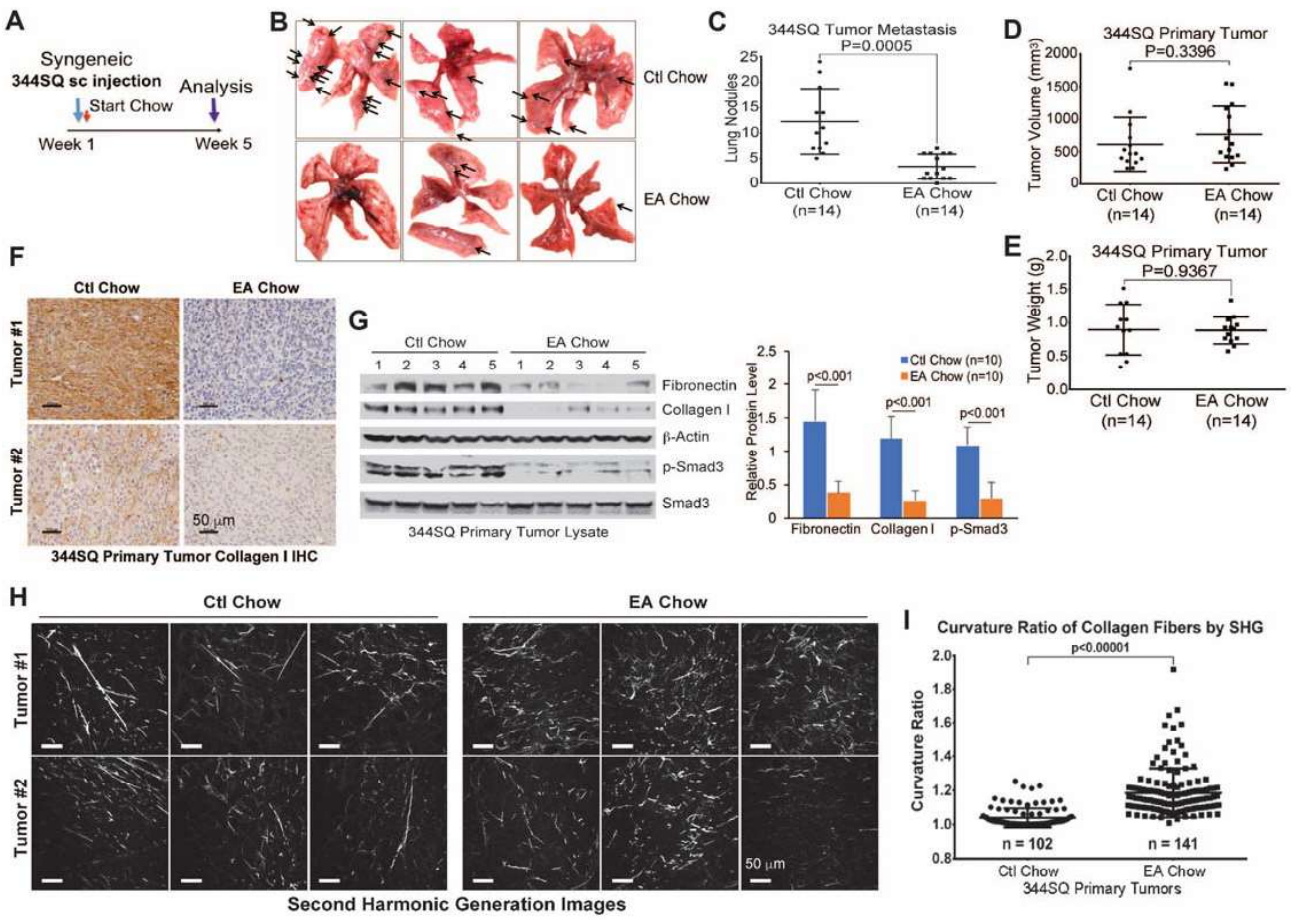

Figure 2. EA-rich diet attenuates 344SQ lung tumor metastasis and primary tumor collagen cross-linking. (**A**) Implantation and treatment in syngeneic lung cancer model. Metastatic 344SQ tumor cells were subcutaneously injected in syngeneic mice at 12-week old and treated with ctl or EA chow for 5 weeks. (**B**) Representative pictures of lung metastasis of 344SQ tumors treated with ctl or EA chow. (**C**) Quantification of lung metastasis of 344SQ tumors treated with ctl or EA chow (n=14 mice per group). (**D**) Total volume of 344SQ tumors treated with ctl or EA chow (n=14 mice per group). (**E**) Total tumor weight (grams) of ctl or EA chow treated 344SQ primary tumors (n=14 mice per group). (**F**) Collagen I immunohistochemistry (IHC) of 344SQ primary tumors treated with ctl or EA chow. Scale bar, 50 μm. (**G**) Ctl or EA chow treated 344SQ primary tumors were lysed and immunoblotted for fibronectin, collagen I, β-actin, p-Smad3, and total Smad3. Quantification of bands normalized to β-actin were pooled from 10 mice per group. Data represent mean±SD. Each protein is analyzed by one-way ANOVA with a Tukey post hoc test. (**H**) Representative second harmonic generation (SHG) images from 344SQ primary tumors treated with ctl or EA chow. (**I**) Quantification of curvature ratio for individual collagen fibers imaged by SHG microscopy of primary 344SQ tumor tissues treated with ctl (n=102 collagen fibers per sample) or EA chow (n=141 collagen fibers per sample). Data for **C-E** and **I** are expressed as mean±SD. P value by unpaired two-tailed t-test.

Figure 3

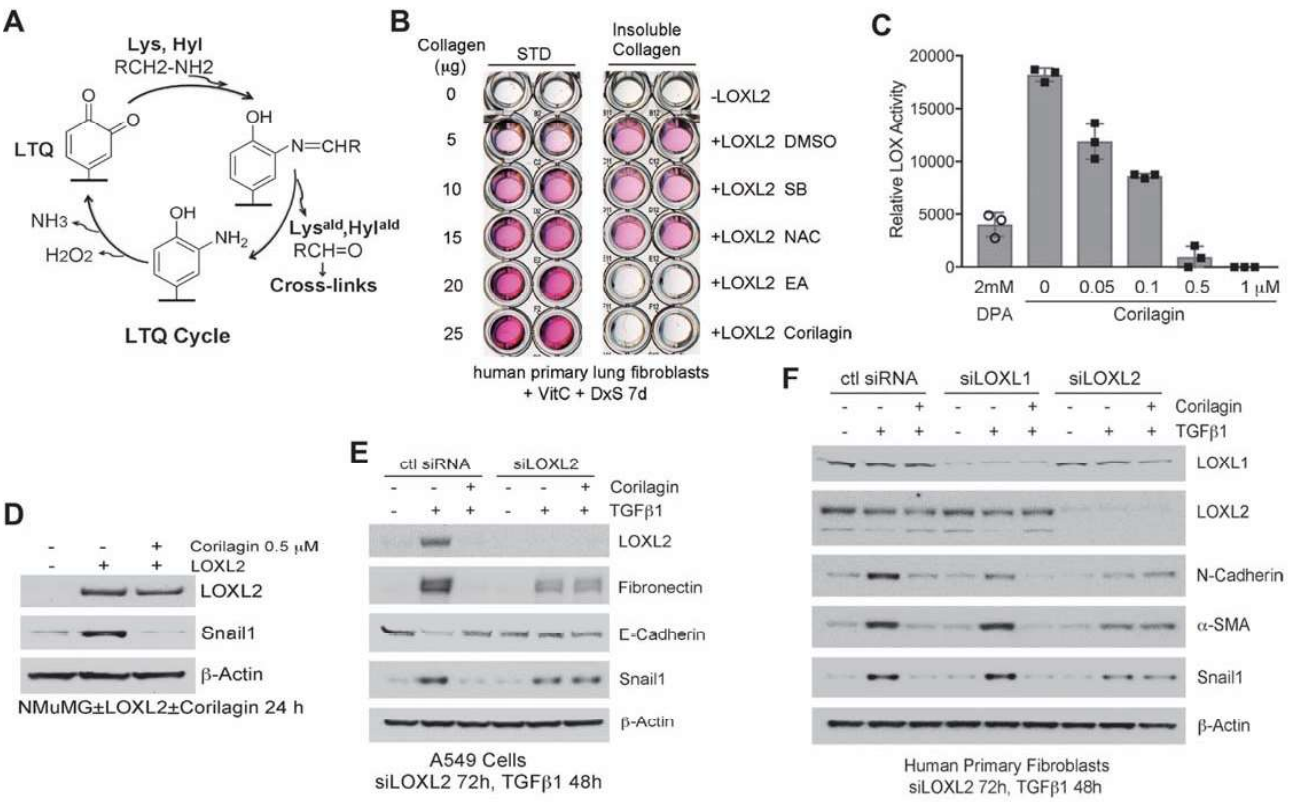

Figure 3. Identification of LOXL2 as the target of EA and corilagin. Requirement for active LOXL2 for corilagin-induced inhibition of EMT and Snail expression. (**A**) LTQ cycle. LTQ converts lysine to allysine and yields an aminophenol intermediate. Subsequent hydrolyses releases allysine and the original cofactor, producing hydrogen peroxide and ammonia as side products. (**B**) Primary human lung fibroblasts cultured in the presence of vitamin C and dextran sulfate were treated with recombinant human LOXL2 and different inhibitors for 7 days. The insoluble cross-linked collagen was extracted and measured by Sircol assay. SB: SB431542, TβRI inhibitor; NAC: N-acetylcysteine, antioxidant. (**C**) Recombinant human LOXL2 was incubated with 2 mM penicilamine (DPA) or different concentrations of corilagin (0-1 μM) for 1 h and LOX activity was measured. Data represent mean±SD. n=3. (**D**) NMuMG cells over-expressing human LOXL2 were incubated with or without 0.5 μM corilagin for 24 h, lysed, and immunoblotted for LOXL2, Snail1, and β-actin. (**E**) A549 cells transfected with siRNA to LOXL2 were stimulated with TGFβ1 or left un-stimulated for 48 h in the presence or absence of 1 μM corilagin. The lysates were immunoblotted for LOXL2, fibronectin, E-cadherin, Snail1, and β-actin. (**F**) Primary human lung fibroblasts transfected with siRNAs to LOXL1 or LOXL2 were stimulated with TGFβ1 or left un-stimulated for 72 h in the presence or absence of 1 μM corilagin and the lysates were immunoblotted for LOXL1, LOXL2, N-cadherin, alpha smooth muscle actin (α-SMA), Snail1, and β-actin. **B, D, E, F** are representative of at least three experiments with similar results.

Figure 4

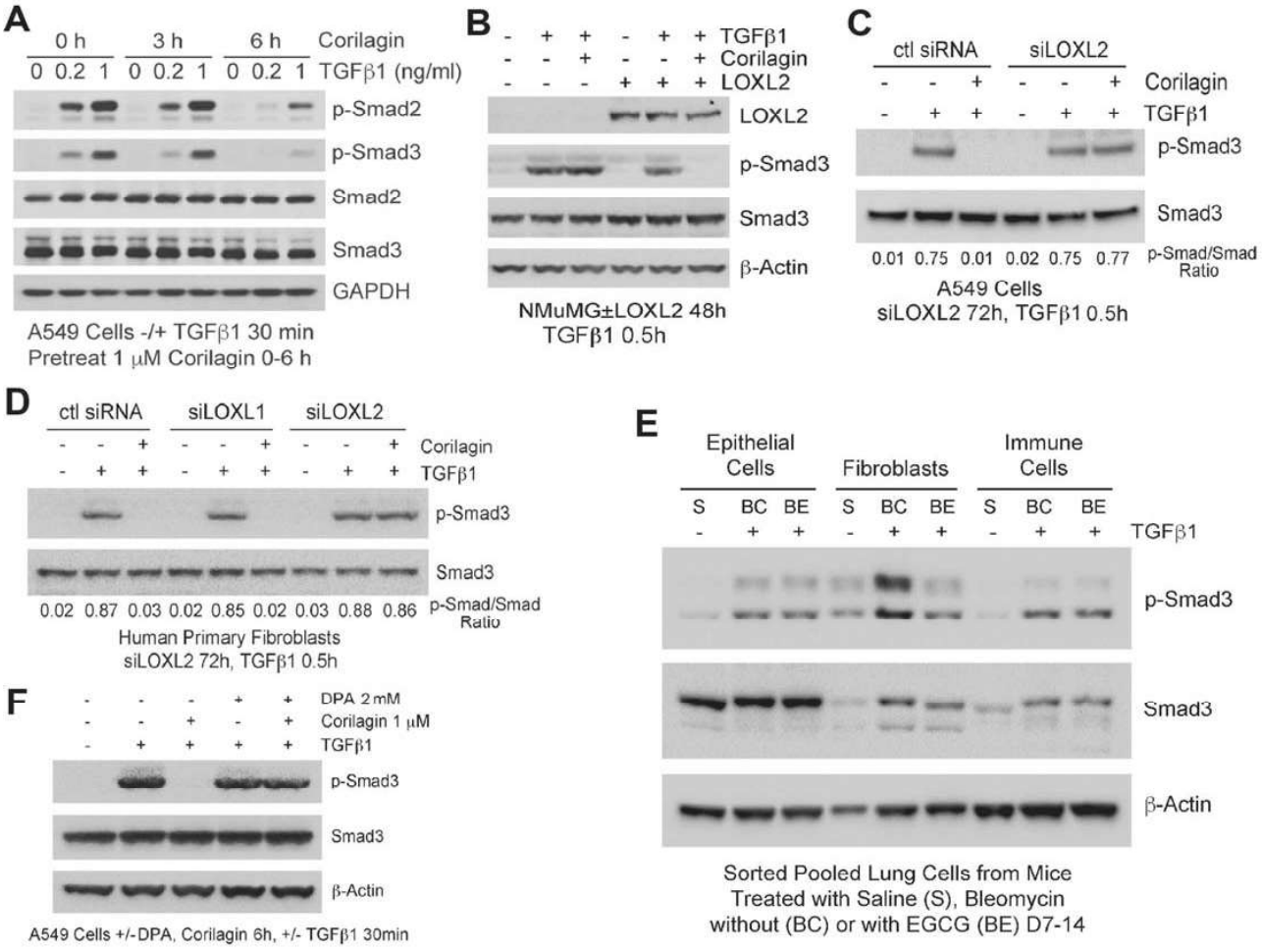

Figure 4. Corilagin inhibition of TGFβ1 signaling is dependent on LOXL2 activity. (**A**) A549 cells pre-treated with 1 μM corilagin for 0 h, 3 h, or 6 h were stimulated with different doses of TGFβ1 (0, 0.2, or 1 ng/ml) for 30 min and the cell lysates were blotted for p-Smad2, p-Smad3, Smad2, Smad3, and β-actin. (**B**) NMuMG cells transfected with human LOXL2 or empty vector were pretreated with 1 μM corilagin or DMSO for 6 h and then incubated without or with TGFβ1 for 30 min. The cell lysates were blotted for LOXL2, p-Smad3, Smad3, and β-actin. (**C-D**) A549 cells transfected with siRNA to LOXL2 (**C**) and primary human lung fibroblasts transfected with siRNAs to LOXL1 or LOXL2 (**D**) were pre-treated with 1 μM corilagin or DMSO for 6 h before incubating without or with TGFβ1 for 30 min. The cell lysates were blotted for p-Smad3 and Smad3. The ratio of p-Smad3/Smad3 for each lane is shown. (**E**) Mouse lung epithelial cells, fibroblasts, and immune cells sorted from mice treated for 14 days with saline (S), bleomycin with vehicle control (BC), or bleomycin with 7 days oral EGCG (100 mg/kg) (BE), were immediately treated with TGFβ1 for 30 min and cell lysates blotted for p-Smad3, total Smad3, and β-Actin. n=5 for each group. (**F**) A549 cells were pre-treated with 1 μM corilagin with or without 2 mM penicilamine (DPA) for 6 h before TGFβ1 stimulation for 30 min. The cell lysates were blotted for p-Smad3, Smad3, and β-actin. The data from **A-D** and **F** are representative of at least three experiments with similar results.

Figure 5

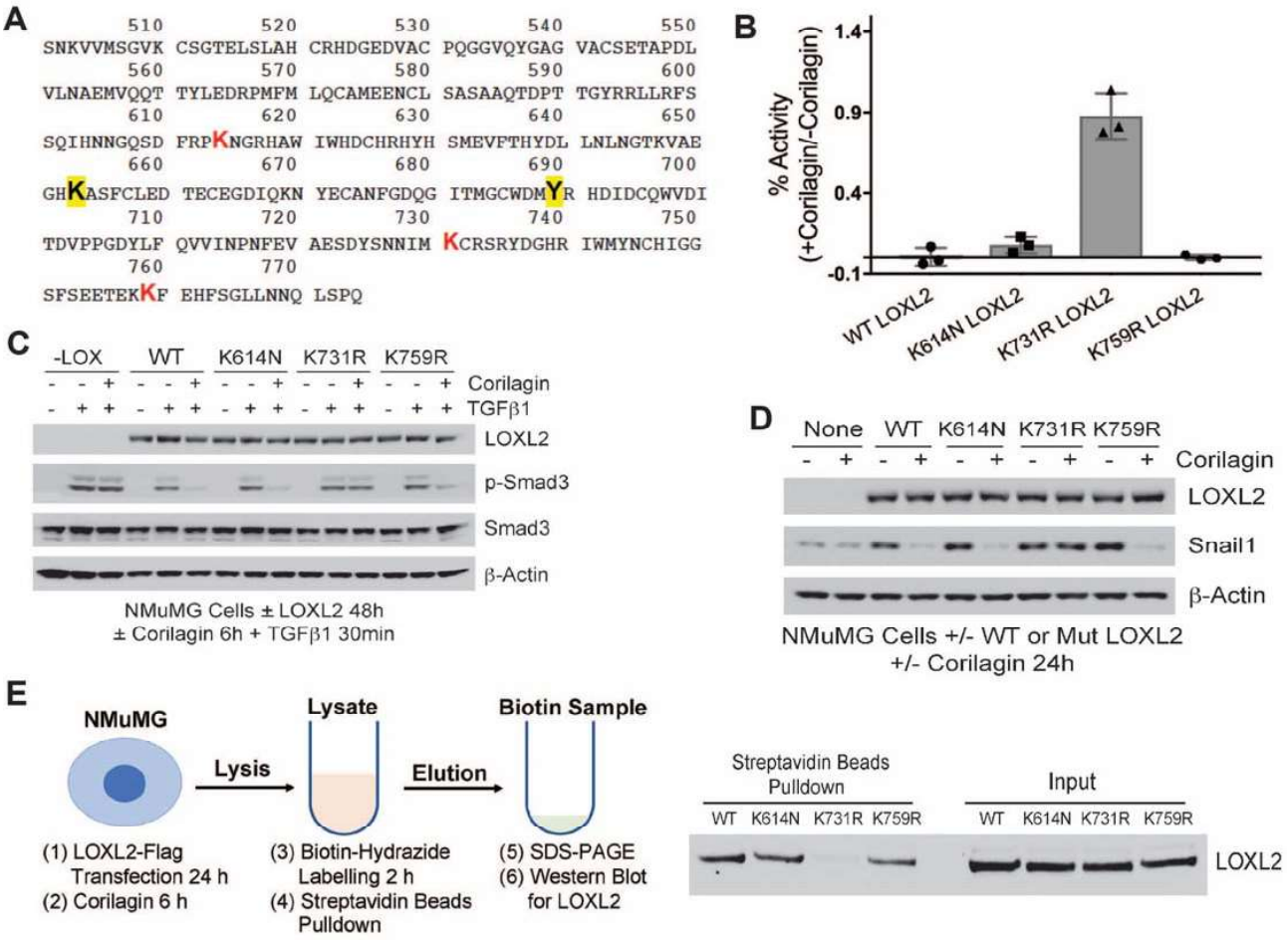

Figure 5. Trihydroxyphenolic motif mimics the LTQ leading to auto-oxidation of LOXL2 K731 and inactivation of LOXL2. (**A**) Catalytic domain sequence of LOXL2. Catalytic domain: P548-S751. LTQ sites are highlighted and bolded (K653 and Y689). The three point mutation sites are in red (K614N, K731R, K759R). (**B**) NMuMG cells transfected with wild-type or mutant human LOXL2 were treated with 1 μM corilagin or DMSO for 6 h. LOX activity of conditioned media from treated cells was measured. Data presented as percent activity of no corilagin control. Mean±SD, n=3. (**C**) NMuMG cells transfected with wild-type or mutant human LOXL2 were pretreated with 1 μM corilagin or DMSO for 6 h and then incubated without or with TGFβ1 for 30 min. The cell lysates were immunoblotted for LOXL2, p-Smad3, Smad3, and β-actin. (**D**) NMuMG cells transfected with wild-type or mutant human LOXL2 were incubated with or without 1 μM corilagin for 24 h and lysates were immunoblotted for LOXL2, Snail1, and β-actin. (**E**) NMuMG cells transfected with wild-type or mutant human LOXL2 incubated with 1 μM corilagin for 6 h and labelled with 2.5 mM biotin-hydrazide for 2 h. The biotin-hydrazide linked carbonylated LOXL2 was pulled down with streptavidin-magnetic beads and the precipitates and input protein were immunoblotted for LOXL2. **C-E** are representative of at least three experiments with similar results.

Figure 6

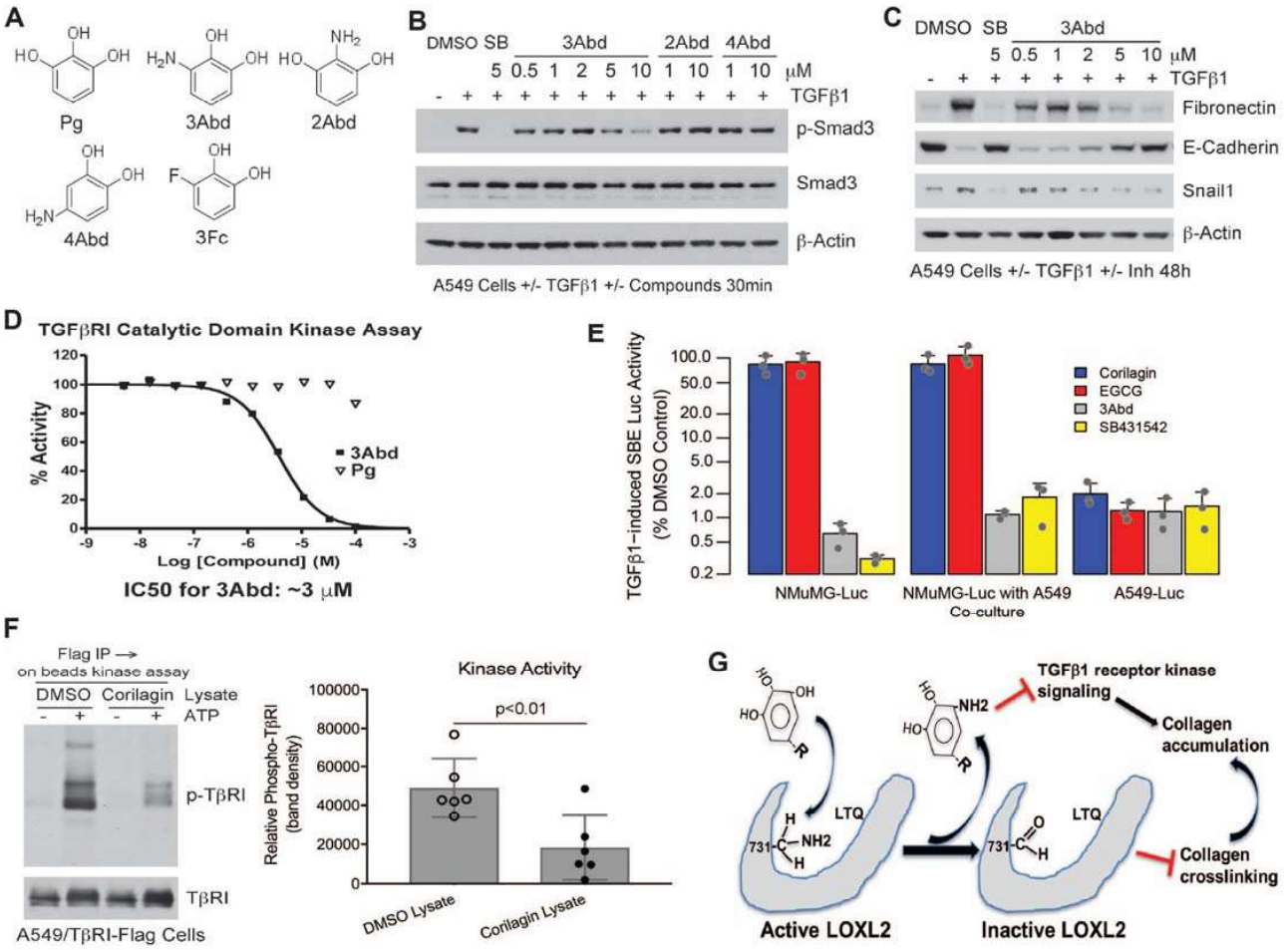

Figure 6. Generation of a novel non-diffusible TβRI kinase inhibitor. (**A**) Structure of pyrogallol (Pg), 3Abd and derivatives. (**B**) A549 cells were stimulated with TGFβ1 for 30 min and lysates immunoblotted for p-Smad3, Smad3, and β-actin. Treatment without pre-incubation: 3Abd (0.5-10 μM), 2Abd or 4Abd (1,10μM). (**C**) A549 cells were stimulated with TGFβ1 for 48 h and lysates immunoblotted for LOXL2, fibronectin, E-cadherin, Snail1, and β-actin. 3Abd (0.5-10 μM). (**D**) Purified ALK5/TGFβRI catalytic domain kinase assay was performed with ten doses of 3Abd or Pg starting from 100 μM. Kinase activity was indicated by ^{33}P-ATP signals and IC50 of 3Abd was calculated as ~3 μM. **B-D** are representative of three experiments with similar results. (**E**) SBE reporter transfected NMuMG and A549 cells were seeded into 96-well plate. Co-cultured wells were seeded with 5K transfected NMuMG cells and 25K non-transfected A549 cells. Cells were pretreated with or without 1 μM corilagin, 1 μM EGCG, 10 μM 3Abd, or 5 μM SB431542 for 6 hours and stimulated with TGFβ1 overnight before lysis for luciferase assay. Data presented as percent TGFβ1-induced SBE luciferase activity of DMSO control in log scale. Mean±SD, n=3. (**F**) Flag-tagged TβRI and TβRII were immunoprecipitated from A549 cells and in vitro kinase assay performed on beads exposed to lysate pretreated with corilagin or DMSO. The final reaction was eluted and analyzed by immunoblotting for phosphotyrosine and TβRI. The phosphotyrosine bands were quantified using Image J and normalized to DMSO control. Data represent mean±SD. P value by unpaired two-tailed t-test of six separate experiments. (**G**) Schematic overview of mechanism. A trihydroxyphenolic-containing compound engages active LOXL2 initiating auto-oxidation of K731 and creating a key allysine inactivating the enzyme. In the process, a 3-aminobenzene-1,2-diol (3Abd)-like metabolite is generated that then blocks TGFβRI kinase. The combined effects block pathological collagen accumulation.

Table 1. The survival of bleomycin-treated mice by day 21 of EA chow and day 17 of EA pump treatment

		EA	Control	Chi Square Test
Chow	Alive	10	6	P=0.0308
	Dead	4	8	
Pump	Alive	10	6	P=0.0154
	Dead	1	5	
Total	Alive	20	12	P=0.0014
	Dead	5	13	

Table 2. Collagen cross-links in 344SQ tumors treated with ctl or EA chow (moles/mole of collagen)

	Ctl Chow Mean (±SD) (n=3)	EA Chow Mean (±SD) (n=3)	Ctl vs EA p value
DHLNL	0.1 (0.00)	0.05 (0.01)	**0.005**
HLNL	0.39 (0.02)	0.25 (0.02)	**0.0015**
HHMD	0.23 (0.07)	0.14 (0.06)	0.26
PYD	0.19 (0.00)	0.26 (0.07)	0.33
DPD	0.039 (0.01)	0.022 (0.01)	**0.0221**

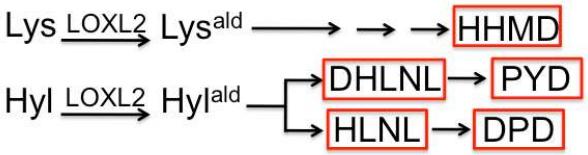

Lys: lysine; Hyl: hydroxylysine; ald: aldehyde;
HHMD: dehydro-histidinohydroxymerodesmosine;
DHLNL: dehydro-dihydroxylysinonorleucine/its ketoamine;
HLNL: dehydro-hydroxylysinonorleucine/its ketoamine;

Supplementary Figures with Legends

Supplemental Figure S1

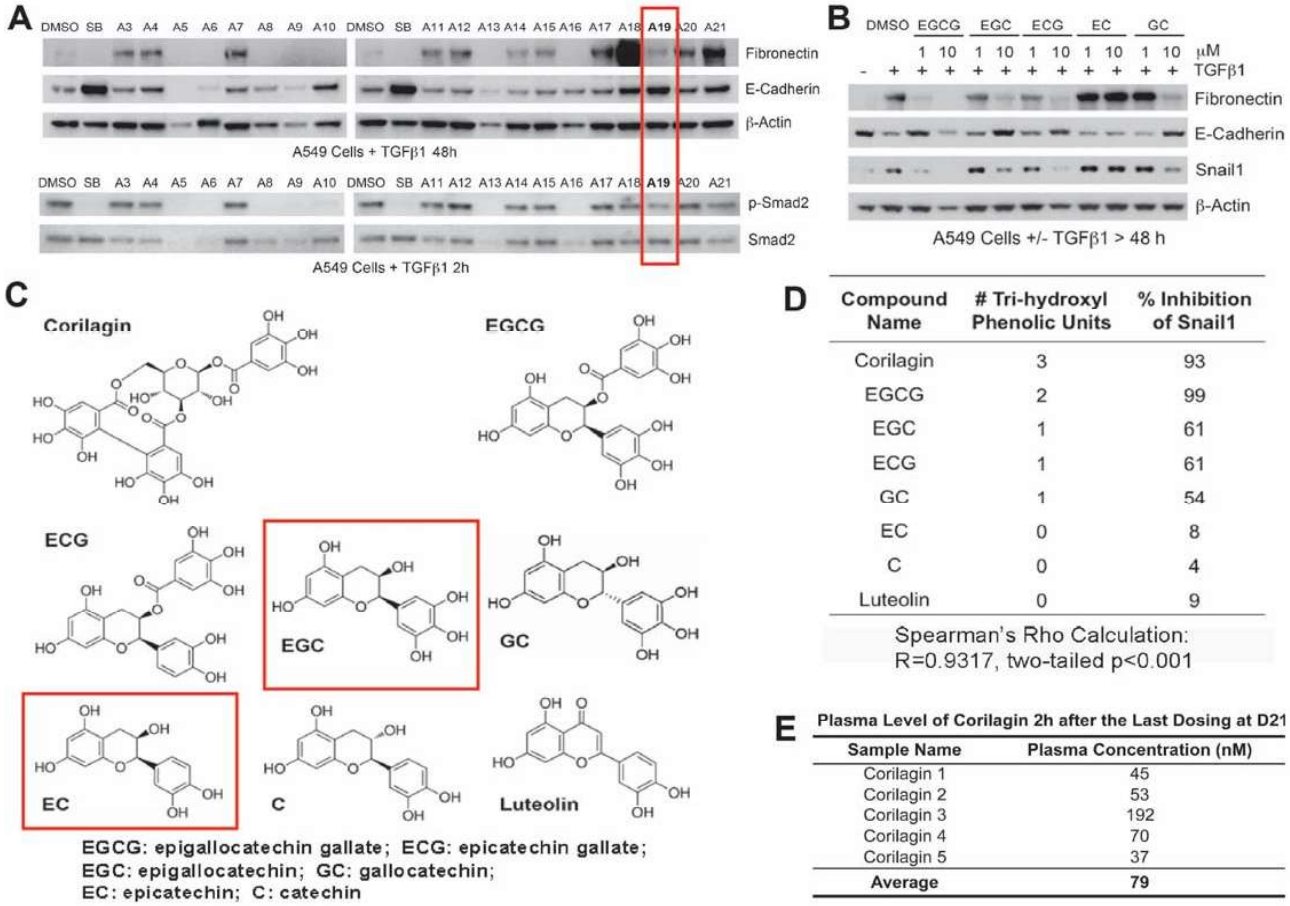

D

Compound Name	# Tri-hydroxyl Phenolic Units	% Inhibition of Snail1
Corilagin	3	93
EGCG	2	99
EGC	1	61
ECG	1	61
GC	1	54
EC	0	8
C	0	4
Luteolin	0	9

Spearman's Rho Calculation:
R=0.9317, two-tailed p<0.001

E

Plasma Level of Corilagin 2h after the Last Dosing at D21

Sample Name	Plasma Concentration (nM)
Corilagin 1	45
Corilagin 2	53
Corilagin 3	192
Corilagin 4	70
Corilagin 5	37
Average	**79**

Supplemental Figure S1. Ellagic acid (EA) and other trihydroxyphenolic compounds inhibit TGFβ1-dependent EMT. (**A**) A549 cells were stimulated with TGFβ1 in the presence of ALK5 inhibitor SB431542 and 21 lead compounds from high-throughput screening for 48 hours. The lysates were blotted for fibronectin, E-cadherin, and β-actin. The cells treated for 2 hours were blotted for p-Smad2 and Smad2. Note, two lead compounds were excluded due to solubility issue. (**B**) A549 cells stimulated with TGFβ1 were treated with different catechins (1 and 10 μM) for 48 h and the lysates were blotted for fibronectin, E-cadherin, snail1, and β-actin. The data shown is a representative of at least three experiments with similar results. (**C**) Structure comparison of corilagin, catechins, and luteolin. (**D**) Correlation of trihydroxyphenolic motif and inhibition of TGFβ1-induced snail1. Data were expressed as percent inhibition of Snail1 by compounds vs DMSO control. Correlation was analyzed by Spearman's Rho Calculation. (**E**) Plasma levels of corilagin 2 hours after the last oral dosing of 100 mg/kg at day 21. n=5.

Supplemental Figure S2

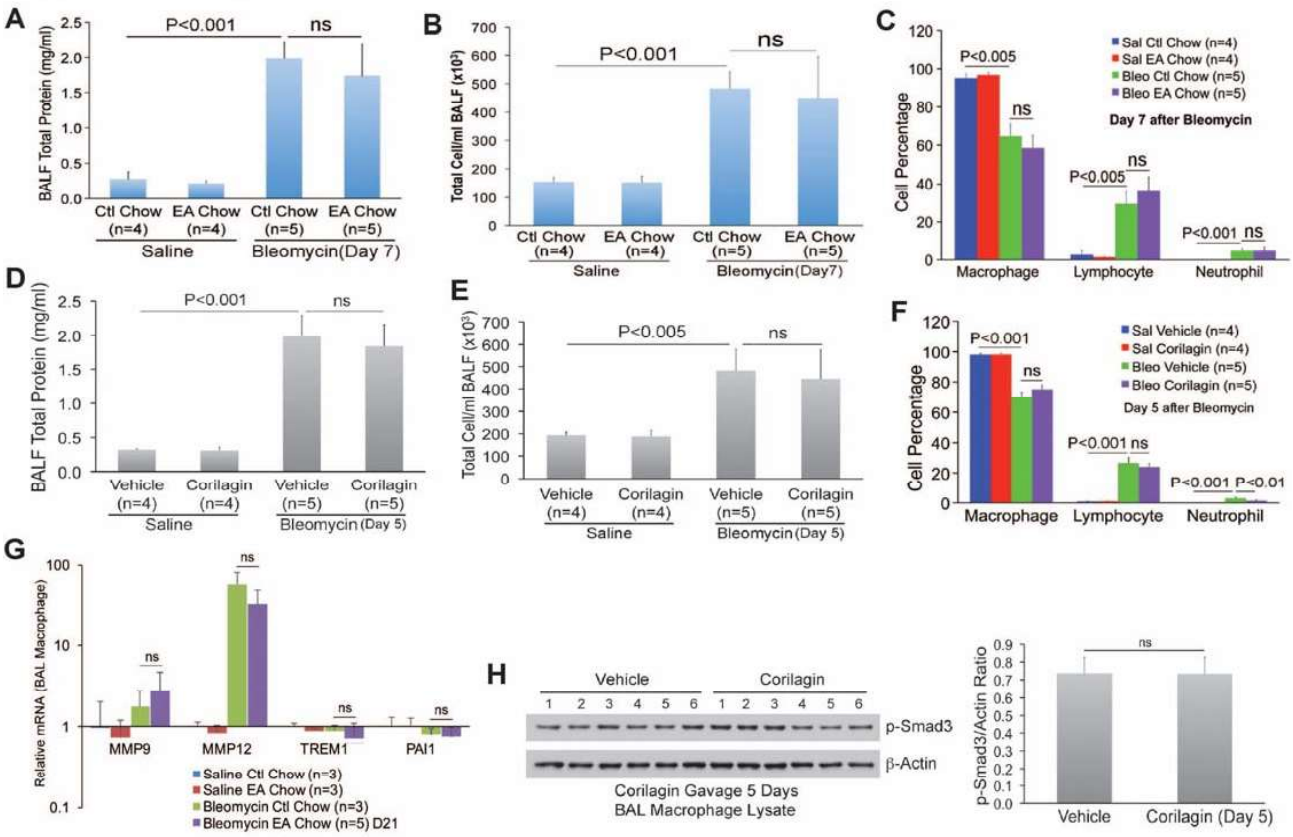

Supplemental Figure S2. Ellagic acid and corilagin do not affect immune cell distribution or macrophage TGFβ1 response in vivo. (**A-C**) Total protein concentration (**A**), total cell counts (**B**), and immune cell distribution (**C**) from bronchoalveolar lavage fluid (BALF) of mice intratracheal injected with saline or bleomycin treated with ctl or EA chow. (**D-F**) Total protein concentration (**D**), total cell counts (**E**), and immune cell distribution (**F**) from BALF of mice intratracheal injected with saline or bleomycin treated with vehicle or corilagin. n=4-5. (**G**) Transcripts of TGFβ1–responsive genes were measured in RNA extracts by qRT-PCR from BALF pellets intratracheal injected with saline or bleomycin for 21 days and treated with EA or control pump (n=3-5/group). Metalloproteinase (MMP)9, MMP12, TREM1, and plasminogen activator type I (PAI)1 mRNA levels are normalized to that of β-actin. Data for **A-G** represent mean±SD. P value by one-way ANOVA with a Tukey post hoc test. "ns", not significant. (**H**) Airway macrophages from BALF of mice intratracheal injected with saline or bleomycin for 5 days and treated with vehicle or corilagin were lysed and blotted for p-Smad3 and β-actin (left). Quantification (mean±SD) of densitometry values of p-Smad3/β-actin ratio (n=6) was shown (right). P value by unpaired two-tailed t-test. "ns", not significant by t-test. The data from **A-F** are representative of at least three experiments with similar results.

Supplemental Figure S3

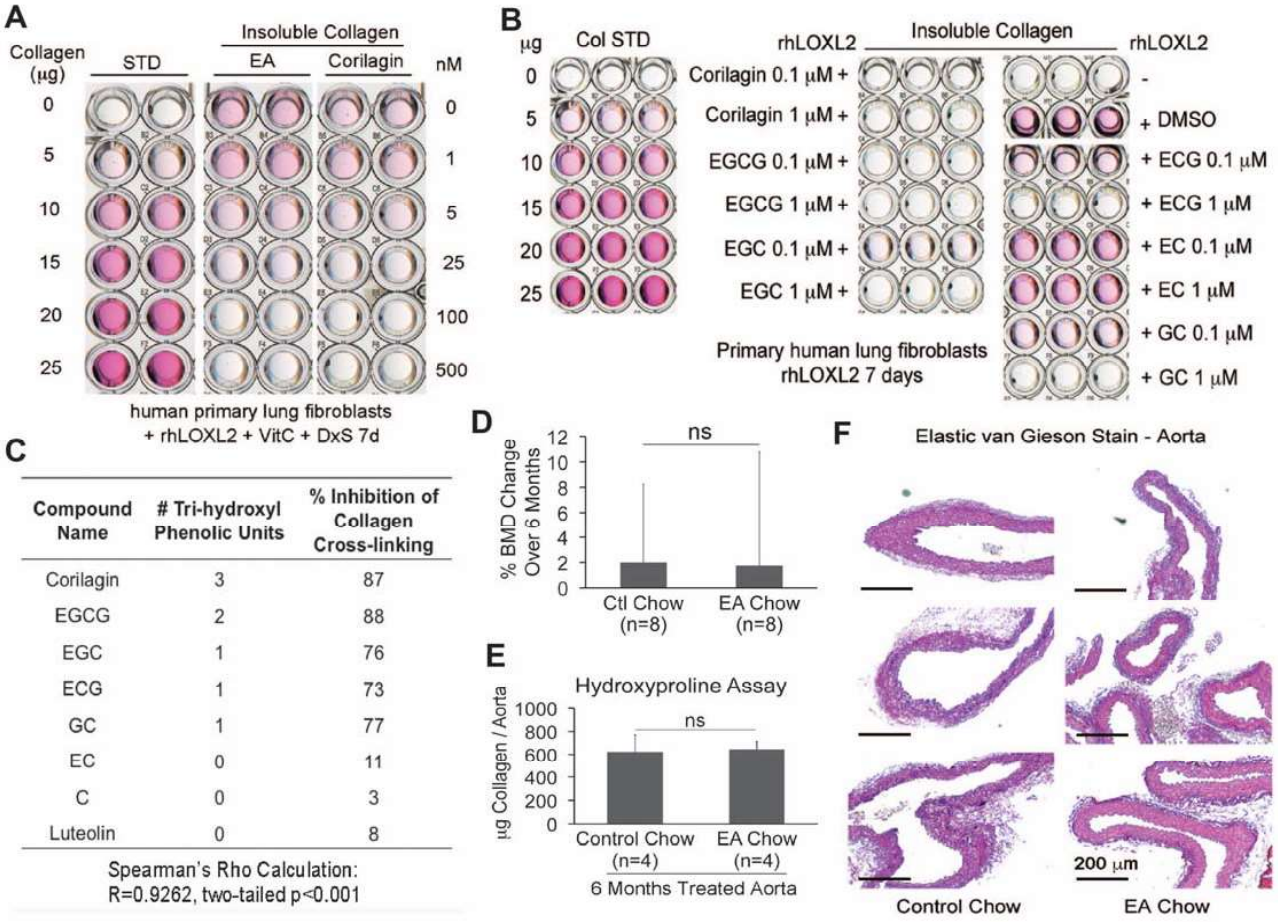

Compound Name	# Tri-hydroxyl Phenolic Units	% Inhibition of Collagen Cross-linking
Corilagin	3	87
EGCG	2	88
EGC	1	76
ECG	1	73
GC	1	77
EC	0	11
C	0	3
Luteolin	0	8

Spearman's Rho Calculation:
R=0.9262, two-tailed p<0.001

Supplemental Figure S3. Trihydroxyphenolic compounds inhibit LOXL2-dependent collagen cross-linking. (**A-B**) Primary human lung fibroblasts cultured in the presence of Vitamin C and Dextran Sulfate were treated with recombinant human LOXL2 (rhLOXL2) in the presence of different concentrations of EA or corilagin (0-500 nM) (**A**) or catechins (**B**) for 7 day. The insoluble cross-linked collagen was extracted and measured by Sircol assay. (**C**) Correlation of trihydroxyphenolic motif and inhibition of rhLOXL2-induced collagen cross-linking. Long-term EA chow treatment does not affect bone mineral density or aorta collagen content. Data were expressed as percent inhibition of collagen cross-linking by compounds vs DMSO control. Correlation was analyzed by Spearman's Rho Calculation. (**D**) Change in bone mineral density (% BMD Change Over 6 Months) from baseline at lumbar spine and proximal femur in mice treated with ctl chow (n=8) or EA chow (n=8). Data are expressed as mean±SD. "ns" indicates not significant (unpaired two-tailed t-test). (**E**) Hydroxyproline analysis of aortas isolated from mice treated with ctl chow (n=4) or EA chow (n=4) for 6 months. Data are expressed as mean±SD. "ns" indicates not significant (unpaired two-tailed t-test). (**F**) Elastic van Gieson stain of paraffin sections of aortas from mice treated with ctl chow (n=3) or EA chow (n=3) for 6 months. Scale bar, 200 µm. The data shown in **A** and **B** are representative of at least three experiments with similar results.

Supplemental Figure S4

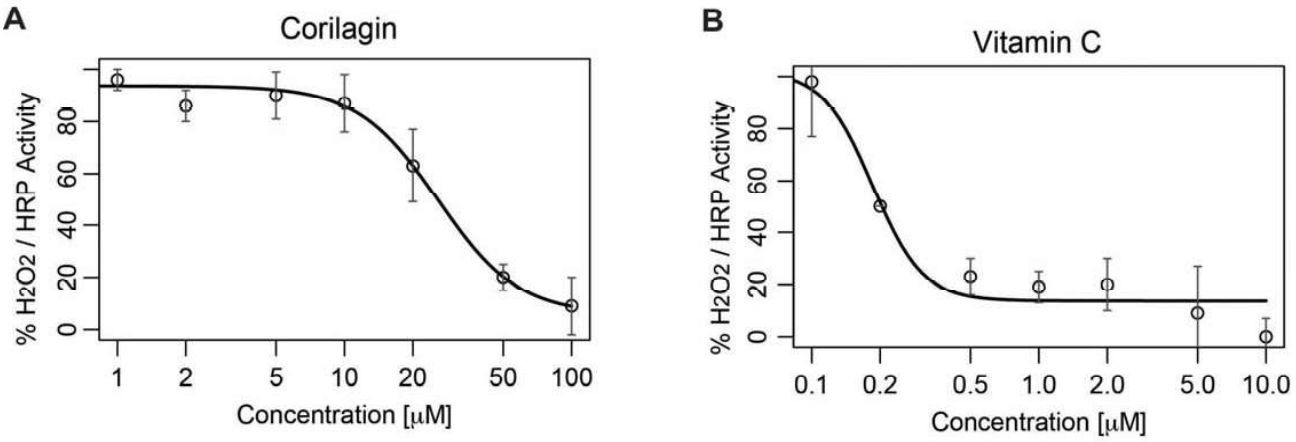

Supplemental Figure S4. Corilagin does not function as an antioxidant. Hydrogen peroxide radical scavenging activity of corilagin (0-100 μM) (**A**) and Vitamin C (0-10 μM) (**B**). Data are presented as mean percent H_2O_2/HRP activity (vs no compound control)±SD of triplicates. A representative of three independent experiments is shown.

Supplemental Figure S5

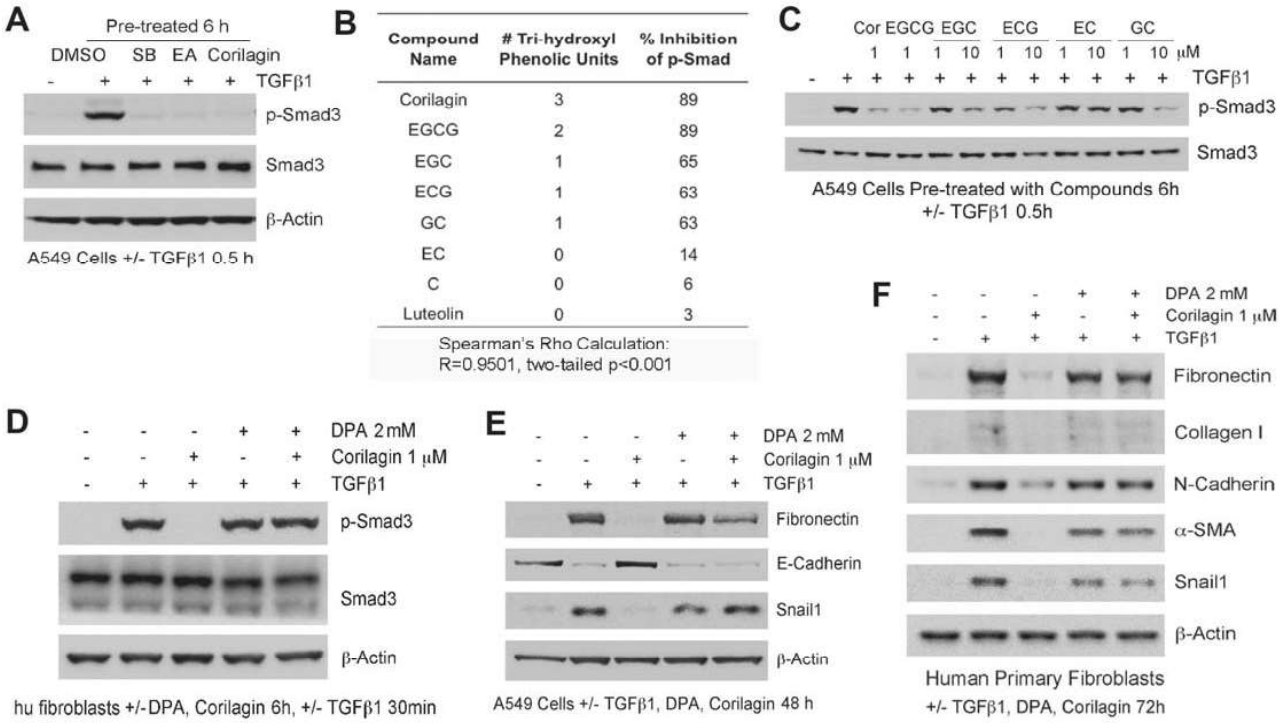

Supplemental Figure S5. Trihydroxyphenolic compounds inhibit TGFβ1 but not EGF signaling. Corilagin inhibition of TGFβ1 responses is dependent on LOXL2 activity. (**A**) A549 cells pre-treated with different inhibitors for 6 h were stimulated with TGFβ1 (4 ng/ml) for 30 min and the cell lysates were blotted for p-Smad3, Smad3, and β-actin. (**B**) Correlation of trihydroxyphenolic motif and inhibition of TGFβ1 signaling. Data were expressed as percent inhibition of p-Smad3 by compounds vs DMSO control. Correlation was analyzed by Spearman's Rho Calculation. (**C**) A549 cells pre-treated with corilagin and catechins for 6 h were stimulated with TGFβ1 for 30 min and the cell lysates were blotted for p-Smad3 and Smad3. (**D**) Primary human lung fibroblasts were pre-treated with 1 μM corilagin with or without 2 mM penicilamine (DPA) for 6 h before TGFβ1 stimulation for 30 min. The cell lysates were blotted for p-Smad3, Smad3, and β-actin. (**E**) A549 cells were stimulated with TGFβ1 or left un-stimulated for 48 h in the presence or absence of 1 μM corilagin with or without 2 mM penicilamine (DPA) and the lysates were blotted for fibronectin, E-cadherin, Snail1, and β-actin. (**F**) Primary human lung fibroblasts were stimulated with TGFβ1 in the presence or absence of 1 μM corilagin with or without penicillamine (DPA) for 72 h. The lysates were blotted for fibronectin, collagen I, N-cadherin, α-SMA, Snail1, and β-actin. All the data shown are representative of at least three experiments with similar results.

Supplemental Figure S6

A **Table I. Correlation of LOXL2 Level and Corilagin Inhibitory Effect on TGFβ1 Response**

Cell Type	Relative LOXL2 Level	Corilagin Inhibition of p-Smad3 (%) Mean (±SD) n=3
A549 (human lung adenocarcinoma)	3070	90 (1)
H358 (human lung adenocarcinoma)	3616	89 (5)
H1299 (human lung adenocarcinoma)	1641	78 (4)
MDA-MB-231 (human breast adenocarcinoma)	30574	93 (2)
Human primary lung fibroblasts	20171	94 (2)
Mouse primary lung fibroblasts	8903	90 (1)
MCF-10A (human mammary epithelial cells)	1	7 (2)
HaCaT (human keratinocytes)	226	8 (1)
NMuMG (mouse mammary epithelial cells)	388	10 (3)
Mouse primary alveolar type II cells	15	3 (1)
Mouse primary alveolar macrophages	6	2 (1)

Spearman's Rho Calculation: R=0.9476, two-tailed p<0.001

B

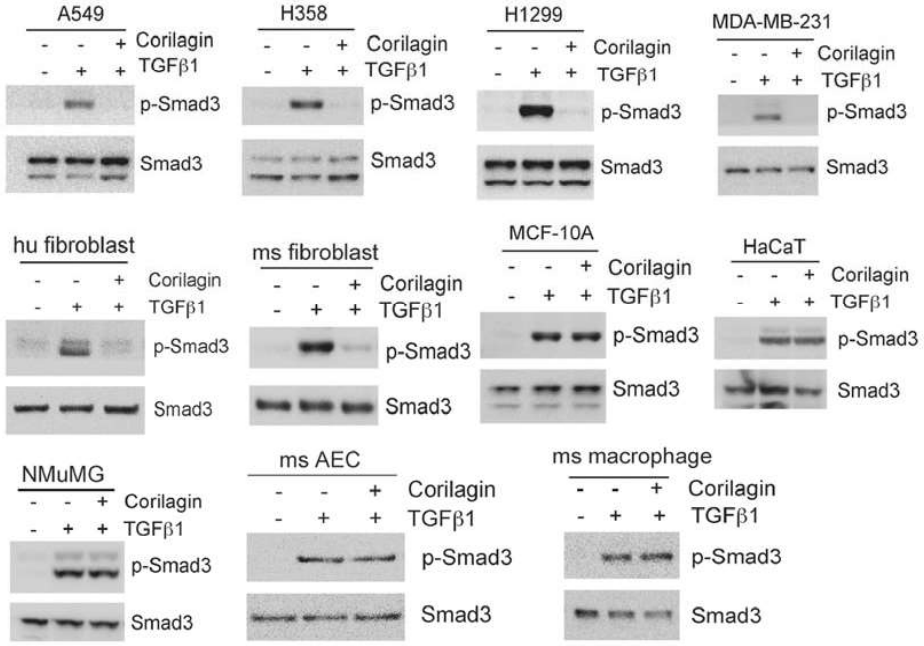

Supplemental Figure S6. Corilagin inhibition of TGFβ1 signaling is dependent upon LOXL2 expression in target cells. (**A**) Correlation of cellular LOXL2 levels and corilagin inhibition of TGFβ1 signaling. LOXL2 levels were determined by qPCR and LOXL2 levels in each cell type were expressed as fold vs that in MCF-10A (1). P-Smad3 inhibition was quantified from three independent experiments and data represent mean percent inhibition by corilagin vs DMSO control±SD. n=3. Correlation was analyzed by Spearman's Rho Calculation. (**B**) Different cells were pre-treated with 1 μM corilagin for 6 h before stimulating with TGFβ1 for 30 min and the cell lysates were blotted for p-Smad3 and Smad3. Results from representative of three experiments for each cell type are shown.

Supplemental Figure S7

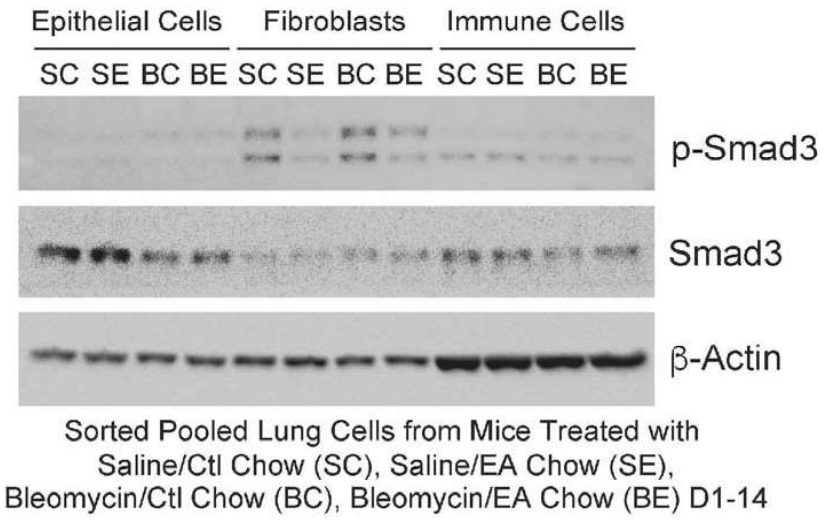

Supplemental Figure S7. Inhibition of TGFβ1 signaling by trihydroxyphenolics is specific to fibroblasts in vivo. Mouse lung epithelial cells, fibroblasts, and immune cells sorted from mice treated for 14 days with saline+control chow (SC, n=5), saline+EA chow (SE, n=5), bleomycin+control chow (BC, n=6), or bleomycin+EA chow (BE, n=3) were lysed and cell lysates blotted for p-Smad3, total Smad3, and β-Actin.

Supplemental Figure S8

A

Kinase	Mean % Control (1μM Corilagin)	Mean % Control (10 μM Corilagin)
Abl	112	114
ALK6	112	111
ALK	85	90
AMPKα1	109	103
ASK1	104	102
Aurora-A	87	77
CaMKI	99	102
CDK1/cyclinB	107	94
CDK2/cyclinA	117	107
CDK6/cyclinD3	96	98
CDK7/cyclinH/MAT1	103	87
CDK9/cyclin T1	104	106
CHK1	72	89
CK1γ1	90	86
CK2α2	18	22
DRAK1	104	102
eEF-2K	101	104
EGFR	18	5
EphA5	77	22
EphB4	16	4
Fyn	72	3
GSK3β	96	100
IGF-1R	101	27
IKKα	100	98
JAK2	96	94
KDR	96	95
LOK	105	113
Lyn	85	8
MAPKAP-K2	90	80
MEK1	100	93
MKK7β	90	23
Mnk2	108	105
MSK2	110	107
MST1	114	116
mTOR	78	47
NEK2	84	72
p70S6K	92	99
PAK2	92	89
PDGFRβ	23	2
PI3 Kinase (p110α/p85α)	51	12
PI3 Kinase (p110β/p85α)	50	15
PI3 Kinase (p110δ/p85α)	48	2
PI3 Kinase (p120γ)	92	73
Pim-1	108	97
PKA	109	106
PKBα	99	94
PKCα	90	91
PKCθ	107	108
PKG1α	105	109
Plk3	104	98
PRAK	37	25
ROCK-I	109	117
Rse	60	25
Rsk1	141	141
SAPK2a	107	114
SRPK1	99	93
ACTR2	98	100
ALK1	106	113
ALK2	100	100
ALK4	100	105
ALK6	122	125
A-Raf	101	93
BMPR2	91	90
B-Raf	91	70
B-Raf(V599E)	85	59
c-RAF	82	55
c-RAF	109	78
IRAK1	92	89
IRAK4	88	88
IRAK4	94	88
LIMK1	98	94
LRRK2	98	96
MLK1	105	110
MLK1	109	111
MLK2	90	84
RIPK1	105	125
RIPK2	101	110
TAK1	108	106
TAK1	104	109
TGFBR1	104	97
TGFBR2	103	98
ZAK	94	73

B

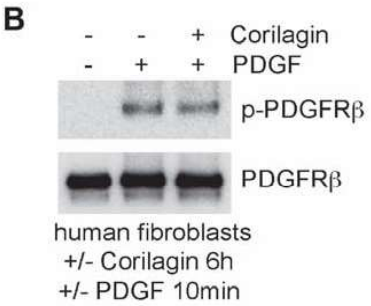

C

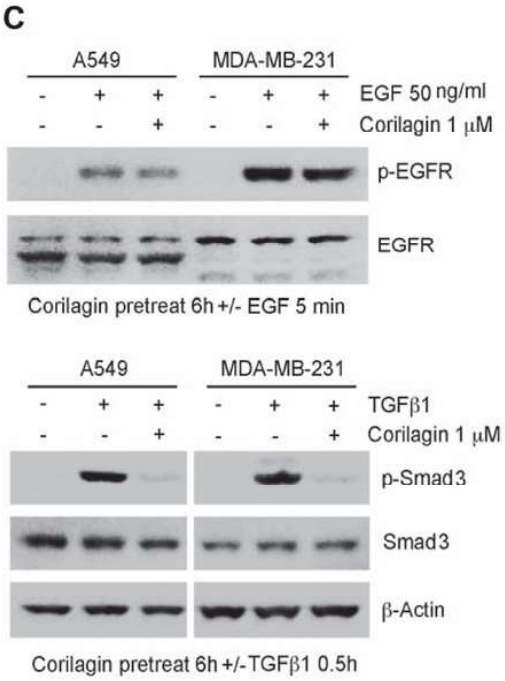

Supplemental Figure S8. Corilagin (1 μM) does not globally block kinase activity. (**A**) Corilagin (1 μM and 10 μM) effects on 82 purified kinase activities measured as percent ATP incorporation for each enzyme compared with DMSO controls. (**B**) A549 cells were pre-treated with 1 μM corilagin for 6 h before stimulating with PDGF (10 ng/ml) for 10 min and the cell lysates were blotted for p-PDGFRβ and total PDGFRβ. (**C**) A549 and MDA-MB-231 cells were pre-treated with 1 μM corilagin for 6 h before stimulating with EGF (50 ng/ml) for 5 min or with TGFβ1 for 30 min and the cell lysates were blotted for p-EGFR and total EGFR or p-Smad3 and Smad3, respectively. **B, C** are representative of three experiments with similar results.

Supplemental Figure S9

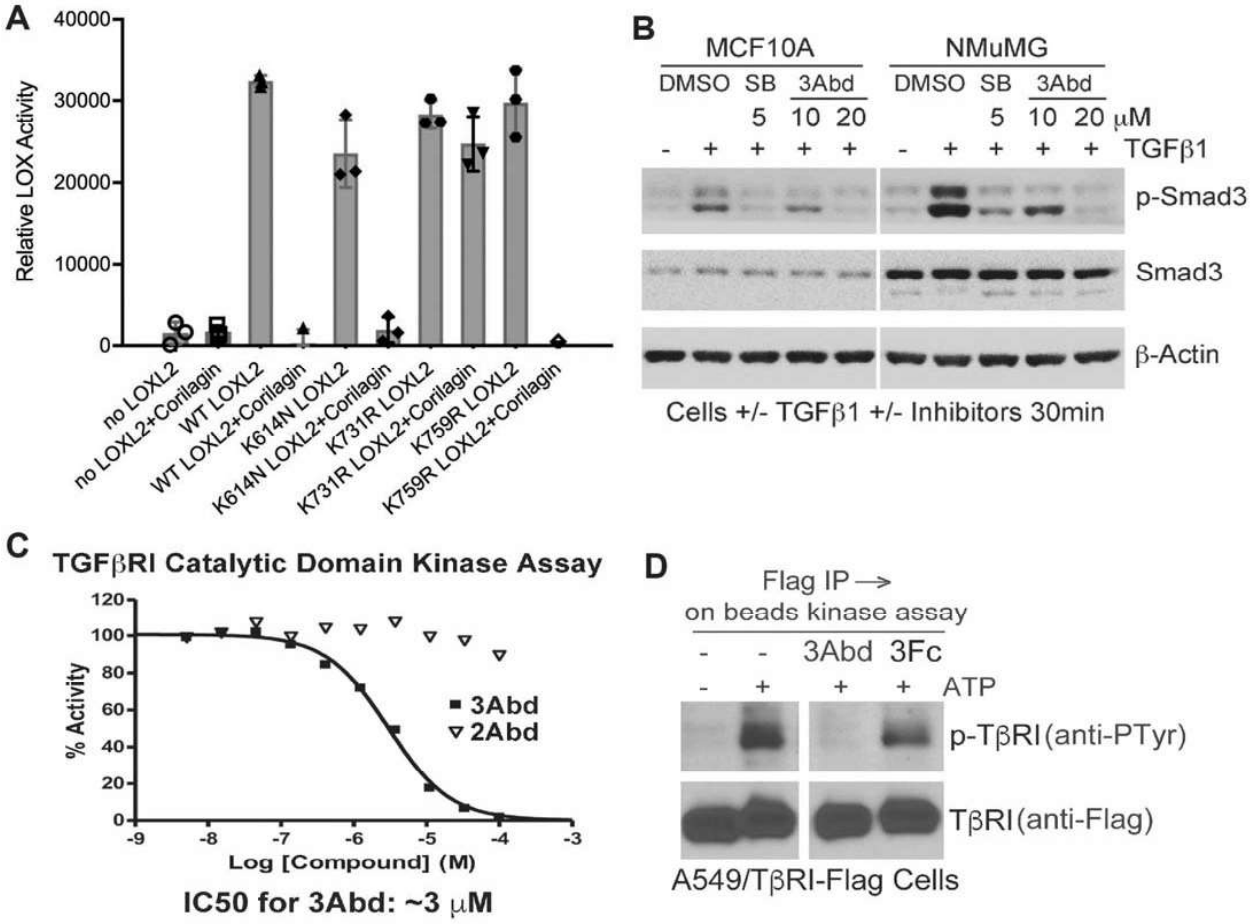

Supplemental Figure S9. Trihydroxyphenolic motif mimics the LTQ leading to auto-oxidation and generation of a novel inhibitor of TGFβR1 kinase. (**A**) NMuMG cells transiently transfected with wild-type or mutant human LOXL2 were treated with 1 μM corilagin or DMSO for 6 h. LOX activity of conditioned media from treated cells was measured. Data presented as relative intensity at Ex/Em 540/590 nm. Data represent mean±SD, n=3. (**B**) MCF-10A and NMuMG cells were stimulated with TGFβ1 for 30 min in the presence or absence of 3Abd (10 and 20 μM) without pre-incubation. Cell lysates were blotted for p-Smad3, Smad3, and β-actin. (**C**) Purified ALK5/TGFβRI catalytic domain kinase assay was carried out in the presence of ten doses of 3Abd or 2Abd starting from 100 μM. The kinase activity was indicated by ^{33}P-ATP signals and the IC50 of 3Abd was calculated. (**D**) A549 cells transfected with Flag-tagged TRI and TRII were immunoprecipitated with anti-Flag antibody and the in vitro kinase assay was performed on beads in the presence or absence of 20 μM 3Abd or 3Cc. The final reaction was eluted and analyzed by immunoblotting for phosphotyrosine and Flag. All the data shown are representative of at least three experiments with similar results.

Supplemental Figure S10

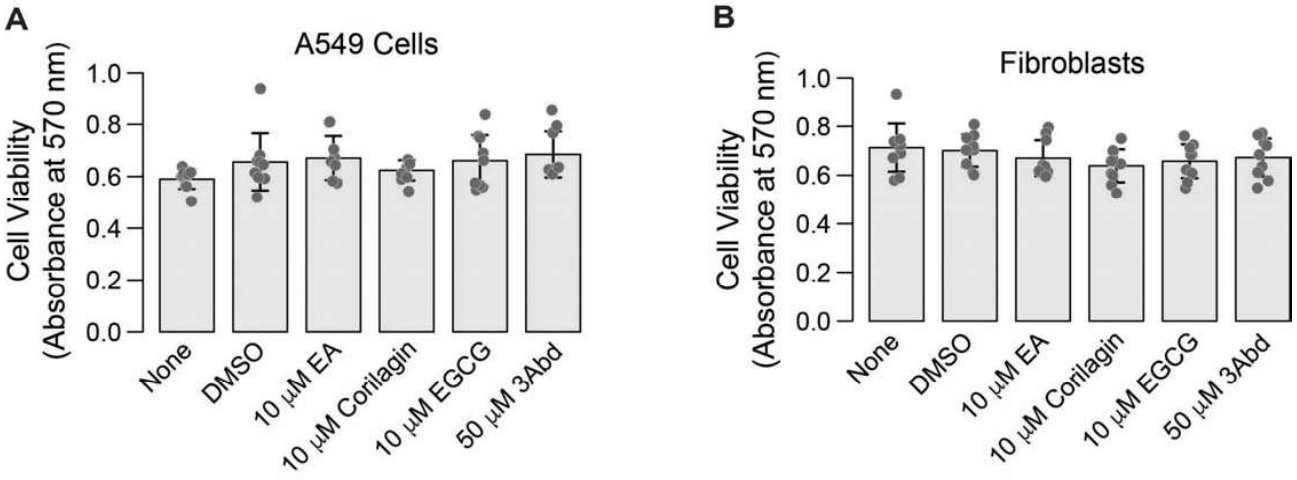

Supplemental Figure S10. Trihydroxyphenolics do not affect cell viability. Effect of EA (10 μM), Corilagin (10 μM), EGCG (10 μM), and 3Abd (50 μM) on cell viability of A549 (**A**) and human primary lung fibroblasts (**B**). Data are presented as mean absorbance at 570 nm±SD. n=9.

Supplemental Figure S11

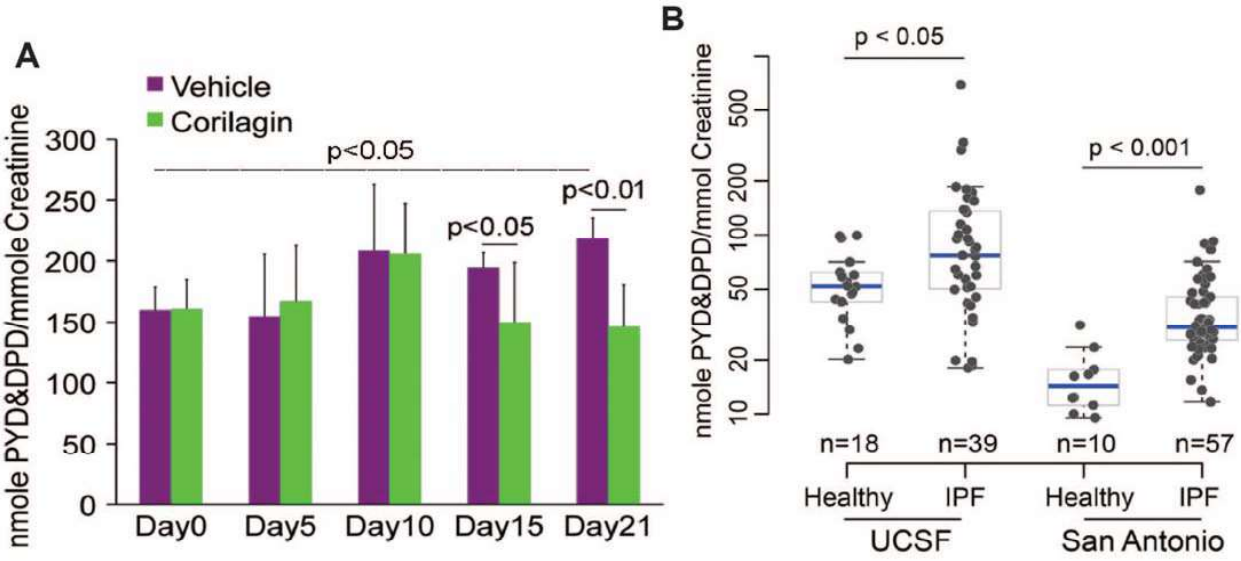

Supplemental Figure S11. Urinary PYD/DPD levels are higher in bleomycin-treated mice and IPF patients than that in controls. (**A**) Mouse pyridinoline (PYD) and deoxypyridinoline (DPD) were measured at different time points (D0-D21) in the urine samples pool-collected from mice injected with bleomycin and treated with vehicle (n=5) or corilagin (n=5). Three urine sample collections at each time point. P value by one-way ANOVA with a Tukey post hoc test. (**B**) Human PYD and DPD were measured in the urine samples collected independently from two cohorts of healthy donors and IPF patients from University of California at San Francisco (UCSF) and University of Texas Health Science Center at San Antonio (San Antonio). The data was analyzed by Mann-Whitney test. Data for **A** and **B** represent mean DPD and PYD/nmol/mmol creatinine±SD.

Supplemental Table 1. Primer and probe sequences for Taqman Quantitative PCR

Name	Sequence
Mouse MMP9 F	5′-TTCCTGGTGGCAGCGC-3′
Mouse MMP9 R	5′-CGGCACGCTGGAATGATC-3′
Mouse MMP9 Probe	5′-/FAM/CCCAGTGCATGGCCGAACTCG/BHQ/-3′
Mouse MMP12 F	5′-TGTGGAGTGCCCGATGTACA-3′
Mouse MMP12R	5′-AGTGAGGTACCGCTTCATCCAT-3′
Mouse MMP12 Probe	5′-/FAM/CATCTTAGAGCAGTGCCCCAGAGGTCAA/BHQ/-3′
Mouse PAI1 F	5′-TGCATCGCCTGCCATTG-3′
Mouse PAI1 R	5′-GACATTTCCACAGTGGACCTTGA-3′
Mouse PAI1 Probe	5′-/FAM/TTGGCCCATGGCACCCTCCA/BHQ/-3′
Mouse Trem1 F	5′-CAAACCGCATCACCACAAAG-3′
Mouse Trem1 R	5′-ACGTGGTTCAGCCACTCCTC-3′
Mouse Trem1 Probe	5′-/FAM/CACTTGATCGCACCCAGAAGGCC/BHQ/-3′

References

1. Thannickal VJ, Zhou Y, Gaggar A, and Duncan SR. Fibrosis: ultimate and proximate causes. *J Clin Invest.* 2014;124(11):4673-7.

2. Friedman SL, Sheppard D, Duffield JS, and Violette S. Therapy for fibrotic diseases: nearing the starting line. *Science translational medicine.* 2013;5(167):167sr1.

3. Bartram U, and Speer CP. The role of transforming growth factor beta in lung development and disease. *Chest.* 2004;125(2):754-65.

4. Han CY, Koo JH, Kim SH, Gardenghi S, Rivella S, Strnad P, et al. Hepcidin inhibits Smad3 phosphorylation in hepatic stellate cells by impeding ferroportin-mediated regulation of Akt. *Nat Commun.* 2016;7:13817.

5. Hu C, Dandapat A, Sun L, Khan JA, Liu Y, Hermonat PL, et al. Regulation of TGFbeta1-mediated collagen formation by LOX-1: studies based on forced overexpression of TGFbeta1 in wild-type and lox-1 knock-out mouse cardiac fibroblasts. *J Biol Chem.* 2008;283(16):10226-31.

6. Sheppard D. Transforming growth factor beta: a central modulator of pulmonary and airway inflammation and fibrosis. *Proc Am Thorac Soc.* 2006;3(5):413-7.

7. Principe DR, DeCant B, Mascarinas E, Wayne EA, Diaz AM, Akagi N, et al. TGFbeta Signaling in the Pancreatic Tumor Microenvironment Promotes Fibrosis and Immune Evasion to Facilitate Tumorigenesis. *Cancer Res.* 2016;76(9):2525-39.

8. Kaminski N, Allard JD, Pittet JF, Zuo F, Griffiths MJ, Morris D, et al. Global analysis of gene expression in pulmonary fibrosis reveals distinct programs regulating lung inflammation and fibrosis. *Proc Natl Acad Sci U S A.* 2000;97(4):1778-83.

9. Levental KR, Yu H, Kass L, Lakins JN, Egeblad M, Erler JT, et al. Matrix crosslinking forces tumor progression by enhancing integrin signaling. *Cell.* 2009;139(5):891-906.

10. Cox TR, Bird D, Baker AM, Barker HE, Ho MW, Lang G, et al. LOX-mediated collagen crosslinking is responsible for fibrosis-enhanced metastasis. *Cancer Res.* 2013;73(6):1721-32.

11. Egeblad M, Rasch MG, and Weaver VM. Dynamic interplay between the collagen scaffold and tumor evolution. *Curr Opin Cell Biol.* 2010;22(5):697-706.

12. Sheppard D. Integrin-mediated activation of latent transforming growth factor beta. *Cancer Metastasis Rev.* 2005;24(3):395-402.

13. Chang TT, Thakar D, and Weaver VM. Force-dependent breaching of the basement membrane. *Matrix biology : journal of the International Society for Matrix Biology.* 2017;57-58:178-89.

14. Vazquez PF, Carlini MJ, Daroqui MC, Colombo L, Dalurzo ML, Smith DE, et al. TGF-beta specifically enhances the metastatic attributes of murine lung adenocarcinoma: implications for human non-small cell lung cancer. *Clin Exp Metastasis.* 2013;30(8):993-1007.

15. Fernandez IE, and Eickelberg O. The impact of TGF-beta on lung fibrosis: from targeting to biomarkers. *Proc Am Thorac Soc.* 2012;9(3):111-6.

16. Yingling JM, Blanchard KL, and Sawyer JS. Development of TGF-beta signalling inhibitors for cancer therapy. *Nat Rev Drug Discov.* 2004;3(12):1011-22.

17. Neuzillet C, Tijeras-Raballand A, Cohen R, Cros J, Faivre S, Raymond E, et al. Targeting the TGFbeta pathway for cancer therapy. *Pharmacol Ther.* 2015;147:22-31.

18. Akhurst RJ, and Hata A. Targeting the TGFbeta signalling pathway in disease. *Nat Rev Drug Discov.* 2012;11(10):790-811.

19. Travis MA, and Sheppard D. TGF-beta activation and function in immunity. *Annual review of immunology.* 2014;32:51-82.

20. Mordasky Markell L, Perez-Lorenzo R, Masiuk KE, Kennett MJ, and Glick AB. Use of a TGFbeta type I receptor inhibitor in mouse skin carcinogenesis reveals a dual role for TGFbeta signaling in tumor promotion and progression. *Carcinogenesis.* 2010;31(12):2127-35.

21. Lacouture ME, Morris JC, Lawrence DP, Tan AR, Olencki TE, Shapiro GI, et al. Cutaneous keratoacanthomas/squamous cell carcinomas associated with neutralization of transforming growth factor beta by the monoclonal antibody fresolimumab (GC1008). *Cancer Immunol Immun.* 2015;64(4):437-46.

22. Anderton MJ, Mellor HR, Bell A, Sadler C, Pass M, Powell S, et al. Induction of heart valve lesions by small-molecule ALK5 inhibitors. *Toxicol Pathol.* 2011;39(6):916-24.

23. Herbertz S, Sawyer JS, Stauber AJ, Gueorguieva I, Driscoll KE, Estrem ST, et al. Clinical development of galunisertib (LY2157299 monohydrate), a small molecule inhibitor of transforming growth factor-beta signaling pathway. *Drug Des Devel Ther.* 2015;9:4479-99.

24. Blackwell TS, Tager AM, Borok Z, Moore BB, Schwartz DA, Anstrom KJ, et al. Future directions in idiopathic pulmonary fibrosis research. An NHLBI workshop report. *American journal of respiratory and critical care medicine.* 2014;189(2):214-22.

25. Bandyopadhyay A, and Raghavan S. Defining the role of integrin alphavbeta6 in cancer. *Curr Drug Targets.* 2009;10(7):645-52.

26. Xi Y, Tan K, Brumwell AN, Chen SC, Kim YH, Kim TJ, et al. Inhibition of epithelial-to-mesenchymal transition and pulmonary fibrosis by methacycline. *American journal of respiratory cell and molecular biology.* 2014;50(1):51-60.

27. Sriram N, Kalayarasan S, Manikandan R, Arumugam M, and Sudhandiran G. Epigallocatechin gallate attenuates fibroblast proliferation and excessive collagen production by effectively intervening TGF-beta1 signalling. *Clin Exp Pharmacol Physiol.* 2015;42(8):849-59.

28. Wang Z, Guo QY, Zhang XJ, Li X, Li WT, Ma XT, et al. Corilagin attenuates aerosol bleomycin-induced experimental lung injury. *Int J Mol Sci.* 2014;15(6):9762-79.

29. Peng DH, Ungewiss C, Tong P, Byers LA, Wang J, Canales JR, et al. ZEB1 induces LOXL2-mediated collagen stabilization and deposition in the extracellular matrix to drive lung cancer invasion and metastasis. *Oncogene.* 2016.

30. Peinado H, Del Carmen Iglesias-de la Cruz M, Olmeda D, Csiszar K, Fong KS, Vega S, et al. A molecular role for lysyl oxidase-like 2 enzyme in snail regulation and tumor progression. *EMBO J.* 2005;24(19):3446-58.

31. Erler JT, Bennewith KL, Nicolau M, Dornhofer N, Kong C, Le QT, et al. Lysyl oxidase is essential for hypoxia-induced metastasis. *Nature.* 2006;440(7088):1222-6.

32. Sethi A, Mao W, Wordinger RJ, and Clark AF. Transforming growth factor-beta induces extracellular matrix protein cross-linking lysyl oxidase (LOX) genes in human trabecular meshwork cells. *Invest Ophthalmol Vis Sci.* 2011;52(8):5240-50.

33. Finney J, Moon HJ, Ronnebaum T, Lantz M, and Mure M. Human copper-dependent amine oxidases. *Arch Biochem Biophys.* 2014;546:19-32.

34. Kagan HM, and Trackman PC. Properties and function of lysyl oxidase. *American journal of respiratory cell and molecular biology.* 1991;5(3):206-10.

35. Yamauchi M, and Sricholpech M. Lysine post-translational modifications of collagen. *Essays Biochem.* 2012;52:113-33.

36. Chen CZ, Peng YX, Wang ZB, Fish PV, Kaar JL, Koepsel RR, et al. The Scar-in-a-Jar: studying potential antifibrotic compounds from the epigenetic to extracellular level in a single well. *Br J Pharmacol.* 2009;158(5):1196-209.

37. Chen CZ, and Raghunath M. Focus on collagen: in vitro systems to study fibrogenesis and antifibrosis state of the art. *Fibrogenesis Tissue Repair.* 2009;2:7.

38. Hecker L, Vittal R, Jones T, Jagirdar R, Luckhardt TR, Horowitz JC, et al. NADPH oxidase-4 mediates myofibroblast activation and fibrogenic responses to lung injury. *Nat Med.* 2009;15(9):1077-81.

39. Chen Y, Guo H, Terajima M, Banerjee P, Liu X, Yu J, et al. Lysyl Hydroxylase 2 Is Secreted by Tumor Cells and Can Modify Collagen in the Extracellular Space. *J Biol Chem.* 2016;291(50):25799-808.

40. Dennler S, Itoh S, Vivien D, ten Dijke P, Huet S, and Gauthier JM. Direct binding of Smad3 and Smad4 to critical TGF beta-inducible elements in the promoter of human plasminogen activator inhibitor-type 1 gene. *EMBO J.* 1998;17(11):3091-100.

41. Raghu G, Brown KK, Collard HR, Cottin V, Gibson KF, Kaner RJ, et al. Efficacy of simtuzumab versus placebo in patients with idiopathic pulmonary fibrosis: a randomised, double-blind, controlled, phase 2 trial. *The Lancet Respiratory medicine.* 2017;5(1):22-32.

42. Hornstra IK, Birge S, Starcher B, Bailey AJ, Mecham RP, and Shapiro SD. Lysyl oxidase is required for vascular and diaphragmatic development in mice. *J Biol Chem.* 2003;278(16):14387-93.

43. Maki JM, Rasanen J, Tikkanen H, Sormunen R, Makikallio K, Kivirikko KI, et al. Inactivation of the lysyl oxidase gene Lox leads to aortic aneurysms, cardiovascular dysfunction, and perinatal death in mice. *Circulation.* 2002;106(19):2503-9.

44. Maki JM, Sormunen R, Lippo S, Kaarteenaho-Wiik R, Soininen R, and Myllyharju J. Lysyl oxidase is essential for normal development and function of the respiratory system and for the integrity of elastic and collagen fibers in various tissues. *Am J Pathol.* 2005;167(4):927-36.

45. Liu X, Zhao Y, Gao J, Pawlyk B, Starcher B, Spencer JA, et al. Elastic fiber homeostasis requires lysyl oxidase-like 1 protein. *Nat Genet.* 2004;36(2):178-82.

46. Peter B, Bosze S, and Horvath R. Biophysical characteristics of proteins and living cells exposed to the green tea polyphenol epigallocatechin-3-gallate (EGCg): review of recent advances from molecular mechanisms to nanomedicine and clinical trials. *Eur Biophys J.* 2017;46(1):1-24.

47. Mereles D, and Hunstein W. Epigallocatechin-3-gallate (EGCG) for clinical trials: more pitfalls than promises? *Int J Mol Sci.* 2011;12(9):5592-603.

48. Zhang HM, Zhao L, Li H, Xu H, Chen WW, and Tao L. Research progress on the anticarcinogenic actions and mechanisms of ellagic acid. *Cancer Biol Med.* 2014;11(2):92-100.

49. Stoner GD, Sardo C, Apseloff G, Mullet D, Wargo W, Pound V, et al. Pharmacokinetics of anthocyanins and ellagic acid in healthy volunteers fed freeze-dried black raspberries daily for 7 days. *J Clin Pharmacol.* 2005;45(10):1153-64.

50. Mertens-Talcott SU, Jilma-Stohlawetz P, Rios J, Hingorani L, and Derendorf H. Absorption, metabolism, and antioxidant effects of pomegranate (Punica granatum l.) polyphenols after ingestion of a standardized extract in healthy human volunteers. *J Agric Food Chem.* 2006;54(23):8956-61.

51. Seeram NP, Henning SM, Zhang Y, Suchard M, Li Z, and Heber D. Pomegranate juice ellagitannin metabolites are present in human plasma and some persist in urine for up to 48 hours. *J Nutr.* 2006;136(10):2481-5.

52. Lee MJ, Maliakal P, Chen L, Meng X, Bondoc FY, Prabhu S, et al. Pharmacokinetics of tea catechins after ingestion of green tea and (-)-epigallocatechin-3-gallate by humans: formation of different metabolites and individual variability. *Cancer epidemiology, biomarkers & prevention : a publication of the American Association for Cancer Research, cosponsored by the American Society of Preventive Oncology.* 2002;11(10 Pt 1):1025-32.

53. Nagle DG, Ferreira D, and Zhou YD. Epigallocatechin-3-gallate (EGCG): chemical and biomedical perspectives. *Phytochemistry.* 2006;67(17):1849-55.

54. Liu J, Liu S, Zhou H, Hanson T, Yang L, Chen Z, et al. Association of green tea consumption with mortality from all-cause, cardiovascular disease and cancer in a Chinese cohort of 165,000 adult men. *European journal of epidemiology.* 2016;31(9):853-65.

55. Lustosa BB, Polegato B, Minicucci M, Rafacho B, Santos PP, Fernandes AA, et al. Green tea (Cammellia sinensis) attenuates ventricular remodeling after experimental myocardial infarction. *International journal of cardiology.* 2016;225:147-53.

56. Kuriyama S, Shimazu T, Ohmori K, Kikuchi N, Nakaya N, Nishino Y, et al. Green tea consumption and mortality due to cardiovascular disease, cancer, and all causes in Japan: the Ohsaki study. *Jama.* 2006;296(10):1255-65.

57. Chapman HA, Li X, Alexander JP, Brumwell A, Lorizio W, Tan K, et al. Integrin alpha6beta4 identifies an adult distal lung epithelial population with regenerative potential in mice. *J Clin Invest.* 2011;121(7):2855-62.

58. Henderson NC, Arnold TD, Katamura Y, Giacomini MM, Rodriguez JD, McCarty JH, et al. Targeting of alphav integrin identifies a core molecular pathway that regulates fibrosis in several organs. *Nat Med.* 2013;19(12):1617-24.

59. Yamauchi M, and Shiiba M. Lysine hydroxylation and cross-linking of collagen. *Methods Mol Biol.* 2008;446:95-108.

Section IV.

TGF-β Receptors and Smads:
Regulatory Complexity and Functional Versatility

Introduction

This section quotes the following published material as it appears in Trends in Cell Biology:

> Budi, E.H., Duan, D. & Derynck, R. Transforming Growth Factor-beta Receptors and Smads: Regulatory Complexity and Functional Versatility. *Trends Cell Biol* **27**, 658-672 (2017).

This review was written in collaboration by Dr. Erine Budi and myself, under the direction of Dr. Rik Derynck. Dr. Budi authored the portion of this review dealing with regulation of TGF-β ligands and receptors at the cell surface, and I wrote the discussion on regulation of the intracellular segment of the signaling pathway.

TGF-β Receptors and Smads:

Regulatory Complexity and Functional Versatility

Erine H. Budi, Dana Duan and Rik Derynck*

Department of Cell and Tissue Biology, and Eli and Edythe Broad Center of Regeneration Medicine and Stem Cell Research, University of California at San Francisco,
San Francisco CA 94143

*To whom correspondence should be addressed:
Rik Derynck
Department of Cell and Tissue Biology
University of California at San Francisco
Broad Center, Room RMB-1027
35 Medical Center Way, San Francisco CA94143-0669
Voice: 415 476 7322
E-mail: rik.derynck@ucsf.edu

Abstract

TGF-β family proteins control cell physiology, proliferation and growth, and direct cell differentiation, thus playing key roles in normal development and disease. The mechanisms of how TGF-β family ligands interact with heteromeric complexes of cell surface receptors to then activate Smad signaling that directs changes in gene expression are often seen as established. Even though TGF-β-induced Smad signaling may be seen as a linear signaling pathway with predictable outcomes, this pathway provides cells with a versatile means to induce different cellular responses. Fundamental questions remain as to how, at the molecular level, TGF-β and TGF-β family proteins activate the receptor complexes and induce a context-dependent diversity of cell responses. Among the areas of progress, we summarize new insights into how cells control TGF-β responsiveness by controlling the TGF-β receptors, and into the key roles and versatility of Smads in directing cell differentiation and cell fate selection.

Introduction

The many roles of TGF-β signaling and the diverse responses to TGF-β and TGF-β family proteins, such as activins and BMPs, in cell physiology, the developing embryo, and the adult organism, have intrigued many scientists over the years. During the last two decades we have seen tremendous activity and much progress in the characterization of the cell surface receptors for TGF-β and TGF-β-related proteins, in our understanding of how TGF-β is presented to and activates its cell surface receptors, and in the mechanisms by which activated TGF-β family receptors induce intracellular signaling that leads to target gene expression. Compared to some other receptor signaling systems, our knowledge still has many important gaps; yet TGF-β signaling is often seen as a well defined signaling pathway (Fig. 1) with a predictable outcome.

The general mechanism by which ligand binding to cell surface receptors leads to activation of gene responses by Smads as intracellular signaling effectors is found in many textbooks and easily summarized in a simple paragraph (Fig. 1). TGF-βs, BMPs, activins and other TGF-β family proteins act as dimers [1] that bind tetrameric cell surface complexes of two "type II" and two "type I" receptor kinases. TGF-βs and activins bind primarily to the type II receptors and promote recruitment of type I receptors, whereas BMPs often bind primarily to type I receptors but mostly require the combination of type II and type I receptors for higher affinity binding [2, 3]. Among the five type II receptors, TGF-β binds specifically the type II receptor named TβRII, which combines with the type I receptor named TβRI or ALK-5, one of seven structurally related type I receptors in vertebrates. The type II and type I receptors are structurally similar, with a rather small glycosylated and disulfide-rich ectodomain, a single transmembrane segment, and a cytoplasmic domain consisting mainly of its defining kinase subdomain structure with an N- and a C-lobe [4]. Ligand-induced assembly of the receptor complex enables the type II receptors, which are thought of as constitutively active kinases, to phosphorylate the glycine-serine-rich domain (GS domain) of the type I receptors, thus resulting in activation of the type I receptor kinases [3]. The activated type I receptor kinases then phosphorylate the intracellular effector Smads, named R-Smads

for receptor-activated Smads, at two C-terminal serines, resulting in their activation, dissociation from the receptor complexes, and subsequent association of two R-Smads with one co-Smad, named Smad4. These trimeric complexes translocate into the nucleus where they associate with high-affinity DNA binding transcription factors at regulatory sequences that allow for DNA binding of Smads together with their interacting transcription factors. TGF-βs and activins activate Smad2 and Smad3 as R-Smads, whereas BMPs activate Smad1, 5, and 8, all of which use Smad4 as co-Smad [2, 3, 5, 6]. Interactions with transcription coregulators in larger nucleoprotein complexes then allow the DNA-bound Smad complexes to activate or repress transcription [5, 6] (Fig. 1). The phosphorylation of serines in Smads by the type I receptors, and in type I receptor GS-domains by the type II receptors, has resulted in the classification of the type II and type I receptors as serine-threonine kinases, which distinguishes them from the receptor tyrosine kinases and receptors that act through associated tyrosine kinases.

The model described above resonates because of its simplicity and linearity, and often attracts the view that the identity of the ligand, and the presence and identities of the receptors and Smads confer a predictable response. However, it has become apparent that TGF-β receptors also activate non-Smad signaling pathways that substantially contribute to the TGF-β response. Furthermore, increasing evidence reveals that the cells themselves can regulate their TGF-β responsiveness by controlling the functional receptor availability, and the master regulatory transcription factors, with which Smads interact. This short overview highlights recent progress into the different levels of regulation that determine the response to TGF-β family proteins, with TGF-β signaling as the best defined model system.

Control of TGF-β ligand activation

All TGF-β family members are expressed as precursors with an N-terminal signal peptide followed by a large pro-domain, a furin protease cleavage site, and a C-terminal mature polypeptide. The mature polypeptide is converted into a disulfide-linked dimer that acts as ligand to the cell surface receptors and activates TGF-β family signaling [1]. Based on studies of a few TGF-β family proteins, the pro-domain functions as a chaperone required for folding and secretion of the mature protein, and remains

noncovalently associated with the mature dimeric ligand. Additionally, the association of the respective pro-domains with the three mature TGF-β dimers confers latency to the secreted TGF-β complexes, i.e. prevents TGF-β from binding to the receptors, thus imposing required activation of the latent complexes to enable TGF-β binding to the cell surface TGF-β receptor complexes [7]. This latency is not seen with the BMPs and activins that have been characterized.

Studies during the last few years have yielded new insights into the mechanisms of TGF-β activation. The latency that prevents TGF-β binding to the receptors results from the non-covalent association of two pro-domains, often called "latency-associated polypeptides" (LAP), with the cleaved and dimerized mature TGF-β ligand. While this LAP-TGF-β small latent complex (SLC) is produced by some cell lines, TGF-β is more commonly secreted and deposited in the surrounding extracellular matrix as a large latent complex (LLC) that consists of the SLC with a latent TGF-β binding protein (LTBP) disulfide-linked to the two LAPs [7] (Fig. 2). Four fibrillin-like LTBPs exist and are encoded by different genes. Three of these bind in defined combinations with TGF-β small latent complexes, act as chaperones during transport and secretion of the latent TGF-β proteins, and facilitate the deposition of the latent complexes in the extracellular matrix. The LLC remains in the extracellular matrix until it is further processed to release active TGF-β [7].

Besides complexes with LTBPs, which are generally expressed, latent TGF-β1 is also found in association with the transmembrane protein GARP (glycoprotein A repetitions predominant), also known as LRRC32, in regulatory T (Treg) cells, platelets, and hepatic stellate cells [8-10]. GARP anchors latent TGF-β to the cell membrane. In regulatory T cells, siRNA-mediated silencing of GARP expression and treatment with GARP antibodies were shown to prevent TGF-β activation [9, 11]. The very different nature of the GARP latent complexes versus LTBP latent complexes suggests separate functions and activation mechanisms.

The roles of selected integrins, in particular αvβ6 and αvβ8, in the activation of TGF-β have been well established [7, 12]. Among the three TGF-β isoforms, the precursor segments of TGF-β1 and TGF-β3 have an integrin-binding arginine-glycine-aspartic acid (RGD) motif in the LAP segment, suggesting both a biochemical basis for integrin-mediated activation of the TGF-β1 and TGF-β3 latent complexes, and the requirement of a different mechanism for TGF-β2 complex activation [7, 12]. Further studies characterized a mechanism that requires cytoskeletal interactions with the β6 integrin, and leads to a physical traction/stress-mediated deformation of the latent complex, which allows for exposure and subsequent liberation of active TGF-β from the latent complex [13-15]. This model is supported by the three-dimensional structure of the latent TGF-β1 complex consisting of two LAPs and a mature TGF-β1 dimer [15, 16]. Furthermore, the integrin dependence of latent TGF-β1 complex activation is supported by phenotypic analyses of mice lacking αvβ6 or αvβ8 integrin, and mice expressing a non-functional variant of the RGD sequence [17, 18].

A substantial body of data also implicates proteases, most notably MT1-MMP and several MMPs, in the activation of TGF-β complexes [7, 19]. Latent TGF-β activation by αvβ8 is not traction-dependent and is inhibited by MMP inhibitors, suggesting a coordinated requirement of integrin-mediated retention of the latent complex and protease-mediated cleavage of the LAP [20]. Such cooperation may not be restricted to αvβ8-mediated activation of latent TGF-β, since a conformational change imposed by integrin binding may render the latent complex more accessible to proteases. The participation of structurally related proteases with complementary or compensatory mechanisms in latent TGF-β activation may preclude unambiguous support for a defined role of a protease from phenotypic analyses of mice with targeted inactivation of a single metalloprotease gene. Besides metalloproteases, other proteases have also been implicated in latent TGF-β activation [7, 19]. Furthermore, TGF-β activation also depends on extracellular matrix proteins, such as fibrillin, fibronectin and thrombospondin, which either directly or indirectly control TGF-β activation through mechanisms that require further

characterization [7]. The large yet very incomplete body of data on latent TGF-β activation suggests a variety of scenarios and mechanisms that depend on physiological and tissue context.

Post-translational control of TGF-β receptor activation and function

Signaling initiates at the plasma membrane when TGF-β binds the TβRII receptors. In the absence of TGF-β, TβRI and TβRII can be found at the cell surface as monomers, homodimers, and heterodimers. Ligand binding stabilizes the tetrameric interaction of two molecules of TβRII with two TβRI [3]. TGF-β1 and TGF-β3 can bind TβRII independent of the type I receptor, while TβRI has much lower affinity for the two ligands and therefore requires TβRII for ligand binding. In contrast, TGF-β2 binding requires the ectodomains of both TβRII and TβRI [21]. Similarly to TGF-β1 and TGF-β3, activins interact primarily with their type II receptors, and this binding is required for activin interaction with the type I receptors. BMPs, however, have higher binding affinity toward the type I receptor, but binding to preformed complex of type II and type I receptors ensures more efficient receptor binding [3].

TGF-β receptor ectodomain glycosylation and shedding

TGF-β family receptors are transmembrane glycoproteins, and the TβRII and TβRI receptors have three and one, respectively, sites of Asn-linked N-glycosylation in their ectodomains [3,22]. The status of TGF-β receptor O-glycosylation, which most commonly occurs on Ser and Thr residues, is unknown. Extracellular domain glycosylation regulates the transport to the cell surface, stability, and/or ligand binding of various transmembrane proteins. Whether and how different types of glycosylations define the TGF-β receptor functions and cell responsiveness to TGF-β have been only minimally explored. Biochemical studies reveals that TβRII N-glycosylation facilitates receptor transport to the cell surface, and, consequently, that inhibition of N-linked glycosylation of TβRII greatly reduces TGF-β responsiveness [23]. Additionally, impaired glycosylation of TβRII lowers its binding affinity for TGF-β, which also may confer decreased TGF-β responsiveness. [24]. Besides cell-intrinsic determinants of glycosylation, high glucose has been shown to promote N- and O-glycosylation of several proteins [25-

27], raising the possibility that high glucose promotes TGF-β receptor glycosylation and ligand affinity. These studies strongly suggest that cells can control their TGF-β responsiveness by modulating receptor glycosylation, and invite further studies to explore this mode of regulation.

Ectodomain shedding also controls the function of the cell surface TGF-β receptors (Fig. 2) and consequently the cell's responsiveness to TGF-β. The transmembrane metalloprotease TACE can directly cleave and thus proteolytically remove the ectodomain of TβRI, but not TβRII, at the cell surface [28]. While this does not affect TGF-β binding to cell surface TβRII, TACE-mediated ectodomain shedding, which is activated in response to Erk or p38 MAPK activation, incapacitates the cell surface TβRII-TβRI complexes and thus prevents TGF-β-induced Smad activation and signaling [28]. The many extracellular signals that induce Erk or p38 MAPK activation therefore act to control TGF-β responsiveness through effects at the cell surface. TACE-mediated ectodomain shedding of TβRI is followed, through the activity of presenilin and γ-secretase, by intracellular release of the TβRI cytoplasmic domain, which is then translocated into the nucleus where it acquires new functions (Fig. 2) [29, 30].

TGF-β receptor phosphorylation.

As with many signaling pathways that are activated by growth factors and cytokines, ligand-induced phosphorylation of the receptors and receptor-associated proteins initiates the activation of signaling pathways. The simple model proposes that TGF-β binding induces a constitutively active type II receptor to phosphorylate serine and/or threonine residues in the juxtamembrane GS domain of the type I receptor, which then confers conformational activation of the type I receptor kinase [3,31]. While GS domain phosphorylation leads to Smad activation through C-terminal phosphorylation by the type I receptor, ligand-induced receptor phosphorylation is more complex (Fig. 2).

Although no induced step has been identified, TGF-β binding may cause TβRII autophosphorylation in trans, which may be required for TβRII function. This scenario is suggested by growth factor-induced auto-/transphosphorylation and activation of receptor tyrosine kinases (RTKs) [32,

33], and may explain why immunoprecipitated TβRII is seen phosphorylated and with kinase activity [34] as a result of antibody-induced TβRII dimerization and phosphorylation. In addition to the phosphorylation of the GS domain, the ligand-activated TβRII may phosphorylate TβRI at sites that complement those resulting from TβRI autophosphorylation. Reciprocally, the activated TβRI may also phosphorylate TβRII at defined sites. Further complexity of the phosphorylation state is imposed by the dual specificity kinase activities of the TβRII and TβRI receptors. Predicted by phylogenetic sequence alignments [35, 36], the type II and type I receptors phosphorylate not only on serine and threonine, but also on tyrosine [37, 38], even though the type I receptors phosphorylate the Smads only at C-terminal serines and are therefore often seen as serine/threonine kinases [3]. Accordingly, TGF-β induces Tyr phosphorylation of both TβRII and TβRI receptors [37, 38]. TβRII Tyr phosphorylation is thought to be required for ligand-induced receptor activation, similarly to the MEKs and Erk MAPKs [37], while TβRI Tyr phosphorylation may enable the TGF-β-induced recruitment of ShcA and ShcA phosphorylation on Ser and Tyr by TβRI, which then initiates Erk MAPK pathway activation [38]. Several protein phosphatases control the receptor phosphorylation, although their roles and targeted residues have not been well defined. PP1c and PP2A target the TβRI receptor [39, 40], while no phosphatases have been identified that target the TβRII receptor. Clearly, a thorough analysis of the TβRII and TβRI phosphorylation is required to better understand how TGF-β and related ligands activate signaling.

A number of transmembrane receptors are acetylated on lysine, or methylated on lysine or arginine, and these modifications have in some cases been linked to a defined function [41-43]. For example, acetylation of the EGF receptor, an RTK, controls endocytosis and the extent of receptor phosphorylation [41, 44]. Also intracellular receptors, such as the glucocorticoid and estrogen receptors, are acetylated and methylated with functional consequences [45, 46]. Because of the increasing evidence with other receptor types, it is logical to assume that also the type II and/or type I receptors are targeted for acetylation and/or methylation. No observations have been reported so far on this subject.

TGF-β receptor ubiquitylation, neddylation and sumoylation

Ubiquitylation and the resulting degradation of TGF-β receptors are one mechanism by which the cell regulates the availability of the TGF-β receptors at the cell surface, and consequently the level of TGF-β responsiveness. Insights during the last few years have revealed a complexity with several ubiquitylating enzymes and multiple de-ubiquitylating enzymes, coined DUBs, that together impose extensive regulation of the cell surface receptor availability [47] (Fig. 2).

Protein ubiquitylation on lysine residues is carried out by the sequential activities of ubiquitin-activating E1 enzymes, ubiquitin-conjugating E2 enzymes, and E3 ubiquitin ligases. The E3 ligases are classified based on the nature of their catalytic domains, with many belonging to the RING group or HECT type ubiquitin ligases [48]. The closely related HECT type E3 ligases Smurf1 (Smad ubiquitin regulatory factor 1) and Smurf2, first identified for their abilities to target receptor-activated Smads for poly-ubiquitylation and degradation, also target the TβRI receptors. In this case, Smurf1 or Smurf2 associate with Smad7, which upon association with TβRI enables Smurf1 or Smurf2 to ubiquitylate TβRI and promote receptor degradation [49, 50]. Other HECT type E3 ligases, specifically NEDD4-2 and WWP1, also target TβRI for ubiquitylation and degradation [51, 52]. The relative contributions of the different E3 ligases and their regulation in different contexts remain to be defined.

Substrate ubiquitylation is balanced by isopeptidases that remove ubiquitin from the substrate and are therefore named deubiquitylases. Several of these, specifically USP4 (ubiquitin specific proteases 4), USP11, USP15, and UCH37 (ubiquitin C-terminal hydrolase), were shown to de-ubiquitylate TβRI, either through direct association with the receptor or indirectly through recruitment by Smad7 or TRAF4, which associate with the TβRII-TβRI receptor complex (Fig. 2) [3]. Direct association of USP4 with TβRI at the plasma membrane and USP4-mediated TβRI deubiquitylation are enhanced in response to Akt activation and Akt-mediated USP4 phosphorylation, and directly oppose TβRI ubiquitylation by Smurf2 in association with Smad7 [53]. USP15 and UCH37, and presumably also USP11, de-ubiquitylate TβRI through their association with Smad7, and thus prevent degradation of TβRI [54-56]. The consequently increased TβRI stability results in enhanced TGF-β responsiveness and signaling. The activities of the

different de-ubiquitylases may depend on the cell type and tissue, and the physiological context. Thus, USP15 may control the pathogenesis of glioblastoma by defining the TGF-β responsiveness; accordingly, depletion of USP15 expression in patient-derived glioblastoma cells reduces their tumorigenicity in a xenograft glioblastoma model [54]. The balance in expression of E3 ubiquitin ligases and deubiquitylases is presumably a major determinant of TGF-β receptor stability and TGF-β responsiveness. Little is known about micro-environmental stimuli and the signaling pathways that control TGF-β receptor stability and degradation, besides the already mentioned stimulation of USP4-mediated TβRI deubitylation in response to Akt activation.

Sumoylation and neddylation involve, like ubiquitylation, the covalent attachment of a short polypeptide to a lysine through the combined actions of E1, E2 and E3 ligases. SUMO (Small Ubiquitin-like Modifier) and NEDD8 (Neural Precursor Cell Expressed, Developmentally Down-Regulated 8) show substantial sequence and structural similarity to ubiquitin. However, unlike poly-ubiquitylation, sumoylation and neddylation do not necessarily target the substrate for degradation, but are associated with a variety of functions [57]. TβRI, but not TβRII, is sumoylated in response to TGF-β through the attachment of SUMO-1 (Fig. 2). TβRI sumoylation depends on the kinase activities of TβRI and TβRII, and on phosphorylation of TβRI. This suggests that substrate phosphorylation is required for recognition by the E3 ligase and sumoylation, as observed with some substrates. As high glucose can promote Smad4 sumoylation [58], TβRI sumoylation may be stimulated by other signaling or factor in addition to TGF-β-induced TβRI phosphorylation, although this remains to be determined. TβRI sumoylation enhances the TGF-β-induced Smad3 recruitment to TβRI and subsequent Smad activation [59]. A mutation in *TGFBR1* that results in a serine to tyrosine substitution at position 385 in TβRI is found in some metastatic breast and head-and-neck cancers [60, 61], and results in decreased TβRI sumoylation and an attenuated TGF-β-induced gene transcription response [59].

In contrast to sumoylation, TβRII, but not TβRI, is neddylated (Fig. 2). TβRII neddylation is mediated by the NEDD8 E2 conjugating Ubc12 enzyme and the E3 ligase c-Cbl (Casitas B-lineage

lymphoma) [62]. Neddylation of TβRII at the endogenous level may not be controlled by TGF-β, but requires the kinase activity of TβRII. TβRII neddylation stabilizes the receptor, presumably by opposing its ubiquitylation and degradation, and promotes TβRII internalization into EEA1-positive endosomes, thereby enhancing cellular TGF-β signaling [62]. Accordingly, substitution of His398 by Leu in c-Cbl, which is seen in some leukemia patients and abolishes the neddylation activity of c-Cbl, results in decreased TβRII levels and decreased TGF-β-induced Smad signaling [62]. Like ubiquitylation, neddylation is balanced by isopeptidases that remove NEDD8 from the substrate. NEDP1 has been shown to attenuate the neddylation of TβRII [62].

Sumoylation can be reversed through the actions of specific isopeptidases that proteolytically remove the SUMO from their substrates, but no biochemical evidence has been reported for a specific isopeptidase for TβRI desumoylation. As TβRI is modified by conjugation of SUMO-1, the isopeptidase SENP1 (Sentrin-specific protease 1) may promote TβRI desumoylation, since it is essential for desumoylating some SUMO-1-conjugated substrates, including the ubiquitin E3 ligase Smurf2 [63], which controls Smad and TβRI stability.

Control of TGF-β receptor distribution defines the TGF-β response

Binding of TGF-β to the receptor complex at the cell surface initiates signaling that activates both Smad-mediated signaling and non-Smad pathways. TGF-β or activin binding to their respective receptor complexes activates Smad2 and Smad3, whereas BMPs, as a general rule, induce activation of Smad1 and Smad5 [3, 6]. Smad signaling, which receives most attention, results in direct activation or repression of target genes. Smad signaling is likely to mediate many if not most direct changes, i.e. not requiring new protein synthesis, in gene expression, but does not explain non-transcriptional responses. Non-Smad responses to ligand binding result in Erk, p38 and JNK MAPK activation downstream of MEK activation, induction of PI3K-Akt-mTOR signaling, and activation of RhoA and other small GTPases [64]. The extent to which non-Smad signaling is activated by liganded TGF-β family receptor complexes depends, like Smad signaling, on cell type and physiological context. However, these responses, at least in cell

culture, are generally weaker than those elicited by RTKs, which prominently activate these pathways, although this may in part result from the lower numbers of cell surface receptors. Activation of other pathways, such as NF-κB signaling, has also been described and may be cell type-dependent. While mechanisms of Smad pathway activation have been extensively studied, much has to be learned in the context of non-Smad signaling.

Smad signaling is mediated by receptors that internalize in clathrin-coated pits and is regulated by receptor- and Smad-associated proteins. Several Smad-interacting proteins promote or repress Smad activation. Most notably, the related FYVE-motif proteins SARA and Hgs/Hrs facilitate the interactions of Smad2 and Smad3 with the type I receptors while associated with the plasma membrane, and promote Smad association with clathrin complexes and Smad internalization [65-67]. The intracellular proteins STRAP and axin, which also participate in Wnt signaling, also regulate Smad recruitment to either inhibit or promote TGF-β-induced Smad signaling [68-71]. Conversely, the transmembrane proteins TMEPAI and C18 ORF1 interfere with Smad activation through their abilities to bind SARA, and thus prevent SARA-mediated Smad recruitment to the receptor [72, 73]. Thus, not only the cell surface levels of TGF-β receptors, but also other proteins at the cell surface and inside the cell are major determinants of Smad activation.

Smad signaling in clathrin pits and clathrin-mediated endosomal compartments may very well be initiated prior to endosomal invagination. Consistent with this notion, the TβRI receptor and SARA were shown to associate with β-adaptin [67, 74]. In contrast, although less characterized, TGF-β-induced activation of Erk MAPK signaling and PI3K-Akt signaling occurs most likely in the caveolar compartment, which would be consistent with the ligand-induced activation of these pathways by RTKs in lipid-rich caveolar microdomains [75-77]. Accordingly, the TβRI and TβRII receptors associate with caveolin-1, and silencing caveolin-1 expression results in repression of TGF-β-induced Akt activation [77]. These observations imply that Smad activation and activation of Erk MAPK or PI3K-Akt signaling emanate from TGF-β receptor complexes that are distinct from the Smad-activating receptor complexes in

different subcellular compartments. Ubiquitin-mediated TβRI degradation has also been assigned to the caveolar compartment [67, 78], which may imply the presence of different subpopulations of receptor complexes in that compartment. Whether activation of p38 MAPK or JNK signaling through TRAF4 or TRAF6 [2] also occurs in association with caveolar domains remains to be better defined.

The two major endocytic routes have been reported to independently mediate TGF-β receptor internalization. However, tracking the intracellular routing of fluorescently labeled TβRI indicates that the two pathways may converge under the control of Rab5 before reaching the early endosome, forming endosomal vesicles that are positive for both caveolin-1 and clathrin. This fusion creates a multi-component and multi-functional organelle containing EEA1, caveolin-1, Rab-5, TβRI, Smad3-SARA complexes, Smad7-Smurf complexes and Rab11, where TGF-β receptors can easily access these different proteins and thus efficiently promote TGF-β signaling, TβRI recycling or degradation [79]. This finding may help explain observations that inhibition of clathrin-mediated endocytosis or disruption of caveolar endocytosis have only slight effects on TGF-β signaling levels.

In addition to the TGF-β-stimulated intracellular routing of receptors, the distribution of TGF-β receptors between clathrin-coated pits and cholesterol-rich caveolae defines the TGF-β signaling and resulting cell responses [3]. The SH2 domain protein p52ShcA interacts with TβRI in competition with Smad3, thus repressing TGF-β-induced Smad activation, and initiates TGF-β-induced Erk MAPK pathway activation. Furthermore, p52ShcA stabilizes the association of TβRI with caveolin-1, thus promoting caveolar localization of TGF-β receptor complexes and facilitating TGF-β-induced Erk MAPK and Akt activation [80]. Whether the p66ShcA isoform, which competes with p52ShcA for association with RTKs, also controls TGF-β receptor distribution at the cell surface remains to be seen. Conversely, another SH2 domain adaptor protein, named Dab2, interacts with TβRI and clathrin, and promotes TGF-β-induced Smad signaling [75], possibly at the expense of non-Smad signaling. These observations illustrate that cells have the ability to control the compartmentalization of the receptor at the cell surface, thus defining the relative intensities of the signaling responses. This regulatory mechanism depends on

adaptor proteins, such as ShcA and Dab2, whose expression and post-translational modifications in response to signaling pathways determine the TGF-β signaling response.

Finally, only a fraction of the TGF-β receptors is found at the cell surface, available for TGF-β-induced signaling activation, whereas the majority is retained inside the cells. This intracellular pool of TβRII and TβRI receptors enables rapid transport of the receptors to the cell surface. The consequently increased receptor levels at the cell surface then confer increased TGF-β responsiveness to either autocrine TGF-β or to TGF-β released and/or activated by other cells. Akt activation, e.g. in response to insulin, induces phosphorylation of the intracellular, membrane-associated RabGAP AS160, and thus promotes the transport of the TGF-β receptors to the cell surface, resulting in increased TGF-β signaling and responsiveness [81]. This control of the cell surface levels of the TGF-β receptors positions Akt signaling as a central regulator of the TGF-β response, and enables not only insulin, but also other Akt activating stimuli such as high glucose and activated RTKs, to define the TGF-β response. This mechanism controlling the cell surface TGF-β receptor levels may be relevant in the context of cancers which often show increased Akt activity.

Smads control gene programs and define cell lineage and cell fate.

Upon TGF-β-induced activation by the type I receptors, Smad3 and Smad2 function as direct transcription regulators that activate or repress the transcription of TGF-β/Smad target genes. In this function, they most commonly act in complexes of two receptor-activated Smads and one Smad4, which serves as transcription coactivator or corepressor [5, 6]. Activated Smad3, either as a homodimer or in combination with Smad2, can combine with Smad4 to effect the transcription responses of most TGF-β/Smad target genes, while a minority of TGF-β targets respond to Smad2 without participation of Smad3 [82]. TGF-β/Smad target genes have regulatory DNA sequences that recruit Smad complexes, most commonly an AGAC or GTCT sequence [83-85]. In tandem, these sequences efficiently activate TGF-β-induced transcription, e.g. in reporter assays, but no TGF-β/Smad target genes are known to activate or repress transcription from tandem Smad binding motifs only [5, 6]. Instead, Smads act through physical

association with other transcriptions factors that bind a more extensive regulatory DNA sequence with high affinity. The juxtaposition of a Smad binding sequence and a high affinity DNA binding element for the partnering transcription factor allows for cooperative DNA binding of the complex under the control of TGF-β. It also positions the high affinity sequence-specific binding partner, which is itself controlled by other signaling pathways, as the central determinant of the TGF-β-induced transcriptional control, thus generating substantial versatility in the transcriptional response, depending on the partnering transcription factor, and, by extension, the cell type and cell physiology [5, 6, 86]. Further complexity of the transcription response is dictated by interacting coregulators that define the amplitude of the transcription response of the target gene [5, 87].

The very nature of Smad-mediated transcription control, i.e. through cooperation with high affinity DNA-binding transcription factors, enables the Smads to play key roles in cell differentiation, both in repression or activation of cell lineage selection and in differentiation progression (Fig. 3) [88]. This is well illustrated in a number of differentiation selection contexts, in response to TGF-β-induced Smad3 activation, activin-induced Smad2 activation, or BMP-induced activation of Smad1 and Smad5. Thus, TGF-β controls mesenchymal differentiation along the myoblast, adipocyte, osteoblast or chondrocyte lineages through interaction of Smad3-Smad4 complexes with the lineage-specific master transcription factors [89]. For example, in myogenic differentiation, TGF-β, acting through Smad3, inhibits the expression and activities of the myogenic transcription factors, including MyoD and myogenin. Association of Smad3 with myogenin or MyoD, and the essential myogenic transcription factor MEF2, prevents the functional assembly of myogenic transcription complexes that normally drive muscle-specific genes and cell differentiation [90, 91]. In osteoblast differentiation, the inhibition of differentiation by TGF-β is mediated by the interaction of activated Smad3 with the master regulatory transcription factor, in this case Runx2, which enables Smad3 to recruit a histone deacetylase to thus prevent Runx2-mediated transcription of osteoblast genes [92]. Clearly, targeted association of Smad3

with lineage-determining master transcription factors enables TGF-β to control cell differentiation (Fig. 3) [89].

Interactions of Smads with master transcription factors also control self-renewal and differentiation of embryonic stem cells [86, 88, 93]. In human embryonic stem cells, TGF-β-activated Smad2 and/or Smad3 associate with master transcription factors that define the pluripotent state, and thus co-localize with Oct4 (POU5F1), Nanog or Sox2 in the genome, including at the genes encoding Oct4, Nanog and Sox2. During differentiation, as the expression of pluripotency transcription factors is repressed, TGF-β-activated Smads shift their allegiance and interact with newly expressed master transcription factors that drive the early differentiation lineages, thus presenting a different pattern of genome occupation [86].

The potent ability of TGF-β to initiate and drive epithelial-mesenchymal transition (EMT) serves as another example of how Smads promote and control cell differentiation. In this transdifferentiation context, Smad-mediated reprogramming of gene and regulatory RNA (miRNAs and lncRNAs) expression greatly contributes to the transition of epithelial cells toward a mesenchymal phenotype, with the apical-basal polarity redirected to a front-rear polarity, which enables the cells to directionally migrate [94-96]. TGF-β-activated Smad3-Smad4 complexes directly activate the expression of the EMT master transcription factors, such as Snail1 or Snail2/Slug and ZEB1 and ZEB2, and then cooperate with these transcription factors in the repression of epithelial genes and activation of a mesenchymal gene expression program [94]. Additionally, TGF-β-activated Smad3 interacts with RNA helicase p68/DDX5 to directly control the generation of precursor miRNAs [97, 98]. Alternative splicing is regulated by Smad3 activation as well, through Smad3-mediated changes in the expression of splicing regulatory proteins [99], and, more directly, association of Smad3 with PCBP1/hnRNPE1 in the hnRNA splicing machinery [100]. Both mechanisms result in isoform switching of proteins that control the epithelial or mesenchymal phenotypes, and have been shown to greatly contribute to EMT.

Smad-Sox interactions in the selection of cell differentiation and cell fate.

Transcription factors of the Sox family are well studied as master regulators of differentiation both during development and in disease. Functional cooperation of Smad2 and/or Smad3 with Sox2 plays key roles in maintaining pluripotency, with over 90% of the top one thousand Smad3 genomic binding sites co-occupied by Oct4, Sox2, and/or Nanog in cultured human embryonic stem cells [86]. In mouse embryonic stem cells, Smad1 and Sox2 also co-localize extensively at regulatory gene sequences with other transcription factors known to regulate pluripotency, such as Nanog and Oct4 [93]. Interestingly, Smad2 and/or Smad3 was found to drive expression of Nanog in human embryonic stem cells through binding to the proximal promoter of the *NANOG* gene [101]. Besides key roles of Smad-Sox2 complexes in pluripotency, Sox2 also controls the specification of neural, skin epithelial, and osteoblast differentiation, among other lineages [102].

Interactions of Smads with other Sox family proteins further illustrate critical roles in lineage specification and differentiation progression. For example, BMP-activated Smad1 cooperates with Sox5 to activate BMP target genes that are required in ectoderm development [103]. During chondrogenesis, BMP signaling induces the expression of Sox5, -6, and -9, while TGF-β-activated Smad3 induces Sox9 expression [104, 105]. In glioblastoma multiforme, Sox4 expression under the control of autocrine TGF-β/Smad3 signaling enables cooperation of Sox4 with Oct4 in the activation of Sox2 expression, which is necessary for the stemness of neuronal and glioblastoma stem cells [106, 107]. In these glioma-initiating cells, TGF-β also activates Smad-dependent expression of LIF, a cytokine required for self-renewal of mouse embryonic stem cells and for *Sox2* expression [108].

Aside from its role in differentiation, the interplay between Smad and Sox4 can lead to cell death, which was shown to occur in pancreatic ductal adenocarcinoma cells [109]. In this context of TGF-β-induced EMT, the balance between Smad4 and Sox4 levels directs the cancer cells either toward tumor formation and cancer progression, or to cell death. When Smad4 is functionally inactivated, e.g. through gene mutation or repression, TGF-β-induced Smad2 and/or Smad3 activation drives the expression of Sox4, which then cooperates with the transcription factor Klf5 to promote self-renewal and

tumorigenesis. However, in cells expressing normal Smad4 levels, the Smad complex containing Smad4 drives the expression of the EMT master transcription factor Snail1, which inhibits *Klf5* expression. Sox4, in conjunction with low Klf5 level, then promotes the expression of the pro-apoptotic genes *Bim* and *Bmf*, leading to EMT-associated apoptosis [109]. Thus Smad4 in cooperation with Sox4 acts as a switch toggling between self-renewal versus EMT followed by cell death as ultimate cell fate.

This role of the functional Smad4-Sox4 crosstalk in EMT is better appreciated in the context of previous findings. EMT is generally seen to protect against cell death, and Snail1 specifically promotes stem cell maintenance and resistance to a variety of apoptotic signals [110-112]. Furthermore, Snail1 and Snail2 expression were seen to directly lead to repression of pro-apoptotic genes and to protect against p53-mediated apoptosis [113]. Additionally, in retinal pigment epithelial cells, TGF-β activates the expression of the anti-apoptotic protein survivin, which protects against cell death and allows for EMT; following depletion of survivin, TGF-β induces cell death and apoptosis [114]. In other cells, TGF-β represses survivin expression, which promotes cell death, thus positioning survivin as a cell fate selection switch between EMT and cell death [114]. Additionally, TGF-β has also been shown to promote cell death by direct activation of the pro-apoptotic DAP-kinase expression by Smad2-Smad3-Smad4 complexes [115]. How the cooperation of Smad4 with Sox4 in the selection of EMT versus cell death relates to these prior observations-- the role of survivin, that Snail transcription factor expression and EMT protect against cell death, the ability of TGF-β to activate apoptosis -- remains to be clarified. Additional studies are required to assess whether the proposed mechanism is cell type- and context-dependent or can be extrapolated to epithelial and carcinoma cells of different origin. More insight into how TGF-β signaling promotes or protects against apoptosis in different cell types is clearly required.

As apparent from this discussion of selected areas of progress in understanding TGF-β signaling, the accepted simple model of TGF-β signaling with ligand binding to heteromeric TβRII-TβRI complexes leading to Smad activation and nuclear translocation to consequently activate or repress TGF-β/Smad target genes is a gross oversimplification that does not explain the highly nuanced and context-dependent

TGF-β responses. While our current knowledge provides the basis to understand the highly versatile TGF-β response, much remains to be learned about the mechanisms that control receptor presentation and activation, the control of cell responsiveness in activation of Smad and non-Smad signaling, and the Smad-mediated control of gene reprogramming and cell fate selection that, in combination with non-Smad signaling, defines the developmental and pathological roles of TGF-β signaling.

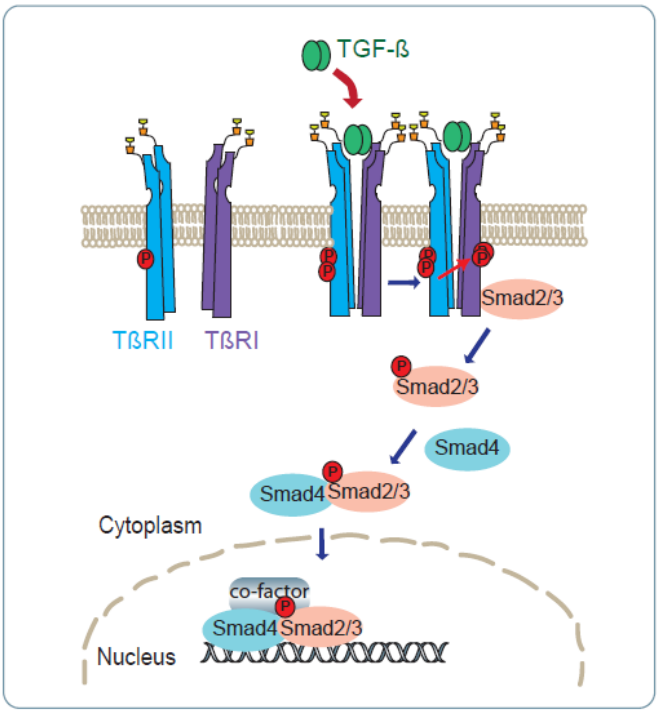

Figure 1. Commonly accepted model of TGF-β-induced Smad activation leading to Smad-mediated gene expression. The TGF-β dimer binds to the type II TGF-β receptor (TβRII), which leads to recruitment of the type I TGF-β receptor (TβRI) into a heteromeric receptor complex, enabling TβRII to transphosphorylate the GS domain of TβRI. The consequently activated TβRI then activates Smad2 and Smad3 by phosphorylation on C-terminal serines. These receptor-activated R-Smads then associate with a co-Smad (Smad4) and the Smad trimers then enter the nucleus where they associate with other transcription cofactors at Smad-binding regulatory DNA sequences of target genes, thus directly activating or repressing target gene expression.

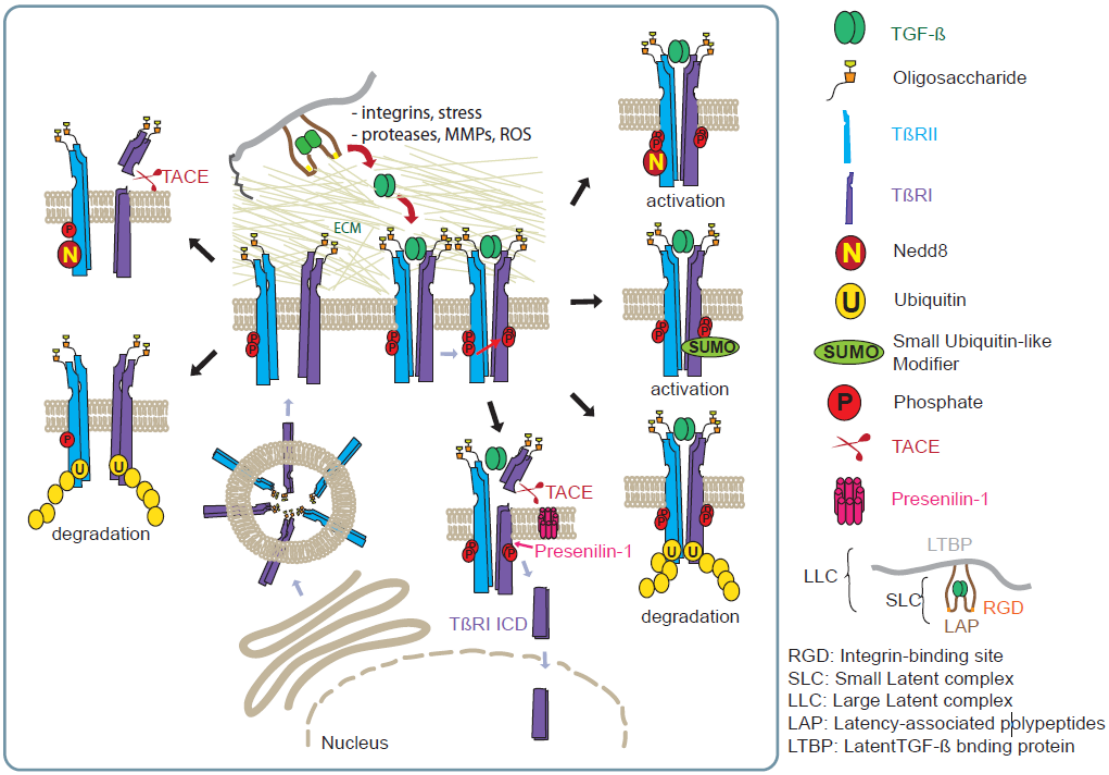

Figure 2. Post-translational modifications of the TGF-β receptors. TGF-β is secreted and stored in the extracellular matrix (ECM) in a large latent complex (LLC). Activation through integrin-mediated action and/ or proteases liberates active TGF-β for receptor binding. At the cell surface, the N-glycosylated TGF-β receptors, TβRI and TβRII are subject to TACE-mediated ectodomain cleavage and/or poly-ubiquitylation leading to degradation, independent of TGF-β stimulation (left). Ligand binding induces phosphorylation of the GS domain in TβRI by the TβRII kinase, as well TβRII and TβRI phosphorylation at multiple sites, TβRII neddylation, TβRI sumoylation, TβRII and TβRI ubiquitylation that can be reversed by de-ubiquitylases, and intracellular release of the TβRI intracellular domain (ICD) following TACE-mediated ectodomain cleavage (right).

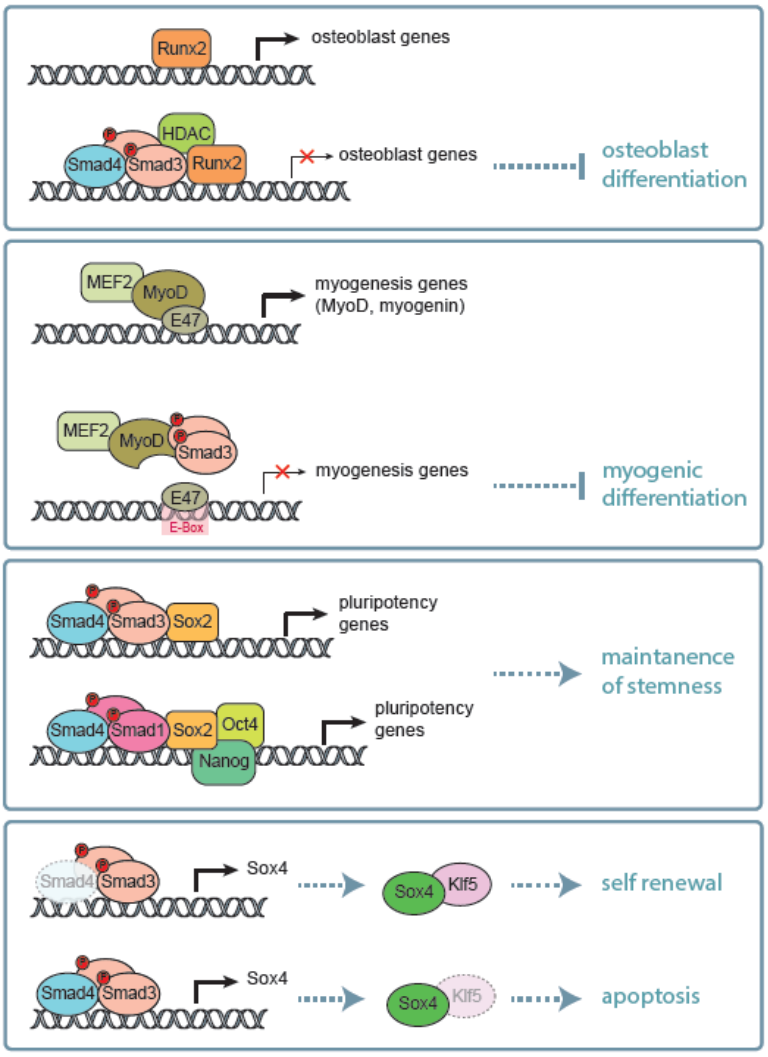

Figure 3. Smad cooperation with master transcription factors defines cell lineage and cell fate decisions. Some examples are illustrated. TGF-β-induced association of Smad3 with Runx2 enables histone deacetylase recruitment to promoter regions of osteoblast genes, resulting in repression of osteoblast differentiation. TGF-β-induced association of Smad3 with the myogenic transcription factors MyoD and MEF2 interferes with association of the myogenic transcription complex with E-proteins at regulatory E-box DNA sequences, thus repressing directed transcription of key myogenesis genes. In embryonic stem cells, activated Smads partner with pluripotency master regulators such as Sox2, Nanog, and Oct4 to drive gene expression programs necessary to maintain pluripotency. Depending on the Smad4 abundance, TGF-β-induced Smad3 activation can drive either self-renewal or an EMT that results in apoptosis through expression of Sox4.

REFERENCES

1. Morikawa, M., *et al.* (2016) TGF-β and the TGF-β family: context-dependent roles in cell and tissue physiology. *Cold Spring Harbor Persp Biol* 8, a021873.

2. Massagué, J. (2012) TGFβ signalling in context. *Nat Rev Mol Cell Biol* 13, 616-630.

3. Heldin, C.H. and Moustakas, A. (2016) Signaling receptors for TGF-β family members. *Cold Spring Harbor Persp Biol* 8, a022053.

4. Derynck, R. (1994) TGF-β-receptor-mediated signaling. *Trends Biochem Sci* 19, 548-553

5. Feng, X.H. and Derynck, R. (2005) Specificity and versatility in TGF-β signaling through Smads. *Annu Rev Cell Dev Biol* 21, 659-693.

6. Hill, C.S. (2016) Transcriptional Control by the SMADs. *Cold Spring Harbor Persp Biol* 8, 022079.

7. Robertson, I.B. and Rifkin, D.B. (2016) Regulation of the bioavailability of TGF-β and TGF-β-related Proteins. *Cold Spring Harbor Persp Biol* 8, 021907.

8. Stockis, J., *et al.* (2009) Membrane protein GARP is a receptor for latent TGF-β on the surface of activated human Treg. *Eur J Immunol* 39, 3315-3322.

9. Tran, D.Q., *et al.* (2009) GARP (LRRC32) is essential for the surface expression of latent TGF-β on platelets and activated FOXP3+ regulatory T cells. *Proc Natl Acad Sci U S A* 106, 13445-13450.

10. Li, Y., *et al.* (2015) Hepatic stellate cells inhibit T cells through active TGF-β1 from a cell surface-bound latent TGF-β1/GARP Complex. *J Immunol* 195, 2648-2656.

11. Wang, R., *et al.* (2012) GARP regulates the bioavailability and activation of TGF-β. *Mol Biol Cell* 23, 1129-1139.

12. Munger, J.S. and Sheppard, D. (2011) Cross talk among TGF-β signaling pathways, integrins, and the extracellular matrix. *Cold Spring Harbor Persp Biol* 3, a005017.

13. Annes, J.P., *et al.* (2004) Integrin αvβ6-mediated activation of latent TGF-β requires the latent TGF-β binding protein-1. *J Cell Biol* 165, 723-734.

14. Wipff, P.J. and Hinz, B. (2008) Integrins and the activation of latent transforming growth factor β1 - an intimate relationship. *Eur J Cell Biol* 87, 601-615.

15. Dong, X., *et al.* (2017) Force interacts with macromolecular structure in activation of TGF-β. *Nature* 542, 55-59.

16. Shi, M., *et al.* (2011) Latent TGF-β structure and activation. *Nature* 474, 343-349.

17. Aluwihare, P., *et al.* (2009) Mice that lack activity of αvβ6 and αvβ8 integrins reproduce the abnormalities of Tgfβ1- and Tgfb3-null mice. *J Cell Sci* 122, 227-232.

18. Yang, Z., *et al.* (2007) Absence of integrin-mediated TGFβ1 activation in vivo recapitulates the phenotype of TGFβ1-null mice. *J Cell Biol* 176, 787-793.

19. Jenkins, G. (2008) The role of proteases in transforming growth factor-β activation. *Int J Biochem Cell Biol* 40, 1068-1078.

20. Mu, D., *et al.* (2002) The integrin αvβ8 mediates epithelial homeostasis through MT1-MMP-dependent activation of TGF-β1. *J Cell Biol* 157, 493-507.

21. Rodriguez, C., *et al.* (1995) Cooperative binding of transforming growth factor (TGF)-β2 to the types I and II TGF-β receptors. *J Biol Chem* 270, 15919-15922.

22. Wells, R.G., *et al.* (1997) Biosynthesis of the type I and type II TGF-β receptors. *J Biol Chem* 272, 11444-11451.

23. Kim, Y.W., *et al.* (2012) TGF-β sensitivity is determined by N-linked glycosylation of the type II TGF-β receptor. *Biochem J* 445, 403-411.

24. Goetschy, J.F., *et al.* (1996) The unglycosylated extracellular domain of type-II receptor for transforming growth factor-β. A novel assay for characterizing ligand affinity and specificity. *Eur J Biochem* 241, 355-362.

25. Fukami, K., et al. (2017) High glucose induces N-linked glycosylation-mediated functional upregulation and overexpression of Cav3.2 T-type calcium channels in neuroendocrine-like differentiated human prostate cancer cells. *J Pharmacol Sci* 133, 57-60.

26. Alisson-Silva, F., et al. (2013) Increase of O-glycosylated oncofetal fibronectin in high glucose-induced epithelial-mesenchymal transition of cultured human epithelial cells. *PloS One 8*, e60471.

27. Bektas, M. and Rubenstein, D.S. (2011) The role of intracellular protein O-glycosylation in cell adhesion and disease. *J Biomed Res* 25, 227-236.

28. Liu, C., *et al.* (2009) TACE-mediated ectodomain shedding of the type I TGF-β receptor downregulates TGF-β signaling. *Mol Cell* 35, 26-36.

29. Gudey, S.K., *et al.* (2014) TRAF6 stimulates the tumor-promoting effects of TGFβ type I receptor through polyubiquitination and activation of presenilin 1. *Science Signal* 7, ra2

30. Mu, Y., *et al.* (2011) TRAF6 ubiquitinates TGFβ type I receptor to promote its cleavage and nuclear translocation in cancer. *Nat Commun* 2, 330.

31. Hata, A. and Chen, Y.G. (2016) TGF-β signaling from receptors to Smads. *Cold Spring Harbor Perspect Biol* 8, 022061.

32. Schlessinger, J. (2000) Cell signaling by receptor tyrosine kinases. *Cell* 103, 211-225.

33. Spaargaren, M., *et al.* (1991) Antibody-induced dimerization activates the epidermal growth factor receptor tyrosine kinase. *J Biol Chem* 266, 1733-1739.

34. Chen, F. and Weinberg, R.A. (1995) Biochemical evidence for the autophosphorylation and transphosphorylation of transforming growth factor-β receptor kinases. *Proc Natl Acad Sci U S A* 92, 1565-1569.

35. Hanks, S.K. and Hunter, T. (1995) Protein kinases 6. The eukaryotic protein kinase superfamily: kinase (catalytic) domain structure and classification. *FASEB J* 9, 576-596.

36. Rask-Andersen, M., *et al.* (2014) Advances in kinase targeting: current clinical use and clinical trials. *Trends Pharmacol Sci* 35, 604-620.

37. Lawler, S., *et al.* (1997) The type II transforming growth factor-β receptor autophosphorylates not only on serine and threonine but also on tyrosine residues. *J Biol Chem* 272, 14850-14859.

38. Lee, M.K., *et al.* (2007) TGF-β activates Erk MAP kinase signalling through direct phosphorylation of ShcA. *EMBO J* 26, 3957-3967.

39. Shi, W., *et al.* (2004) GADD34-PP1c recruited by Smad7 dephosphorylates TGFβ type I receptor. *J Cell Biol* 164, 291-300.

40. Batut, J., *et al.* (2008) Two highly related regulatory subunits of PP2A exert opposite effects on TGF-β/Activin/Nodal signalling. *Development* 135, 2927-2937.

41. Goh, L.K., *et al.* (2010) Multiple mechanisms collectively regulate clathrin-mediated endocytosis of the epidermal growth factor receptor. *J Cell Biol* 189, 871-883.

42. Hsu, J.M., *et al.* (2011) Crosstalk between Arg 1175 methylation and Tyr 1173 phosphorylation negatively modulates EGFR-mediated ERK activation. *Nat Cell Biol* 13, 174-181.

43. Liao, H.W., *et al.* (2015) PRMT1-mediated methylation of the EGF receptor regulates signaling and cetuximab response. *J Clin Invest* 125, 4529-4543.

44. Song, H., *et al.* (2011) Acetylation of EGF receptor contributes to tumor cell resistance to histone deacetylase inhibitors. *Biochem Biophys Res Commun* 404, 68-73.

45. Ito, K., *et al.* (2006) Histone deacetylase 2-mediated deacetylation of the glucocorticoid receptor enables NF-κB suppression. *J Exp Med* 203, 7-13.

46. Le Romancer, M., *et al.* (2008) Regulation of estrogen rapid signaling through arginine methylation by PRMT1. *Mol Cell* 31, 212-221.

47. Liu, S., *et al.* (2016) Regulation of the TGF-β pathway by deubiquitinases in cancer. *Int J Biochem Cell Biol* 76, 135-145.

48. Rotin, D. and Kumar, S. (2009) Physiological functions of the HECT family of ubiquitin ligases. *Nat Rev Mol Cell Biol* 10, 398-409.

49. Ebisawa, T., *et al.* (2001) Smurf1 interacts with transforming growth factor-β type I receptor through Smad7 and induces receptor degradation. *J Biol Chem* 276, 12477-12480.

50. Kavsak, P., *et al.* (2000) Smad7 binds to Smurf2 to form an E3 ubiquitin ligase that targets the TGFβ receptor for degradation. *Mol Cell* 6, 1365-1375.

51. Kuratomi, G., *et al.* (2005) NEDD4-2 (neural precursor cell expressed, developmentally down-regulated 4-2) negatively regulates TGF-β (transforming growth factor-β) signalling by inducing ubiquitin-mediated degradation of Smad2 and TGF-β type I receptor. *Biochem J* 386, 461–470.

52. Komuro, A., *et al.* (2004) Negative regulation of transforming growth factor-β (TGF-β) signaling by WW domain-containing protein 1 (WWP1). *Oncogene* 23, 6914-6923.

53. Zhang, L., *et al.* (2012) USP4 is regulated by AKT phosphorylation and directly deubiquitylates TGF-β type I receptor. *Nat Cell Biol* 14, 717-726.

54. Eichhorn, P.J., *et al.* (2012) USP15 stabilizes TGF-β receptor I and promotes oncogenesis through the activation of TGF-β signaling in glioblastoma. *Nat Med* 18, 429-435.

55. Wicks, S.J., *et al.* (2005) The deubiquitinating enzyme UCH37 interacts with Smads and regulates TGF-β signalling. *Oncogene* 24, 8080-8084.

56. Al-Salihi, M.A., *et al.* (2012) USP11 augments TGFβ signalling by deubiquitylating ALK5. *Open Biology* 2, 120063.

57. Kerscher, O., *et al.* (2006) Modification of proteins by ubiquitin and ubiquitin-like proteins. *Annu Rev Cell Dev Biol* 22, 159-180.

58. Zhou, X., et al. (2014) High glucose induces sumoylation of Smad4 via SUMO2/3 in mesangial cells. *Biomed Res Int* 2014, 782625.

59. Kang, J.S., *et al.* (2008) The type I TGF-β receptor is covalently modified and regulated by sumoylation. *Nat Cell Biol* 10, 654-664.

60. Chen, T., et al. (1998) Transforming growth factor-β type I receptor kinase mutant associated with metastatic breast cancer. *Cancer Res* 58, 4805-4810.

61. Chen, T., et al. (2001) Novel inactivating mutations of transforming growth factor-β type I receptor gene in head-and-neck cancer metastases. *Int J of Cancer* 93, 653-661.

62. Zuo, W., *et al.* (2013) c-Cbl-mediated neddylation antagonizes ubiquitination and degradation of the TGF-β type II receptor. *Mol Cell* 49, 499-510.

63. Chandhoke, A.S., *et al.* (2016) The ubiquitin ligase Smurf2 suppresses TGFβ-induced epithelial-mesenchymal transition in a sumoylation-regulated manner. *Cell Death Differ* 23, 876-888.

64. Zhang, Y.E. (2017) Non-Smad signaling pathways of the TGF-β family. *Cold Spring Harbor Persp Biol* 9, a022129.

65. Tsukazaki, T., *et al.* (1998) SARA, a FYVE domain protein that recruits Smad2 to the TGF-β Receptor. *Cell* 95, 779-791.

66. Miura, S., *et al.* (2000) Hgs (Hrs), a FYVE domain protein, is involved in Smad signaling through cooperation with SARA. *Mol Cell Biol* 20, 9346-9355.

67. Le Roy, C. and Wrana, J.L. (2005) Clathrin- and non-clathrin-mediated endocytic regulation of cell signalling. *Nat Rev Mol Cell Biol* 6, 112-126.

68. Datta, P.K. and Moses, H.L. (2000) STRAP and Smad7 synergize in the inhibition of transforming growth factor-β signaling. *Mol Cell Biol* 20, 3157-3167.

69. Guo, X.*, et al.* (2008) Axin and GSK3- control Smad3 protein stability and modulate TGF-β signaling. *Genes Dev* 22, 106-120.

70. Furuhashi, M.*, et al.* (2001) Axin facilitates Smad3 activation in the transforming growth factor β signaling pathway. *Mol Cell Biol* 21, 5132-5141.

71. Liu, W.*, et al.* (2006) Axin is a scaffold protein in TGF-β signaling that promotes degradation of Smad7 by Arkadia. *EMBO J* 25, 1646-1658

72. Watanabe, Y.*, et al.* (2010) TMEPAI, a transmembrane TGF-β-inducible protein, sequesters Smad proteins from active participation in TGF-β signaling. *Mol Cell* 37, 123-134.

73. Nakano, N.*, et al.* (2014) C18 ORF1, a novel negative regulator of transforming growth factor-β signaling. *J Biol Chem* 289, 12680-12692.

74. Yao, D.*, et al.* (2002) Transforming growth factor-β receptors interact with AP2 by direct binding to β2 subunit. *Mol Biol Cell* 13, 4001-4012.

75. Shapira, K.E.*, et al.* (2014) Dab2 inhibits the cholesterol-dependent activation of JNK by TGF-β. *Mol Biol Cell* 25, 1620-1628.

76. Zuo, W. and Chen, Y.G. (2009) Specific activation of mitogen-activated protein kinase by transforming growth factor-β receptors in lipid rafts is required for epithelial cell plasticity. *Mol Biol Cell* 20, 1020-1029.

77. Meyer, C.*, et al.* (2013) Caveolin-1 abrogates TGF-β mediated hepatocyte apoptosis. *Cell Death Dis* 4, e466.

78. Di Guglielmo, G.M.*, et al.* (2003) Distinct endocytic pathways regulate TGF-β receptor signalling and turnover. *Nat Cell Biol* 5, 410-421.

79. He, K.*, et al.* (2015) Internalization of the TGF-β type I receptor into caveolin-1 and EEA1 double-positive early endosomes. *Cell Res* 25, 738-752

80. Muthusamy, B.P., *et al.* (2015) ShcA protects against epithelial-mesenchymal transition through compartmentalized inhibition of TGF-β-induced Smad activation. *PLoS Biology* 13, e1002325.

81. Budi, E.H., *et al.* (2015) The insulin response integrates increased TGF-β signaling through Akt-induced enhancement of cell surface delivery of TGF-β receptors. *Science Signal* 8, ra96.

82. Takimoto, T., *et al.* (2010) Smad2 and Smad3 are redundantly essential for the TGF-β-mediated regulation of regulatory T plasticity and Th1 development. *J Immunol* 185, 842-855.

83. Dennler, S., *et al.* (1998) Direct binding of Smad3 and Smad4 to critical TGF β-inducible elements in the promoter of human plasminogen activator inhibitor-type 1 gene. *The EMBO J* 17, 3091-3100.

84. Zawel, L., *et al.* (1998) Human Smad3 and Smad4 are sequence-specific transcription activators. *Mol Cell* 1, 611-617.

85. Jonk, L.J., *et al.* (1998) Identification and functional characterization of a Smad binding element (SBE) in the JunB promoter that acts as a transforming growth factor-β, activin, and bone morphogenetic protein-inducible enhancer. *J Biol Chem* 273, 21145-21152.

86. Mullen, A.C., *et al.* (2011) Master transcription factors determine cell-type-specific responses to TGF-β signaling. *Cell* 147, 565-576.

87. Massagué, J. (2012) TGFβ signalling in context. *Nat Rev Mol Cell Biol* 13, 616-630.

88. Mullen, A.C. and Wrana, J.L. (2017) TGF-β family signaling in embryonic and somatic stem-cell renewal and differentiation. *Cold Spring Harbor Persp Biol* 9, a022186.

89. Grafe, I., *et al.* (2017) TGF-β family signaling in mesenchymal differentiation. *Cold Spring Harbor Persp Biol* In Press

90. Liu, D., *et al.* (2001) TGF-β inhibits muscle differentiation through functional repression of myogenic transcription factors by Smad3. *Genes Dev* 15, 2950-2966.

91. Liu, D., *et al.* (2004) TGF-β-activated Smad3 represses MEF2-dependent transcription in myogenic differentiation. *EMBO J* 23, 1557-1566.

92. Kang, J.S., *et al.* (2005) Repression of Runx2 function by TGF-β through recruitment of class II histone deacetylases by Smad3. *EMBO J* 24, 2543-2555.

93. Chen, X., *et al.* (2008) Integration of external signaling pathways with the core transcriptional network in embryonic stem cells. *Cell* 133, 1106-1117.

94. Lamouille, S., *et al.* (2014) Molecular mechanisms of epithelial-mesenchymal transition. *Nat Rev Mol Cell Biol* 15, 178-196.

95. Yuan, J.H., *et al.* (2014) A long noncoding RNA activated by TGF-β promotes the invasion-metastasis cascade in hepatocellular carcinoma. *Cancer Cell* 25, 666-681

96. Gonzalez, D.M. and Medici, D. (2014) Signaling mechanisms of the epithelial-mesenchymal transition. *Science Signal* 7, re8.

97. Warner, D.R., *et al.* (2004) Functional interaction between Smad, CREB binding protein, and p68 RNA helicase. *Biochem Biophys Res Commun* 324, 70-76.

98. Davis, B.N., *et al.* (2008) SMAD proteins control DROSHA-mediated microRNA maturation. *Nature* 454, 56-61.

99. Horiguchi, K., *et al.* (2012) TGF-β drives epithelial-mesenchymal transition through δEF1-mediated downregulation of ESRP. *Oncogene* 31, 3190-3201.

100. Tripathi, V., *et al.* (2016) Direct Regulation of alternative splicing by SMAD3 through PCBP1 is essential to the tumor-promoting role of TGF-β. *Mol Cell* 64, 549-564.

101. Xu, R.H., *et al.* (2008) NANOG is a direct target of TGF-β/activin-mediated SMAD signaling in human ESCs. *Cell Stem Cell* 3, 196-206.

102. Sarkar, A. and Hochedlinger, K. (2013) The sox family of transcription factors: versatile regulators of stem and progenitor cell fate. *Cell Stem Cell* 12, 15-30.

103. Nordin, K. and LaBonne, C. (2014) Sox5 Is a DNA-binding cofactor for BMP R-Smads that directs target specificity during patterning of the early ectoderm. *Dev Cell* 31, 374-382.

104. Lee, H.L., *et al.* (2016) Transforming growth factor-β-induced KDM4B promotes chondrogenic differentiation of human mesenchymal stem cells. *Stem Cells* 34, 711-719.

105. Wu, M., *et al.* (2016) TGF-β and BMP signaling in osteoblast, skeletal development, and bone formation, homeostasis and disease. *Bone Research* 4, 16009.

106. Ikushima, H., *et al.* (2009) Autocrine TGF-β signaling maintains tumorigenicity of glioma-initiating cells through Sry-related HMG-box factors. *Cell Stem Cell* 5, 504-514.

107. Ikushima, H., *et al.* (2011) Glioma-initiating cells retain their tumorigenicity through integration of the Sox axis and Oct4 protein. *J Biol Chem* 286, 41434-41441.

108. Penuelas, S., *et al.* (2009) TGF-β increases glioma-initiating cell self-renewal through the induction of LIF in human glioblastoma. *Cancer Cell* 15, 315-327.

109. David, C.J., *et al.* (2016) TGF-β tumor suppression through a lethal EMT. *Cell* 164, 1015-1030.

110. Vega, S., *et al.* (2004) Snail blocks the cell cycle and confers resistance to cell death. *Genes Dev* 18, 1131-1143.

111. Barrallo-Gimeno, A. and Nieto, M.A. (2005) The Snail genes as inducers of cell movement and survival: implications in development and cancer. *Development* 132, 3151-3161.

112. Franco, D.L., *et al.* (2010) Snail1 suppresses TGF-β-induced apoptosis and is sufficient to trigger EMT in hepatocytes. *J Cell Sci* 123, 3467-3477.

113. Kurrey, N.K., *et al.* (2009) Snail and slug mediate radioresistance and chemoresistance by antagonizing p53-mediated apoptosis and acquiring a stem-like phenotype in ovarian cancer cells. *Stem cells* 27, 2059-2068.

114. Lee, J., *et al.* (2013) TGF-β1 regulates cell fate during epithelial-mesenchymal transition by upregulating survivin. *Cell Death Disease* 4, e714.

115. Jang, C.W., *et al.* (2002) TGF-β induces apoptosis through Smad-mediated expression of DAP-kinase. *Nat Cell Biol* 4, 51-58.

Publishing Agreement

It is the policy of the University to encourage the distribution of all theses, dissertations, and manuscripts. Copies of all UCSF theses, dissertations, and manuscripts will be routed to the library via the Graduate Division. The library will make all theses, dissertations, and manuscripts accessible to the public and will preserve these to the best of their abilities, in perpetuity.

Please sign the following statement:

I hereby grant permission to the Graduate Division of the University of California, San Francisco to release copies of my thesis, dissertation, or manuscript to the Campus Library to provide access and preservation, in whole or in part, in perpetuity.

Author Signature

12-28-2017

Date